Am J Nucl Med Mol Imaging 2012;2(2):174-220
www.ajnmmi.us /ISSN:2160-8407/ajnmmi1202002

Review Article

Current imaging strategies in rheumatoid arthritis

Merissa N Zeman, Peter JH Scott

Department of Radiology, University of Michigan Medical School, Ann Arbor, MI, USA

Received February 5, 2012; accepted February 28, 2012; Epub March 28, 2012; Published April 15, 2012

Abstract: As remission has now become a realistic therapeutic goal in the clinical management of RA due to the introduction and widespread adoption of biologic agents, there is a greater need for earlier diagnoses and objective methods for evaluating disease activity and response to treatment. In this capacity, advanced imaging strategies are assuming an expansive clinical role, particularly as they take advantage of newer imaging technologies and the shift toward imaging at the molecular level. Molecular imaging utilizes target-specific probes to non-invasively visualize molecular, cellular, and physiological perturbations in response to the underlying pathology. Probes for nuclear and MR imaging have been and are being developed that react with discrete aspects of inflammatory and destructive pathways specific to RA. These probes in addition to new MR sequences and contrast agents have the potential to provide an earlier and more reliable assessment of clinical outcome, disease activity, severity, and location, and therapeutic response. Furthermore, these imaging strategies may enable a more fundamental understanding of critical pathophysiological processes and the advent of new molecular therapies. This review will discuss these advances in both nuclear medicine and MRI strategies for imaging RA with a particular emphasis on molecular imaging.

Keywords: Molecular imaging, magnetic resonance imaging, nuclear imaging, rheumatoid arthritis

Introduction

Rheumatoid arthritis (RA) is a chronic, systemic inflammatory disease of unknown etiology that affects 0.5-1.0% of the general population [1]. Although heterogeneous, RA is primarily characterized by symmetric, erosive synovitis, which, if uncontrolled, can lead to joint and cartilage damage, multiple co-morbidities, significant disability, and reduction in quality of life, **Figure 1** [2, 3]. That being said, recent advances in therapeutic interventions have greatly improved the outlook of this disease. In particular, the introduction and widespread adoption of biologic agents, which target specific molecules critical for the sustenance of RA, has revolutionized the clinical management of patients [4-6]. Several studies have demonstrated that biologic agents in combination with conventional disease-modifying antirheumatic drugs (DMARDs), such as methotrexate (MTX), significantly reduce clinical symptoms, slow or arrest erosive changes, and allow for disease remission [7-9].

Optimal patient outcomes greatly depend on aggressive and efficacious treatment that is initiated early in the disease course [10]. This not only requires timely diagnoses, but also objective measures for monitoring disease activity and therapeutic response. Currently, rheumatologists primarily rely on clinical examination, laboratory parameters, and conventional radiography (CR) for patient evaluation. While this approach is a mainstay of rheumatology, the utility of such testing is limited in many respects. Clinical measures of pain and swelling are subjective and have been shown to have moderate sensitivity and specificity. Similarly, laboratory parameters, such as erythrocyte sedimentation rate (ESR) and C-reactive protein (CRP) serum concentrations, are unreliable and highly unspecific. While CR clearly delineates bone erosions and joint space narrowing, it does not provide any information about disease activity or non-osseous components of RA, and it has low sensitivity in early disease.

In light of these shortcomings, advanced imaging strategies are assuming an increasingly prominent role in the investigation and routine assessment of RA patients. Central to this paradigm shift in disease management has been the

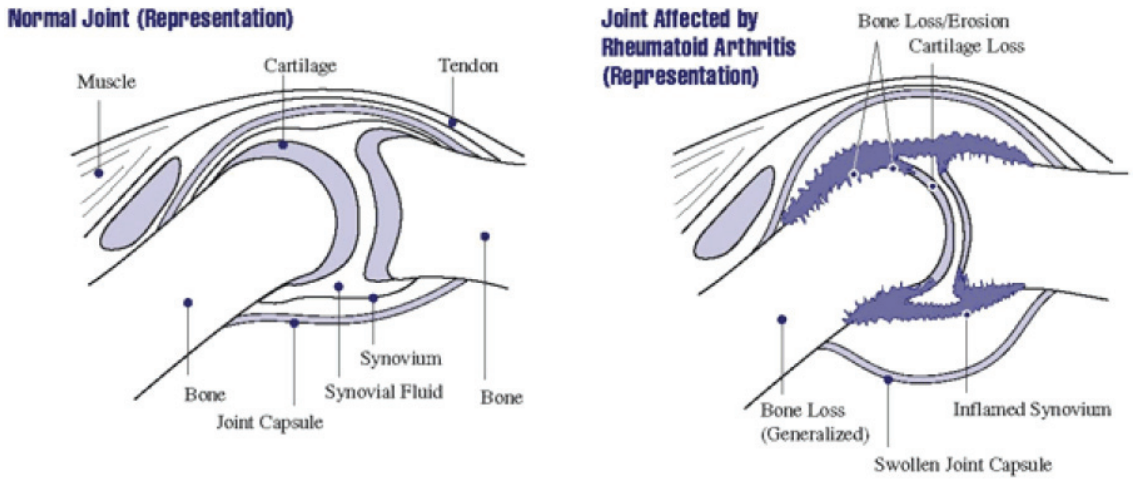

Figure 1. A joint (the place where two bones meet) is surrounded by a capsule that protects and supports it. The joint capsule is lined with a type of tissue called synovium, which produces synovial fluid that lubricates and nourishes joint tissues. In rheumatoid arthritis, the synovium becomes inflamed, causing warmth, redness, swelling, and pain. As the disease progresses, the inflamed synovium invades and damages the cartilage and bone of the joint. Surrounding muscles, ligaments, and tendons become weakened. Rheumatoid arthritis also can cause more generalized bone loss that may lead to osteoporosis (fragile bones that are prone to fracture) (Image courtesy of the National Institute of Arthritis and Musculoskeletal and Skin Diseases (NIAMS) (http://www.niams.nih.gov/Health_Info/Rheumatic_Disease/default.asp - last accessed February 2012)).

rapid emergence of new imaging technologies (for a review see [11]) and the field of molecular imaging, which utilizes target-specific probes to non-invasively visualize molecular, cellular, and physiological perturbations in response to the underlying pathology [12]. As more is learned about the pathophysiological changes indicative of RA, imaging agents that specifically react with discrete aspects of inflammatory and destructive pathways are being constructed primarily for nuclear medicine imaging modalities, such as positron emission tomography (PET), single photon emission computed tomography (SPECT), and scintigraphy. These targeted probes relay information about molecules driving RA and thus enable a more fundamental understanding of critical pathophysiological processes, the development of new molecular therapies, an earlier and more reliable prognosis, assessment of disease activity and severity, and treatment response [12]. Additionally, as evidence suggests there is a subclinical phase of RA, in which cellular and molecular changes precede any anatomic, physiological, or metabolic alterations, molecular imaging may allow for diagnoses early in the disease course prior to the appearance of irreversible erosions [12-14]. While mostly experimental, molecular imaging has recently been applied to magnetic resonance imaging (MRI) as well. Through the advent of new sequences and targeted contrast agents, MRI not only provides high-resolution images with good soft tissue contrast at the anatomical level, but is now also capable of offering more 'physiological' data about disease pathways. This paper will explore the advances in both nuclear medicine and MRI strategies for imaging RA with a particular emphasis on molecular imaging.

RA pathophysiology: targets for treatment and molecular imaging

While the etiology of this disease is currently unknown, a number of pathophysiological processes and molecules specific to RA have been identified and well characterized. Genetically pre-disposed individuals are believed to develop RA through a number of inflammatory pathways triggered in response to endogenous and/or exogenous antigens that resemble self-determinants. Critical to the initiation of the disease, HLA-DR-positive antigen-presenting cells (APCs) are thought to present these antigens to auto-reactive $CD4^+$ T Helper (T_H) cells in secondary lymphoid organs. A linkage of RA to "the shared epitope" of the HLA-DRB1*04 cluster has been determined and is in support of

this hypothesis [15]. $CD4^+$ T_H cells are subsequently stimulated through interactions between their T-cell receptor (TCR)-CD3 complex and CD4 molecule and the type II major histocompatibility complex (MHC-II) with the antigenic determinant on the surface of the APCs. T cell activation additionally needs a co-stimulatory signal from the recognition of CD80 or CD86 by its CD28 cell-surface molecule [16, 17].

Activated T_H cells proliferate and infiltrate into the synovial tissue, where they release interferon-γ (IFN-γ), interleukin-2 (IL-2), and interleukin-4 (IL-4) [18]. These pro-inflammatory cytokines not only activate other T_H cells, but also macrophages, fibroblasts, osteoclasts, and chondrocytes [19, 20]. Similar to T_H cells, macrophages, when activated, increasingly migrate into synovial tissue. This is consistent with the finding that macrophages and T_H cells make up the majority of inflammatory cell infiltrates in early and late RA [13, 14]. Stimulated macrophages and fibroblasts, in turn, produce other pro-inflammatory cytokines, including tumor necrosis factor-α (TNF-α), interleukin-1 (IL-1), and interleukin-6 (IL-6), as well as chemokines, prostaglandins, proteases, and growth factors [21-23]. From the multitude of released immune mediators, B lymphocytes are stimulated to produce autoantibodies such as rheumatoid factor (RF), which is present in >80% of RA patients. Neutrophils are recruited as well to the synovial joints, but they are more prevalent in the synovial fluid than lining.

Activated endothelial vasculature helps coordinate and perpetuate this mass infiltration of mononuclear cells into inflamed synovium. In the presence of IL-1β and TNF-α, endothelial cells in postcapillary venules upregulate cell adhesion molecules (CAMs), which assist in the rolling, binding, and transendothelial migration of leukocytes [24]. Increased microvascular permeability and hyperemia, non-specific mechanisms of the acute inflammatory response, may add to the accumulation of leukocytes in inflamed synovium; moreover, these processes, in addition to locally expanded diffusion space, account for the enhanced extravasation of macromolecules and small proteins into the interstitial space during the acute phase of the disease [25]. As RA becomes chronic, synovial proliferation, supported by neovascularization, leads to pannus formation. This hypertrophic and hyperplastic synovial tissue is highly invasive, particularly at the interface between the synovium and juxta-articular bone and cartilage, and is responsible for marginal erosions and joint space narrowing. The destructive nature of this tissue is likely the result of fibroblast-like synoviocyte and chondrocyte production and release of metalloproteinases, which degrade proteoglycans and collagen [26-28]. Bone resorption due to activation of osteoclasts, however, appears to be the main mechanism through which bone erosions occur [27]. Over time, these destructive forces coupled with mechanical stress cause variable changes in peri-articular bone and soft tissue structures. These changes manifest clinically as chronic joint swelling, tenderness, pain, and eventual destruction. Overall, RA can be viewed as a series of coordinated events in the synovial, vascular, and bone compartments. The mechanisms that both initiate and perpetuate this disease within and between these compartments all represent potential targets for molecular imaging and therapeutic intervention and will be discussed in detail below.

Nuclear medicine imaging strategies

Role of nuclear medicine in the management of RA

While more established imaging techniques focus on morphological changes, nuclear medicine provides functional data about disease activity, which is critical for therapy decision-making and patient follow-up. In particular, by measuring long-term alterations in imaging parameters that serve as surrogates for synovitis, nuclear imaging allows for the objective monitoring of treatment response in RA patients. As current drug regimens are relatively expensive, determining patient response early in the treatment course is a cost-effective solution. Additionally, it is important to determine which patients are likely to develop high-risk lesions or a more severe disease course, as it may call for more aggressive treatment or more frequent monitoring. As nuclear probes visualize disease processes that are active even prior to irreversible anatomic changes, imaging with these probes may allow for the early prediction of disease outcomes.

Furthermore, nuclear imaging has the potential to accurately select patients that are likely to

respond to a particular treatment based on the articular presence of the drug target. Due to the high intra- and inter-individual variation in these target molecules in the joints of RA patients, a pre-treatment scan with a radiotracer that localizes the therapeutic target in inflamed tissues may be useful in predicting treatment efficacy and planning appropriate therapies. This approach could also provide an explanation for the failure of any targeted therapy or a justification for the use of a specific treatment. As a logical extension, nuclear imaging can allow for a more personalized therapeutic program tailored to the specific perturbations in inflammatory and destructive pathways that are active in the joints of each patient. Individualized patient management is particularly important, considering RA has heterogeneous clinical manifestations and is often thought of as a collection of disorders. While still mostly experimental, the clinical role of nuclear medicine in imaging RA is greatly expanding, particularly as this field takes advantage of new imaging technologies for PET and SPECT and targeted molecular probes. We are gradually seeing this shift to molecular imaging in nuclear medicine, but note that non-specific agents are still widely available for imaging RA as well.

Positron emission tomography (PET) imaging

[^{18}F]FDG

2-[^{18}F]Fluoro-2-deoxy-$_{D}$-glucose ([^{18}F]FDG) is a well-characterized radiolabeled glucose analog that when used in conjunction with PET reflects metabolic changes in tissues. Increased uptake of [^{18}F]FDG is mediated through glucose transporter type 1 (GLUT1) and glucose transporter type 3 (GLUT3) cell-surface proteins, which are overexpressed in hypermetabolic cells [29]. Upon entering the cell, [^{18}F]FDG is rapidly phosphorylated to [^{18}F]FDG-6-phosphate by the primary glycolytic enzyme, hexokinase, whose upregulation additionally accounts for the enhanced [^{18}F]FDG uptake observed in rapidly proliferating cells [29]. Unlike phosphorylated glucose, [^{18}F]FDG-6-phosphate cannot undergo further metabolism, effectively trapping this molecule intracellularly. Due to the inclination toward anaerobic glycolysis and consequently the elevated metabolic demand for glucose in cancerous cells, [^{18}F]FDG PET has been widely employed in the field of oncology for tumor staging, diagnosis, and therapeutic evaluation. [^{18}F]FDG accumulation, however, is not specific for neoplastic tissue. For example, macrophages, neutrophils, and young granulation tissue increasingly take up glucose, and thus, [^{18}F]FDG, as a consequence of activation and respiratory (oxidative) burst [30-32]. Due to the involvement of these cells in the maintenance of inflammatory processes, it was hypothesized that [^{18}F]FDG PET may serve as a useful tool for the study of RA. [^{18}F]FDG PET has since been employed in a number of pre-clinical and clinical RA studies (reviewed in [33]).

Recently, Matsui and co-workers provided the proof-of-mechanism for this imaging approach in a murine collagen-induced arthritis (CIA) model and *in vitro* [^{3}H]FDG uptake study [34]. [^{18}F]FDG PET was shown to accurately delineate swollen joints *in vivo*. As confirmed histologically, moderate [^{18}F]FDG uptake was noted in regions of interstitial inflammatory cell recruitment, synovial cell hyperplasia, and edema early in the disease course. In comparison, later -developing sites of pannus formation and bone destruction demonstrated high levels of [^{18}F]FDG accumulation, highlighting the capacity of this imaging strategy to reflect the progression of arthritis. Within these inflammatory regions, proliferating fibroblasts were determined to exhibit the highest levels of [^{3}H]FDG uptake, followed by neutrophils. Furthermore, while resting macrophages were not shown to significantly contribute to [^{3}H]FDG accumulation, hypoxic conditions and the presence of pro-inflammatory cytokines such as TNF-α (a microenvironment common in rheumatoid joints) greatly enhanced [^{3}H]FDG uptake in these cells as well as fibroblasts, but not neutrophils. Contrastingly, [^{3}H]FDG uptake was considerably lower for T lymphocytes, indicating that these inflammatory cells only play a negligible role in [^{18}F]FDG accumulation *in vivo*. Altogether, these findings suggest that proliferating fibroblasts and macrophages, particularly when in a hypoxic, pro-inflammatory cytokine-rich microenvironment, are the primary contributors to regional [^{18}F]FDG uptake *in vivo* in pannus and interstitial inflammatory cell infiltrates. This study supports the notion set forth by a number of clinical studies (as discussed below) that [^{18}F]FDG PET accurately reflects the disease activity of RA.

Palmer and colleagues were the first to evaluate the validity of quantifying joint inflammation and

changes in metabolic activity in response to treatment in RA patients using [18F]FDG PET [35]. In this pivotal work, Gadolinium-enhanced MRI and [18F]FDG PET images of wrist lesions were acquired for 12 patients with inflammatory arthritis (6 RA patients and 3 patients with psoriatic arthritis) undergoing anti-inflammatory therapy. Clinical examination and imaging studies were conducted at 3 intervals: baseline, after 2 weeks of treatment with prednisone or NSAIDs, and after 12-14 weeks of low-dose methotrexate (MTX) treatment. For each session, volume of enhancing pannus (VEP) was calculated from axial, fat-suppressed MR images for correlation with [18F]FDG PET parameters (total uptake value (TUV) and regional uptake value (RUV)) and clinical findings. Visual comparison of images revealed that regions of greatest PET signal corresponded to areas of enhancing pannus on MRI [35]. While decreases in pannus volume and [18F]FDG uptake in response to treatment paralleled clinical improvement (in terms of pain, tenderness, and swelling) of the imaged wrist, none of the [18F]FDG PET or MRI parameters was associated with overall treatment outcome. The authors suggested that this lack of correlation with treatment outcome could be the result of a small patient population or the strict cut-offs imposed by the Paulus index as to what qualifies as a treatment response (need 20% improvement in each of 4 of 6 possible measures). Palmer and co-workers concluded that Gadolinium-enhanced MRI and [18F]FDG PET allow for the quantification of volumetric and metabolic changes in synovitis and the comparison of efficacies of anti-inflammatory treatments [36].

Expanding on this previous study, Beckers and co-workers investigated the ability of [18F]FDG PET to detect synovitis and quantify its metabolic activity in 21 RA patients, as compared to standard measures of disease activity [37]. In a joint-by-joint analysis, PET findings were found to significantly correlate with those of regional clinical (swelling and tenderness) and sonographic assessments. Furthermore, both the degree of PET positivity (visual analysis) and mean standardized uptake values (SUVs) were found to increase with synovial thickness in all joints (except metatarsophalangeal-1 joints), as measured by ultrasound (US), and the number of clinical or US parameters present simultaneously. On an individual patient level, strong correlations were additionally cited for PET-derived parameters (number of PET-positive joints and cumulative SUV) and disease duration as well as global measures of disease activity, including clinical joint counts for swelling and tenderness, erythrocyte sedimentation rate (ESR) and C-reactive protein (CRP) serum levels, the patient and physician global assessments, the disease activity score and the simplified disease activity index, and US-derived. Based upon these findings, the authors suggest that [18F]FDG PET offers unique information concerning the metabolic activity of synovitis specific to each patient.

According to Brenner *et al.*, these findings, while promising, do not necessarily procure a role for [18F]FDG PET in the routine clinical assessment of RA patients [38]. As a relatively costly technique, [18F]FDG PET must provide clinically relevant data that cannot be obtained from standard clinical and laboratory measures of disease activity to have a broader application in the study of RA. Consequently, evidencing the capacity of [18F]FDG PET to monitor disease activity and response to treatment is of particular importance. In another study by Beckers *et al.*, 16 RA patients underwent clinical and biological evaluation, dynamic Gadolinium-enhanced MRI, US, and [18F]FDG PET imaging of knee joints at baseline and after 4 weeks of anti-TNF-α treatment [39]. Consistent with previous studies, SUVs were significantly correlated with all MRI-derived parameters, synovial thickness, and serum levels of matrix metalloproteinase (MMP) 3 and CRP [35, 37]. PET-positive knee joints were determined to have higher SUVs, MRI parameters, and greater synovial thickness as measured by US than PET-negative knee joints.

While a number of studies have shown that [18F]FDG PET is capable of detecting treatment-related changes in disease activity, very few have investigated whether PET findings can predict clinical outcomes early in the course of treatment [36, 39, 40]. In a small explorative study with 16 RA patients, Elzinga and colleagues demonstrated that early changes in regional [18F]FDG uptake in the joints of RA patients undergoing anti-TNF-α (infliximab) treatment were representative of later changes in global disease activity, as assessed clinically [41]. While these findings support the notion that [18F]FDG PET allows for the sensitive detection of early changes in disease activity that are

highly predictive of subsequent responses to treatment, larger studies are needed to confirm.

Although these results are already promising, new advances in PET technology, including multimodal image co-registration, may serve to enhance the utility of this imaging technique in the study of RA. In particular, PET/CT hybrid acquisition offers higher spatial resolution and simultaneous integration of morphologic and functional data and thus has rapidly become standard clinic protocol. Despite these advantages, only a limited number of studies have evaluated this technology in RA patients. For example, in a case study by Vogel *et al.*, [^{18}F]FDG PET/CT was reported to not only have the capability of calculating the degree of inflammation in the tarsus of an RA patient, but also precisely localizing the disease activity to the particular joints causing the complaints [42]. Contrastingly, neither physical examination nor conventional radiography could offer this information. Due to the involvement of multiple joints, as visualized by [^{18}F]FDG PET/CT, a triple arthrodesis of the tarsus was performed, with successful pain reduction, demonstrating that this imaging technique provides clinically relevant information that can be utilized in patient management. Additional case studies have demonstrated that [^{18}F]FDG PET/CT accurately detects extra-articular inflammatory sites such as subcutaneous nodules and hypermetabolic lymph nodes and synovitis of the atlanto-axial and knee joints [43-45]. Furthermore, although not substantiated, it is plausible that PET/CT allows for improved discrimination between juxta-articular disease and articular processes. Goerres *et al.* did note that PET imaging alone was able to delineate inflammation of the tendon sheaths and bursae [40], but mild cases may not be apparent due to the low spatial resolution of dedicated PET scanners. Having an anatomic framework, as is provided with PET/CT, may help in the evaluation of these cases.

Of particular interest, Kubota and colleagues reported that whole-body [^{18}F]FDG PET/CT imaging accurately and sensitively reflected the metabolic disease activity and joint anatomy in 14 patients with active RA and 4 patients in remission [46, 47]. More specifically, [^{18}F]FDG joint uptake, total joint score, global SUV_{max}, and the mean number of joints with at least a moderate uptake of [^{18}F]FDG were significantly higher for patients with active disease as compared to those in remission. Additionally, painful/swollen joints had a higher [^{18}F]FDG uptake score and SUV_{max} than did clinically uninvolved joints. A representative [^{18}F]FDG PET/CT image of a patient with recurrent RA can be seen in **Figure 2**, showing increased radiotracer uptake in multiple large joints and clearly delineating inflammatory foci (**Figure 2A**). While the wrist, elbow, and knee joints could be easily interpreted as PET positive, more complicated large joints such as the hip and shoulder require PET images with anatomical correlation to CT findings, as increased FDG uptake by enthesopathies must be differentiated from synovitis arising from RA (**Figures 2B** and **2C**). To compare, a conventional bone scan only showed mild arthritic changes in the large joints of the same patient, suggesting that this modality is not as sensitive as [^{18}F]FDG PET/CT (**Figure 2D**).

CT correlation was also necessary for interpretation of findings in the atlanto-axial joint. As compression of the spinal cord and brainstem are potentially serious complications of the involvement of the atlanto-axial joint in RA patients, early detection of this high-risk lesion is clinically important. In this study, 28% (5/18) of the RA patients exhibited increased [^{18}F]FDG uptake in the atlanto-axial joint, but most were asymptomatic. The authors speculated that these hypermetabolic lesions are most likely indicative of active subclinical synovitis. This finding is consistent with that of other studies, which have found that there is a high prevalence of asymptomatic cervical spine subluxation in this patient population [44, 48]. [^{18}F]FDG PET/CT may thus allow for the early identification of patients at risk for developing subluxation of the atlanto-axial joint. In addition, this imaging technique may have prognostic value for a more severe disease course in RA patients, as it has been reported that the presence of arthritis in large joints, particularly arthritis in the knee joint, is predictive of a destructive disease course [49]. Overall, whole-body [^{18}F]FDG PET/CT has the advantage of allowing for the accurate assessment of the extent and severity of the disease even at subclinical levels.

In addition to PET/CT, PET/MRI technology has also been studied in RA patients. As this technology has only recently been developed, the distribution of dedicated PET/MRI scanners is fairly limited. Co-registered PET/MRI hybrid acquisition, however, is rapidly becoming an important nuclear medicine strategy. Chaudhari and colleagues showed that this technology

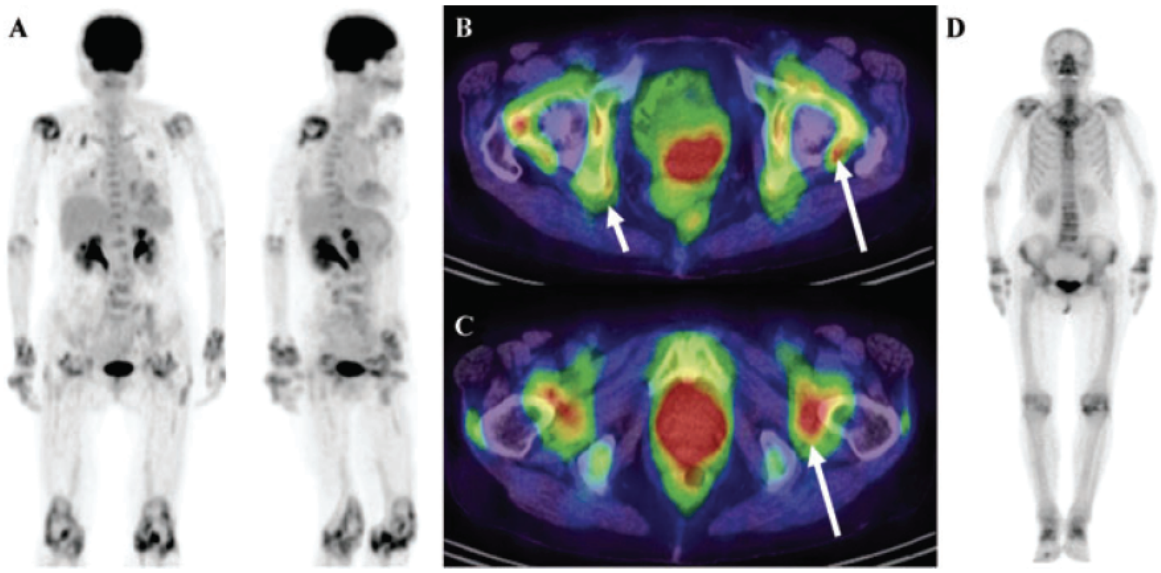

Figure 2. A 74-year-old woman with 3.5-year history of RA who experienced a recurrence and was being considered for infliximab therapy. (A) Anterior and RAO MIP image obtained using FDG-PET/CT shows typical RA lesions in the large joints. (B and C) Axial PET/CT fusion image of the hip joint in the same patient. The large arrows indicate synovitis in the acetabulum and femoral head. The small arrows indicate enthesopathies at the ischium and greater trochanter (D) Bone scan of the same patient shows mild changes in the joints. (Reprinted from Kubota K, Ito K, Morooka M, Minamimoto R, Miyata Y, Yamashita H, Takahashi Y and Mimori A. FDG PET for rheumatoid arthritis: basic considerations and whole-body PET/CT. Ann NY Acad Sci 2011; 1228: 29-38; by permission of John Wiley and Sons).

could be employed to monitor the early response to anti-TNF-α therapy in the wrist joint of an RA patient [50]. This study, however, did not use a fully integrated PET/MRI system. Instead, the patient underwent extremity [^{18}F]FDG PET/CT imaging separately following MR image acquisition; the CT image was used for post-acquisition PET/MRI image co-registration. While this study demonstrates the capability of this technology, it does not showcase its complete range of advantages. Since using separate PET/CT and MRI scanners does not allow for simultaneous acquisition of image data, there is room for spatial and temporal misalignment between PET and MRI images. In comparison, dedicated PET/MRI scanners greatly reduce these artifacts through simultaneous acquisition of PET and MRI data without sacrificing sensitivity or spatial resolution. While they did not specifically evaluate an RA patient, El-Haddad and co-workers used a fully integrated PET/MRI scanner in a case study to accurately delineate a meniscal tear associated with synovitis [51].

To date, there has only been one study that has successfully performed a true hybrid PET/MRI examination of an RA patient. In a recent study by Miese *et al.*, a patient with early RA underwent simultaneous PET/MRI scanning of the hand using a prototype of an APD-based magneto-insensitive Brain PET detector (Siemens Healthcare, Erlangen, Germany) operated within a standard 3T MR scanner (MAGNETOM Trio, Siemens) [52]. Increased [^{18}F]FDG uptake was noted surrounding the metacarpophalangeal (MCP) II and III joints, which corresponded to sites of synovitis and tenovaginitis as identified on contrast-enhanced MRI (**Figure 3**). A maximum SUV of 3.1 was measured for the palmar portion of MCP II, which was shown to correlate with marked synovial thickening and contrast enhancement on MRI. No significant [^{18}]FDG uptake was seen within the joint spaces or bony structures. Contrastingly, conventional radiographic evaluation was determined to be negative. These results suggest that [^{18}F]FDG PET/MRI is a potentially useful tool in the early diagnosis of RA.

[^{11}C]Choline

Choline is a water-soluble essential nutrient that functions as a neurotransmitter (upon acetyla-

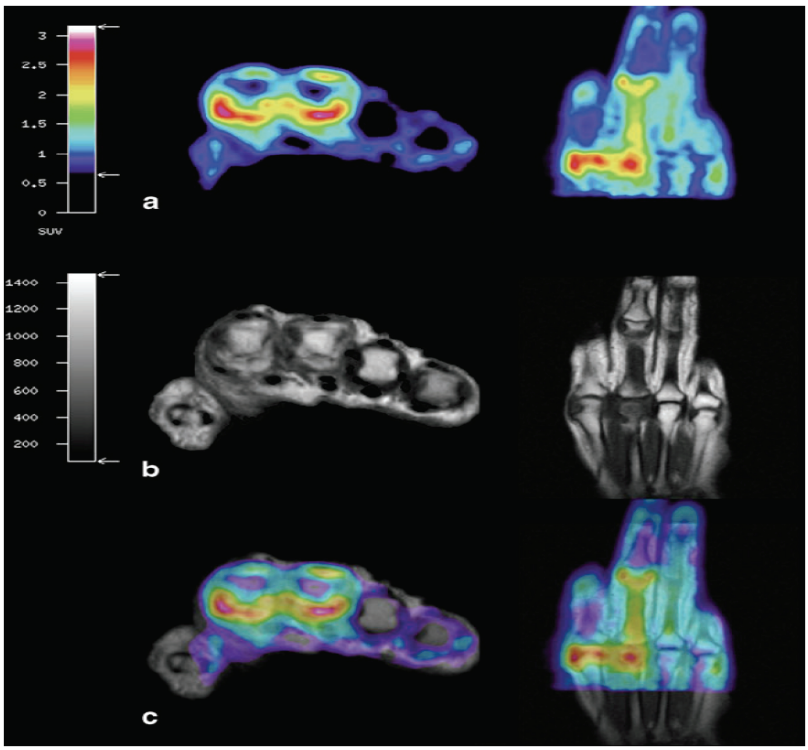

Figure 3. Hybrid ^{18}F-FDG PET–MRI of the hand in early RA. a axial and coronal display of PET co-registered with b axial and coronal T1-weighted MRI. c True hybrid ^{18}F-FDG PET–MRI of the hand. (Reprinted with kind permission from Springer Science+Business Media: Miese F, Scherer A, Ostendorf B, Heinzel A, Lanzman RS, Kropil P, Blondin D, Hautzel H, Wittsack HJ, Schneider M, Antoch G, Herzog H and Shah NJ. Hybrid ^{18}F-FDG PET-MRI of the hand in rheumatoid arthritis: initial results. Clin Rheumatol 2011; 30: 1247-1250, Figure 1).

tion to acetylcholine in cholinergic nerve endings), a methyl group donor (through degradation to its primary metabolite, betaine), and a precursor to phospholipids (the main constituent of all eukaryotic cell membranes) [53]. Free choline is taken up by dividing cells and predominantly phosphorylated by choline kinase to phosphorylcholine, in the first step of the cytidine diphosphocholine (CDP) pathway [53]. This commits choline to the biosynthesis of phospholipids, particularly phosphatidylcholine (lecithin), and integration into eukaryotic cell membranes. Previous studies have determined that rapidly dividing cells, and their greater need for cell membrane components as compared to normal tissues, result in increased choline uptake through energy-dependent choline specific transport mechanisms and simple diffusion secondary to hyperemia and hyperperfusion [54-56]. Consequently, choline, when radiolabeled with carbon-11, can serve as an *in vivo* biomarker of cellular proliferation.

[^{11}C]Choline PET imaging has been shown to clearly delineate various brain tumors, lymph node metastases of esophageal cancer, and lung carcinoma [57-62]. Due to the minimal renal excretion of [^{11}C]choline, the primary indication for this imaging procedure is the detection and staging of prostate cancer and other cancers of the urogenital tract (bladder and uterine cancer) [63, 64]. Non-neoplastic applications are currently under investigation, as the rate of [^{11}C]choline uptake in tissues solely correlates with the level of cellular growth, irrespective of histologic grade [59]. Since arthritic pannus and nearby vessels undergo similar proliferative changes to those exhibited during malignant transformation, it was hypothesized that [^{11}C]choline PET could be utilized in the assessment of RA and other arthritic diseases.

Roivainen and co-workers evaluated the capacity of [^{11}C]choline PET to detect and quantify arthritic synovial proliferation by imaging the joints of 10 patients with synovitis and comparing the results with [^{18}F]FDG PET and Gadolinium-DTPA (Gd-DTPA)-enhanced MRI findings [65]. In particular, maximum standardized uptake values (SUV_{max}) and kinetic influx constants (K_i), as obtained from the graphic analysis described by Patlak *et al.*, were calculated for both PET radiotracers and compared to MRI parameters (synovial volume and rate of enhancement) [66]. In all patients, the PET signal intensities for [^{11}C]choline and[^{18}F]FDG were significantly

increased in diseased synovia, in contrast to clinically unaffected joints. Similarly, when visually compared to coronal Gd-DTPA-enhanced T1-weighted MR images, regions of highest [^{18}F] FDG and [^{11}C]choline signal on PET coincided well with contrast-enhanced hypertrophic synovial tissue (pannus). From these findings, the authors suggested a possible role for [^{11}C] choline PET in the functional imaging of RA.

A clear advantage of [^{11}C]choline PET is the ability to quantitatively measure reproducible disease activity parameters through SUV_{max} and/or graphic analysis. Similar standardized uptake values of [^{11}C]choline to those measured in Roivainen *et al.* [65] were obtained in a later study by the same group [67]. Moreover, due to the short half-life of carbon-11, [^{11}C]choline delivers a relatively low radiation burden to the patient [68]. Finally, as [^{11}C]choline can only be synthesized at facilities equipped with on-site cyclotrons, effectively limiting its broader distribution and application, [^{18}F]choline is currently under development. To date, however, there have not been any pre-clinical or clinical studies that have evaluated its efficacy in imaging RA or other arthritic diseases [69].

(R)-[^{11}C]PK11195

While both [^{18}F]FDG and [^{11}C]choline are sensitive to changes in cellular proliferation, their uptake is not specific to inflammation; normal physiologic variants, malignancy, infection, and other benign pathological processes can result in hypermetabolic PET lesions. For this reason, there is an increasing need for PET radiotracers that allow for more specific visualization of rheumatoid synovial tissue through direct targeting of underlying inflammatory pathways. Due to the cardinal role of macrophage infiltration in the propagation and extension of RA, radiotracers that target this process are of special interest. *(R)*-[^{11}C]PK11195 is a recently developed isoquinolone carboxamide PET radiotracer that targets cells of the monocyte-macrophage lineage by selectively binding as an antagonist to the peripheral benzodiazepine receptor (PBR), or newly renamed translocator protein (TSPO) [70-73]. TSPO is an 18 kDa protein that is expressed on the outer mitochondrial membrane- and to a lesser extent nucleus and plasma membrane- of mononuclear phagocytes, other leukocyte subsets, peripheral organs, and neuronal, hematopoietic, and lymphatic tissues [71, 73-76]. While TSPO was originally discovered as a second high-affinity binding site for benzodiazepines, particularly diazepam, it has since been determined that this transmembrane protein serves many functions; more specifically, TSPO is thought to be a component of the trimeric mitochondrial permeability transition pore (MPTP) and play a role in the regulation of steroidogenesis and apoptosis, heme biosynthesis, cell proliferation, and immune regulation [73, 75-79].

Since activated macrophages and polymononuclear cells upregulate TSPO during inflammation, TSPO-targeting radiotracers can serve as surrogate markers for disease activity and macrophage recruitment to inflammatory foci. This imaging technique has been validated for the assessment of various inflammatory neurological disorders; in particular, *(R)*-[^{11}C] PK11195 PET imaging allows for the differentiation of neuroinflammatory lesions from normal tissues by mapping out glial cell activation and recruitment [80-82]. van der Laken and coworkers were the first to extend the application of *(R)*-[^{11}C]PK11195 PET to the study of RA by comparing the imaging findings for 11 RA patients and 8 healthy controls to clinical data and immunohistochemical analysis of excised synovial tissue samples [83]. *(R)*-[^{11}C]PK11195 uptake correlated well with clinical severity of synovitis. Severely inflamed joints exhibited the highest accumulation of *(R)*-[^{11}C] followed by mild to moderately inflamed joints. Uptake values for these joints were, on average, significantly higher than those for clinically uninflamed and control joints, which intimates that *(R)*-[^{11}C]PK11195 imaging is sensitive in its detection of both severe and moderate inflammation. The increased PET signal in inflamed joints was determined to be a consequence of specific PBR-mediated uptake of *(R)*-[^{11}C]PK11195 by activated macrophages, as confirmed by immunohistochemical staining of synovial tissues. Accordingly, severely inflamed joints demonstrated the highest degree of macrophage recruitment and PBR expression. In comparison, control knee joints of healthy volunteers displayed minimal PBR expression and macrophage infiltration, and, concomitantly, no significant accumulation of radioactivity on PET.

Of interest, though not confirmed in this study, van der Laken and colleagues conjectured that *(R)*-[^{11}C]PK11195 PET imaging may detect sub-

clinical synovitis [83]. In support of this hypothesis, mean SUV ratios for clinically uninflamed joints in RA patients were noted to be approximately 50% higher ($P<0.05$) than those of control joints in healthy volunteers. These findings are consistent with those of previous studies that have established that macrophage infiltration into synovial joints is a common feature of asymptomatic synovitis in early RA [13, 14]. Furthermore, as the presence and number of macrophages in rheumatoid synovia correlate with the progression of radiographic joint erosions, the application of *(R)*-[^{11}C]PK11195 imaging to RA may prove to be relevant to patient management.

Gent and co-workers recently confirmed that *(R)*-[^{11}C]PK11195 PET can observe subclinical synovitis in arthralgia patients [84]. In this prospective pilot study, high resolution *(R)*-[^{11}C]PK11195 images of the metacarpophalangeal (MCP), proximal interphalangeal (PIP), and wrist joints of 29 seropositive arthralgia patients, 6 healthy volunteers (negative controls), and 3 patients with established RA (positive controls) were acquired and subsequently scored semi-quantitatively for joint uptake minus background activity by 2 independent readers. Patients were followed prospectively for 24 months to determine progression to RA. Four of 29 arthralgia patients (i.e. 4 of the 9 arthralgia patients that progressed to RA) were determined to have PET positive scans with moderate to high radiotracer uptake in the joints of 3 of these patients. To compare, healthy volunteers did not exhibit any PET positive joints while significant *(R)*-[^{11}C]PK11195 accumulation was noted in all clinically involved joints of RA patients. During the follow-up period, all four subjects with PET positive scans showed progression and developed clinical arthritis in at least 1 MCP, PIP, and/or wrist joint(s). Unexpectedly, five patients with negative scans developed clinical synovitis within 24 months. Incongruent PET and clinical findings in 3 of these patients were easily explained by the fact that the newly diagnosed arthritic lesions were not present in the hands and wrists. Since the researchers used a small animal and human brain 3D PET scanner for image acquisition, the field of view (FOV) was not large enough to allow visualization of joints beyond the hands and wrists. The remaining 2 arthralgia patients that developed arthritis, despite having negative PET scans, only showed subtle signs of disease activity throughout the follow-up period, and 1 of these patients even entered remission spontaneously at 10 months.

There are also drawbacks to using *(R)*-[^{11}C]PK11195 however. Although the absolute standardized uptake values of *(R)*-[^{11}C]PK11195 in arthritic joints are comparable to those reported for [^{18}F]FDG, high non-specific binding of this radiotracer in hand muscles, soft tissues surrounding the nails, and bone marrow greatly reduces signal-to-noise ratios [83, 84]. High physiologic uptake has also been noted in the kidneys, lungs, liver, and heart [85-87]. This, in turn, could limit the detection of mild arthritic lesions. Although not evaluated in the trial of Gent *et al*. [84], it is important to note that co-registration of PET and CT scan images, which is the current standard clinical protocol, may allow for the accurate differentiation between articular and peri-articular uptake of *(R)*-[^{11}C]PK11195 by providing accurate anatomic localization. In addition, this radiopharmaceutical is not ideal for imaging, as it has low bioavailability, high plasma protein binding, high lipophilicity, and a relatively low binding affinity (K_i=1-4 nM) [85, 88, 89]. Consequently, numerous TPSO-targeting radiotracers with improved imaging properties are currently under development [90]. Such probes that have entered pre-clinical and clinical trials include [^{11}C]DPA-713, [^{11}C]DAA1106, [^{11}C]PBR28, [^{11}C]AC-5216, [^{18}F]PBR06, [^{18}F]DPA-714, and [^{18}F]FEDAA1106 [89, 91-100]. As ligands labeled with fluorine-18 have a longer half-life than their carbon-11 labeled counterparts, they are favored moving forward with this imaging strategy.

Scintigraphy and SPECT imaging

Non-specific Imaging Agents

[^{67}Ga]Citrate

[^{67}Ga]citrate (Neoscan®) is a well-characterized non-conjugated γ-emitting radiotracer that localizes in acute and chronic inflammatory, infectious, and neoplastic lesions. Upon intravenous administration, cationic $^{67}Ga^{3+}$, similar in behavior to the ferric ion, binds to circulating blood plasma proteins, such as transferrin and ferritin, and to a minority of leukocytes [101-103]. The resultant ^{67}Ga-bound protein complex, and to a minor extent, free and neutrophil-associated [^{67}Ga]citrate, extravascates increas-

ingly at sites of inflammation due to locally augmented microvascular permeability and expanded extracellular diffusion space [102, 104-107]. As there is limited reabsorption of macromolecules at these sites, [^{67}Ga]citrate progressively accumulates in inflammatory foci, including rheumatoid synovia. Following the trapping of ^{67}Ga-bound macromolecules in the inflammatory interstitial space, transchelation of ^{67}Ga to lactoferrin, ferritin, and/or bacterial siderophores may occur [101, 102, 108, 109]. The enhanced neutrophil secretion of lactoferrin in synovial fluid, and expression of ferritin in inflamed synovia are additional mechanisms by which [^{67}Ga]citrate concentrates in these tissues [102]. Although not as well-supported in the literature, transferrin receptor-mediated endocytosis of the [^{67}Ga]citrate-transferrin complex by synovial macrophages may play a partial role in the localization of this radiotracer in affected joints of RA patients [103, 110]. This mechanism is currently under review, serving as the rationale for the development of new ^{99m}Tc-labeled conjugated transferrin probes [111].

While it is well-documented that [^{67}Ga]citrate scintigraphy is a sensitive imaging technique for inflammation, there are several disadvantages that preclude its widespread use in the evaluation of RA patients. In particular, due to its release of high-energy γ radiation (91-393 keV) and long physical half-life ($t_{1/2}$= 78.3 hours), ^{67}Ga imposes a relatively high radiation burden on patients [112]. Moreover, similar to other radiolabeled macromolecules, [^{67}Ga]citrate has a slow plasma clearance when bound to serum proteins. Slow blood clearance is unfavorable because it results in high background activity and longer acquisition times so as to attain optimal target-to-background ratios [103, 113]. Further limiting the clinical application of [^{67}Ga]citrate is its lack of specificity. Although [^{67}Ga]citrate imaging is able to sensitively detect RA disease activity and extent, it cannot accurately distinguish active inflammation from infection or even neoplasm [103, 114-116]. Therefore, [^{67}Ga]citrate scintigraphy has been relegated to a secondary role in imaging patients with RA as well as other inflammatory and infectious diseases.

[^{99m}Tc]- and [^{111}In]HIG

Polyclonal human immunoglobulin G (HIG) is a non-antigen IgG antibody that when labeled with either ^{99m}Tc or ^{111}In behaves as a biomarker for infection and inflammation. HIG scintigraphy is an inexpensive, accessible tool that allows visualization of inflammatory foci, and thus, its use has been widely explored in RA. A number of studies have indicated that this imaging technique detects local joint inflammation in RA patients with a higher sensitivity than that of clinical examination, conventional bone scanning, and leukocyte scintigraphy [117-119]. Pons and co-workers found a correlation between articular HIG uptake, as assessed visually and quantitatively, and clinical scores for swelling, suggesting that HIG scintigraphic findings accurately reflect disease severity [120]. Furthermore, highlighting its prognostic value, a study by de Bois *et al.* demonstrated that this imaging strategy is able to predict progression to RA in arthralgia patients [121]. Similar to [^{67}Ga]citrate, however, HIG is a non-specific marker for inflammation. It accumulates at sites of inflammation due to a local increase in vascular permeability and diffusion space, and hyperemia [122]. Consequently, HIG scintigraphy is only of limited clinical relevance. For example, it is incapable of distinguishing between joints with active disease and those with inflammation from secondary joint destruction. It also has no utility in evidence-based biologic therapy. HIG imaging is sensitive, but its non-specificity has greatly diminished its clinical role, as newer radiopharmaceuticals with higher specificity have been developed.

[^{99m}Tc]Diphosphonates

Unlike previous radiotracers, ^{99m}Tc-labeled diphosphonate analogs, such as methylene diphosphonate (MDP), hydroxy methylene diphosphonate (HDP), and dicarboxy propane diphosphonate (DPD), are not primarily inflammation-seeking agents. Instead, their uptake reflects alterations in bone metabolism, especially increased obsteoblastic activity occurring in response to underlying pathology. Conventional bone scintigraphy has shown some utility in the evaluation of RA, as it allows localization of arthritic joints and provides functional and quantitative information about disease activity [123-125]. Three-phase bone scanning (blood flow phase, immediate blood pool phase, and delayed imaging phase) may allow detection of acute RA. Blood flow and blood pooling phases typically exhibit increased uptake secondary to hyperemia and augmented microvascular per-

meability (same vascular changes as those in surrounding inflamed synovium) during the acute phase of RA [126]. In addition, delayed images demonstrate higher radiotracer deposition in diseased juxta-articular bone, reflecting increased bone turnover and remodeling in response to joint inflammation and cartilage destruction [126]. This technique, while a sensitive tool in identifying osseous changes, is not specific for RA and lacks the spatial resolution of radiography or MRI [127]. Moreover, as ^{99m}Tc -labeled diphosphonates accumulate to a variable degree in all joints, differentiation between normal bone and juxta-articular physiologic uptake and mild arthritic changes is difficult [128]. As a further disadvantage, bone scintigraphy cannot reliably differentiate between active disease and inflammation in chronically damaged joints [128, 129].

To improve the sensitivity, spatial resolution, and overall image quality of this approach, Ostendorf and colleagues evaluated and compared [^{99m}Tc]DPD multi-pinhole SPECT (MPH-SPECT) to conventional bone scintigraphy and MRI for the detection of bone changes in 13 patients with early RA and 9 patients with early osteoarthritis (OA) [130]. Recently developed MPH-SPECT systems have been previously shown to have a 50-fold increased sensitivity and spatial resolution of less than 1 mm as a consequence of their inclusion of collimators that have up to 20 pinholes [131, 132]. In the Ostendorf *et al*. study, MPH-SPECT, in comparison to conventional bone scanning, demonstrated better radiotracer localization and spatial resolution and was able to detect a greater number of diseased joints [130]. As 10 of 13 RA patients had a central tracer distribution and 7 of 9 OA patients had an eccentric pattern, the authors suggested that this distinction may have relevance to our understanding of RA pathogenesis. Furthermore, the sensitivity of this technique was found to be comparable to that of MRI. Hybrid SPECT/CT also allows for fusion of functional and anatomic information, but despite these advancements in tomographic technology, bone scanning has mainly been superseded by other imaging techniques for the assessment of RA patients.

[^{99m}Tc]- and [^{111}In]-labeled Leukocytes

Directly labeling autologous leukocytes with [^{99m}Tc]hexamethylpropylene amine oxime ([^{99m}Tc]HMPAO) or [^{111}In]oxine, radiolabeled complexes that easily penetrate cell membranes and become trapped intracellularly as a result of their high lipophilicity and charge neutrality, is in wide clinical use for the evaluation of a number of infectious and inflammatory diseases [133, 134]. As mononuclear cells and neutrophils are highly recruited to inflamed synovial tissue and fluid, respectively, leukocyte imaging has been described for use in RA. In a preliminary study, Gaál and co-workers found a significant correlation ($P<0.01$) between the global scores for [^{99m}Tc]HMPAO-labeled neutrophil accumulation in the hands and feet of 21 RA patients and the number of clinically swollen joints [135]. The authors concluded that leukocyte scintigraphy or SPECT is an inexpensive and widely available tool that can be utilized in the localization and estimation of synovitis in RA. Al-Janabi and co-workers additionally demonstrated that this imaging technique is sensitive to alterations in disease activity following treatment with intra-articular steroid injections [136]. Autologous monocytes have also been successfully labeled with [^{99m}Tc]HMPAO and assessed in RA [134, 137]. Thurlings and colleagues reported that [^{99m}Tc]HMPAO-labeled monocyte scintigrahpic findings positively correlate with the swollen joint count and number of macrophages, as confirmed by immunohistochemical staining, in biopsied synovial tissue from 8 RA patients [138]. While it is clear that radiolabeled leukocyte joint scintigraphy allows delineation of inflammation and distribution of disease with high sensitivity, it lacks specificity for RA, ultimately limiting its clinical utility.

Specific imaging agents

[^{99m}Tc]J001X

To improve specificity, receptor-specific radiolabeled probes that indirectly track leukocyte migration and recirculation in chronic inflammatory diseases have been developed. As discussed earlier, radiotracers that target macrophages are of interest because this cell subpopulation is highly recruited to rheumatoid synovia and plays a critical role in the inflammatory process. *In vitro* studies have shown that macrophages specifically bind to bacterial proteoglycans, providing a rationale for the use of radiolabeled proteoglycan derivatives in macrophage scintigraphy [139-141]. J001X, a 34 kDa acylated poly-(1,3)-$_D$-galactoside isolated from

membrane proteoglycans of a non-pathogenic strain of *Klebsiella pneumoniae*, is a newly designed probe that when coupled with ^{99m}Tc allows the visualization of mononuclear phagocyte trafficking [142, 143]. Although similar in structure to the immunogenic bacterial lipopolysaccharide (LPS), J001X has been greatly modified to not trigger phagocytic activation, while still retaining its specificity for cells of the monocyte-macrophage lineage [139, 140, 144]. CD14 (a glycosylphosphoinositol-anchored LPS receptor found on macrophages and neutrophils) and CD11b (the α-chain of the complement receptor-3 (CD11b/CD18) β_2 leukocyte integrin expressed on mononuclear phagocytes, granulocytes, and NK cells) mediate this specific receptor-ligand interaction [143, 145].

The imaging potential of [^{99m}Tc]J001X scintigraphy has been widely explored for numerous tumoral, inflammatory, and infectious processes in both human patients and experimental animal models. [^{99m}Tc]J001X scintigraphy has successfully delineated alveolitis and mediastinal berylliotic lymph nodes in baboons; acute localized radiation changes in pigs; pyrogranulomas in sheep; and osteoarthritic lesions induced by severance of cruciate ligaments in rabbits [146-150]. Similarly in humans, macrophage imaging with [^{99m}Tc]J001X, administered as an aerosol, was able to localize inflammatory lesions in sarcoidosis and scleroderma [151]. The assessment of pulmonary involvement in RA patients was explored as a possible application of [^{99m}Tc]J001X scintigraphy, but with mixed results [152]; scintigraphic findings were incompatible with those from high-resolution CT, pulmonary function tests, and bronchoalveolar lavage.

Of interest for purposes of studying RA, this nuclear medicine technique has been investigated in an antigen-induced arthritis model in rabbits [153]. Scintigraphic images demonstrated [^{99m}Tc]J001X focal uptake in active arthritic lesions with high contrast to normal tissues. In comparison, these same inflammatory lesions could not be clearly discerned with [^{99m}Tc]O_4^- and [^{99m}Tc]albumin nanocolloids due to a lower scintigraphic contrast, despite the increased uptake of these non-specific agents in the acute phase of the disease. Furthermore, at the advanced disease stage when non-specific inflammatory processes were normalized, uptake of radiolabeled nanocolloids was minimal while [^{99m}Tc]J001X scans remained positive for macrophage infiltration. These results support previous conclusions that [^{99m}Tc]J001X scintigraphy can serve as a functional imaging strategy that directly reflects the extent of macrophage recruitment and thus evolves with disease activity. To justify the use of this imaging technique in future RA clinical trials, the authors optimized the labeling procedure for the intravenously injectable formulation of [^{99m}Tc]J001X [153, 154]. While this study offers promising results, no clinical trials have been performed to determine the efficacy of [^{99m}Tc]J001X scintigraphy in diagnosing early RA and monitoring disease activity and treatment response to date.

[^{99m}Tc]RP128

Like [^{99m}Tc]J001X, [^{99m}Tc]RP128 scintigraphy visualizes leukocyte recruitment, a process critical for sustaining RA and other inflammatory diseases. RP128, a bifunctional peptide chelate, specifically targets neutrophils and mononuclear phagocytes by binding to receptors expressed on the surface of these cell subpopulations [155]. As a general mechanism, the targeting domain of [^{99m}Tc]RP128, an antagonistic pentapeptide tuftsin analogue (TKPPR), mediates the receptor-specific interaction and binds to tuftsin receptors with a fourfold greater affinity than does their endogenous ligand, tuftsin [156]. Tuftsin is a tetrapeptide (TKPR) derived from proteolytic cleavage of the Fc domain of the heavy chain of IgG that promotes chemotaxis and phagocytosis of its target cells [157]. Tuftsin receptors, as mediators of these key immune functions, represent important molecular targets, and their upregulation in activated macrophages serves as the basis for [^{99m}Tc]RP128 imaging.

Despite promising pre-clinical studies that have cited a positive correlation between [^{99m}Tc]RP128 uptake and quantitative measures of inflammation, there has only been one study that investigated the utility of [^{99m}Tc]RP128 scintigraphy in imaging RA patients. In a Phase I study, Caveliers and co-workers simultaneously evaluated the safety, normal biodistribution, and dosimetry in 8 healthy controls, and the validity of employing [^{99m}Tc]RP128 as a probe to delineate inflamed synovia in 10 RA patients [155]. The biodistribution study favorably revealed low radiotracer uptake in all major organs, except in the kidneys and bladder and, to a lesser extent, the synovia of several joints.

Due to the slower washout of articular activity and low background noise, synovial joints in all subjects could be clearly discerned. The accumulation of [^{99m}Tc]RP128 in normal joints, however, was moderate in comparison to the markedly increased uptake observed in a large number of clinically affected joints in RA patients. Consequently, [^{99m}Tc]RP128 scintigraphy was able to detect inflammatory lesions in RA patients with a sensitivity of 69% for swollen joints, 76% for painful joints, and 73% for joints with bone erosions. Unfortunately, as synovial biopsies were not performed in this study, accuracy of the results could not be confirmed and further evaluation of this radiotracer is needed.

[^{99m}Tc]- and [^{111}In]anti-E-selectin

Another strategy to visualize the continuous leukocyte recruitment and infiltration into inflamed synovium involves targeting cell adhesion molecules (CAMs). CAMs are responsible for the binding of leukocytes to activated endothelial vasculature as well as their subsequent transendothelial migration [158, 159]. While various adhesion molecules have served as targets for therapeutic intervention and imaging in other inflammatory diseases, E-selectin is the only one to be successfully described in the molecular imaging of RA. E-selectin (CD62E, ELAM-1) is a transmembrane glycoprotein that is transiently expressed on the luminal surface of activated vascular endothelium during a normal inflammatory response [24]. Following induction by interleukin-1 (IL-1), tumor necrosis factor-α (TNF-α), and bacterial LPS, E-selectin mediates the initial tethering and rolling of granulocytes, monocytes, and some lymphocytes, via specific interactions with its carbohydrate-based ligands [24, 158-161]. E-selectin is a potentially useful target for the detection of synovitis, because while this molecule is not expressed in resting endothelium, there is increasing evidence that its upregulation in postcapillary venules helps promote the sustained influx of leukocytes into inflamed tissues in RA [162-167]. As an added advantage, E-selectin is directly accessible to intravenously administered agents due to its location on the luminal surface of blood vessels.

[^{111}In]1.2B6 monoclonal antibody (mAb), an indium-labeled murine IgG_1 antibody that recognizes human E-selectin, was first validated for *in vivo* imaging of synovitis in porcine models of arthritis in 1994 [168, 169]. [^{111}In]1.2B6 mAb was shown to immunolocalize to activated endothelial venules in inflamed synovia and regional draining lymph nodes with better sensitivity and specificity than radiolabeled control IgG_1 antibody. Although these early, preclinical studies offered promising results, concerns were raised over the immunogenicity of this radiopharmaceutical. Due to its murine origin, 1.2B6 mAb has the potential to elicit a human anti-mouse antibody (HAMA) response, limiting long-term repeat follow-up imaging with this radiotracer. Furthermore, 1.2B6 mAb has intact Fc regions, which are thought to generate host immunity through non-specific activation of Fc-γ receptor-bearing effector cells. To reduce the likelihood of these clinical complications, researchers elected to study $F(ab')_2$ fragments of 1.2B6 mAb, devoid of its Fc portions. A number of animal studies have validated this substitution [170, 171]. Preliminary clinical studies corroborated these earlier works, demonstrating that [^{111}In]1.2B6 $F(ab')_2$ scintigraphy allows for clear visualization of inflamed joints in RA patients through radioimmunodetection of activated vascular endothelium, as early as 4 hours and optimally at 24 hours post-injection [172, 173]. In addition, this imaging technique was shown to be superior to both ^{111}In- and ^{99m}Tc-labeled HIG scintigraphy in terms of sensitivity, specificity, lower background activity, higher radiotracer uptake, and better image contrast. However, due to the higher radiation burden imparted to the patient and lower spatial resolution of ^{111}In-labeled radiopharmaceuticals, a ^{99m}Tc-labeled anti-E-selectin radiotracer was subsequently developed and tested in RA patients.

In a two part study, Jamar and colleagues evaluated the validity of using [^{99m}Tc]1.2B6 Fab fragments in RA patients as compared to [^{111}In] 1.2B6 $F(ab')_2$ and [^{99m}Tc]HDP [128]. For the double-isotope comparative study, planar images were acquired 4 and 20-24 hours following administration of either [^{111}In]1.2B6 $F(ab')_2$ or [^{99m}Tc]1.2B6 Fab in 10 RA patients and 2 healthy volunteers. Additionally, 16 RA patients underwent scintigraphic evaluation for comparison between [^{99m}Tc]1.2B6 Fab and [^{99m}Tc]HDP (740 MBq (20 mCi)) at 4 hours post-injection of either radiotracer. [^{99m}Tc]1.2B6 Fab scintigraphic findings were found to be congruent with those of [^{111}In]1.2B6 $F(ab')_2$. Deviations in radiotracer distribution were noted, but could mostly be attributed to the differences in normal

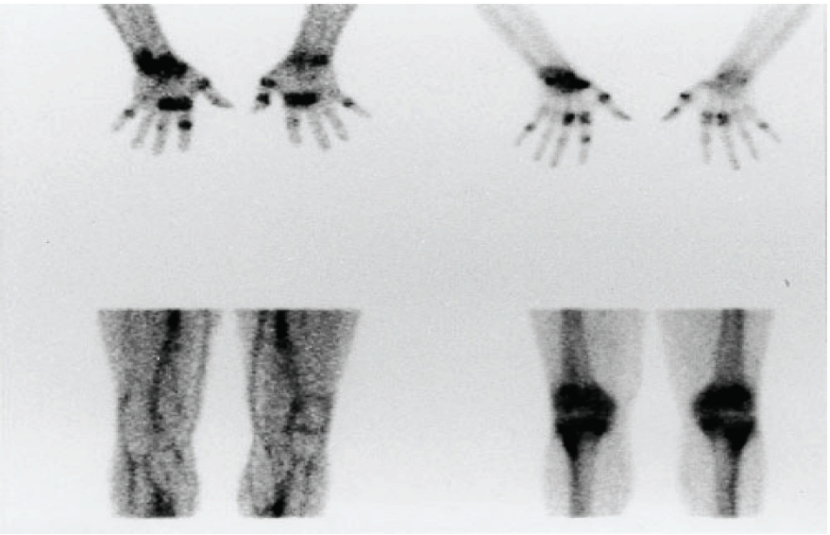

Figure 4. Images obtained 4 h after injection of ^{99m}Tc-1.2B6-Fab (left) and ^{99m}Tc-HDP (right) in two patients with RA. The images on the top correlate well; the bottom images show discordance between the lack of uptake of the mAb fragment and diffuse bony uptake. (Reprinted from Jamar F, Houssiau FA, Devogelaer JP, Chapman PT, Haskard DO, Beaujean V, Beckers C, Manicourt DH and Peters AM. Scintigraphy using a technetium-99m labelled anti-E-selectin Fab fragment in rheumatoid arthritis. Rheumatology (Oxford) 2002; 41: 53-61; by permission of Oxford University Press).

biodistribution of ^{99m}Tc- and ^{111}In-labeled antibody fragments. Due to the comparable results between the radiotracers and the fact that image quality and contrast were superior for the ^{99m}Tc-labeled radiotracer at the earlier scan, the substitution of [^{99m}Tc]1.2B6 Fab for ^{111}In-labeled F(ab')$_2$ is not only valid, but also advantageous, as it allows for a one day imaging protocol.

In the second subset of RA patients, radiolabeled anti-E-selectin, despite its lower joint-to-soft tissue uptake ratios and persistence of vascular activity, served as a significantly better discriminant ($P<0.0001$) of active joint inflammation than [^{99m}Tc]HDP, as a consequence of its specific uptake by activated vascular endothelium and lack of accumulation in normal joints. Conversely, although [^{99m}Tc]HDP images were of high-quality, they exhibited variable diffuse and non-specific bone uptake over a majority of joints, regardless of clinical involvement, greatly diminishing its capacity to differentiate between clinically active and normal or chronically damaged joints (**Figure 4**).

A similar approach that utilizes a binding peptide as the delivery agent for targeting E-selectin has also been described [174]. In a rat-adjuvant arthritis model, [^{99m}Tc]E-selectin binding peptide ([^{99m}Tc]ESbp) accurately localized inflammatory foci through selective, high-affinity binding (K_D= 2-5 nM) to E-selectin in activated endothelium [175]. To date, the clinical role of both E-selectin nuclear medicine imaging strategies has yet to be fully clarified, particularly in light of the advent of E-selectin-targeted MRI and optical imaging approaches [176-178].

[^{99m}Tc]- and [^{111}In]Octreotide

Similar to the previous approach, octreotide targets endothelium activation and macrophage recruitment. Octreotide is a long-acting somatostatin analogue that when radiolabeled allows for the *in vivo* visualization of somatostatin receptor distribution and density. Somatostatin and its receptors are clinically relevant due to their ubiquitous nature and regulatory involvement in several physiological processes. While first reported as a growth hormone release-inhibiting factor and neurotransmitter in the hypothalamus, somatostatin was subsequently assigned other important functions, including inhibition of motor activity in the gastrointestinal tract and release of a number of exocrine and endocrine secretions [179-181]. These mainly suppressive functions are mediated through 5 distinct G-protein-coupled receptor subtypes (sst_{1-5}) widely distributed in the central nervous system and peripheral tissues [182]. Hyperexpression of these receptors is well documented in a variety of pathological conditions and serves as a basis for octreotide imaging [183-185].

Currently, [^{111}In]DTPA-D-Phe^1-octreotide ([^{111}In] pentetreotide, OctreoScan®), an ^{111}In-labeled DTPA-conjugated octreotide peptide that specifically targets $sst_{2,3,5}$, is routinely used for the

scintigraphic and/or SPECT imaging of primary neuroendocrine tumors and their metastases as well as other somatostatin receptor-bearing malignancies [186-191]. Non-neoplastic applications of this imaging technique have only recently been explored [185]. The demonstration of somatostatin's role in the modulation of the immune response prompted investigations into the value of somatostatin receptor scintigraphy in chronic inflammatory diseases and other immune-mediated disorders [192]. The possibility of utilizing this imaging technique for the *in vivo* study of RA was raised only after researchers coincidentally observed uptake of radiolabled octreotide in the arthritic joints of a sarcoidosis patient [193]. As a logical progression, it was supposed and subsequently confirmed that the synovia of affected joints in RA patients overexpress somatostatin receptors, the target of octreotide. In particular, immunohistochemical staining of diseased synovial tissue samples from RA patients revealed expression of sst_2 on activated venule endothelial cells and infiltrating mononuclear phagocytes [193-195]. Constitutive expression of sst_1 and sst_2 on fibroblast-like synovial cells, as the result of TNF-α induction, has additionally been noted [196]. In comparison, the synovial tissue from a patient with clinically and biochemically confirmed RA who successfully underwent treatment did not stain for these receptors to any significant degree [196]. This suggests a role for octreotide imaging not only in disease localization, but also monitoring therapeutic response.

Van Hagen and co-workers conducted a pilot study to evaluate octreotide imaging in a cohort of 14 RA patients [193]. Somatostatin receptor scintigraphic findings were found to correlate well with clinical parameters. Increased [^{111}In] pentetreotide uptake allowed for the visualization of inflamed synovia with a lesion-related sensitivity of 76%. The specific uptake of octreotide by somatostatin receptors expressed in diseased joints was confirmed with *in vitro* autoradiographic studies. In comparison, no radiotracer accumulation was observed in the joints of control patients.

Somatostatin receptor imaging continues to be an area of interest for the assessment of rheumatoid arthritis, particularly as this approach has implications for therapy. A number of studies have indicated that therapy with somatostatin analogues improves symptoms in RA patients and attenuates inflammatory processes such as synovial proliferation and IL-6 and IL-8 production [196-199]. Positive scintigraphic findings may therefore serve as a rationale for treatment with unlabeled somatostatin analogues. However, to the best of our knowledge, no clinical studies have evaluated this novel role for octreotide imaging.

[^{99m}Tc]Anti-CD3 mAb

As mature T lymphocytes play a large role in the pathogenesis and extension of RA, radiopharmaceuticals that target this cell population can serve as a useful tool in evaluating disease course and localization. Radiolabeling monoclonal antibodies (mAbs) directed against CD3 is a recently developed method that allows for the selective imaging of T lymphocyte migration into rheumatoid synovium. The CD3 antigen consists of 2 heterodimeric glycoproteins (CD3-δ/ε and CD3-γ/ε), embedded almost exclusively in the cell membranes of $CD4^+$ and $CD8^+$ T lymphocytes [200]. This protein complex noncovalently associates with the T-cell receptor (TCR) and 2 TCR-ζ accessory chains, and collectively, they are responsible for T-cell activation [201, 202]. The CD3 antigen more specifically participates in signal transduction, following the binding and recognition of the major histocompatibility complex (MHC) proteins by the TCR [201, 202].

Muromonab (Orthoclone OKT®3) was the first specifically engineered anti-CD3 mAb. This murine IgG_{2a} antibody binds to epitopes of human CD3-ε, resulting in the early, temporal activation of peripheral T cells followed by a sharp inhibition and modulation of T cell functions [203]. As a potent immunosuppressant, OKT3 is indicated for the treatment of acute allograft rejection [204]. Recently, however, interest has turned toward radiolabeling OKT3 for use in immunoscintigraphic imaging of rheumatic diseases. In a study of 7 RA patients and 2 patients with psoriatic arthritis, Marcus and coworkers demonstrated that the [^{99m}Tc]OKT3 scintigraphic findings correlated well with patient history and physical examination [205]. Increased focal radiotracer uptake was present in a minority of asymptomatic joints, but this is likely indicative of subclinical synovitis. Consequently, the authors suggested that [^{99m}Tc] OKT3 scintigraphy may allow for earlier diagnosis of RA and psoriatic arthritis. Unfortunately, 2

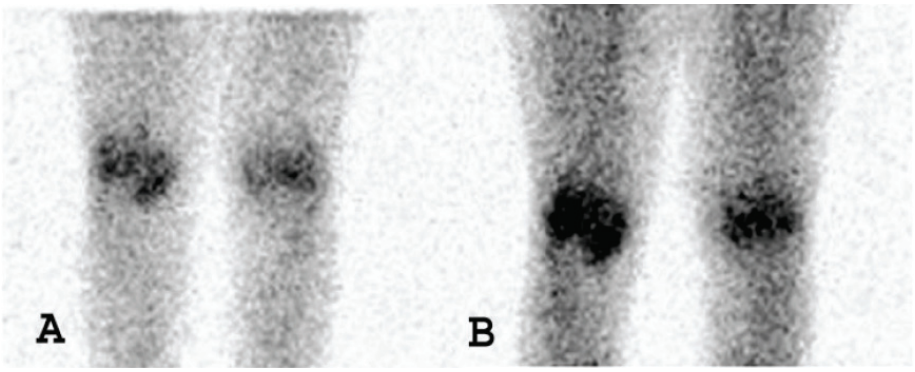

Figure 5. Scintigraphy with ^{99m}Tc-anti-CD3 of the knees shows an increase in the uptake of these areas in late images. Images taken (A) 1 h and (B) 3 h after endovenous injection of the radiopharmaceutical. (Reprinted from Lopes FP, de Azevedo MN, Marchiori E, da Fonseca LM, de Souza SA and Gutfilen B. Use of ^{99m}Tc-anti-CD3 scintigraphy in the differential diagnosis of rheumatic diseases. Rheumatology (Oxford) 2010; 49: 933-939; by permission of Oxford University Press).

patients in this study experienced shaking chills and neck pain approximately 1 hour post-injection of the anti-CD3 mAb. These adverse events appear consistent with cytokine release syndrome and will likely limit the use of OKT3 in RA patients [203, 206].

Despite these possible complications, Martins and colleagues further investigated the application of [^{99m}Tc]OKT3 imaging to the detection of synovitis in 38 RA patients [207]. Anterior planar scans showed increased focal [^{99m}Tc]OKT3 accumulation in 68.8% of tender joints, 71.8% of swollen joints, and 88.1% tender and swollen joints. Correspondingly, [^{99m}Tc]OKT3 scintigraphic findings significantly correlated with swollen joints, tender joints, and the visual analogue scale (VAS) ($p<0.05$). Moreover, [^{99m}Tc]OKT3 scintigraphy allowed the differentiation of patients in remission from those with active synovitis, according to their disease activity score. Unlike the previous study, there were no reported adverse events.

[^{99m}Tc]OKT3 scintigraphy not only has the capacity to assess disease activity, but also the ability to distinguish juvenile idiopathic arthritis (JIA) and RA patients from those with other rheumatic diseases, such as gouty arthritis (GA) and osteoarthritis (OA). As these patients can present clinically with overlapping signs and symptoms, this distinction is critical to optimal patient management and therapeutic intervention. In a study by Lopes and colleagues, the joints of 77 patients with rheumatic diseases (44 RA, 5 JIA, 15 OA, and 13 GA patients) were evaluated by [^{99m}Tc]OKT3 scintigraphy [208]. Since activated T lymphocytes play a large role in the pathophysiological processes of RA and JIA, but not in OA or GA, there were observable differences in the [^{99m}Tc]OKT3 uptake patterns obtained for the patients with each respective disease. As expected, there was high initial radiotracer uptake in the inflamed joints of RA and JIA patients, and a subsequent increase in accumulation visualized on the delayed scans (**Figure 5**).

Contrastingly, the initial radiotracer uptake was absent or minimal in cases of OA followed by a decrease in uptake observed at the delayed scan. This is consistent with the fact that the inflammatory process in OA is independent of T cell activation by the TCR/CD3 complex. Accordingly, no uptake was noted in any of the painful joints of OA patients. For joints (n=4) where the presence of edema was the main complaint, however, there was 1 joint for which the scan showed mild radiotracer accumulation. Moreover, another scan exhibited slightly increased [^{99m}Tc]OKT3 uptake when OA joints (n=6) with pain and edema were considered. Interestingly, a patient with previously diagnosed OA had an elevated ESR and early and delayed scintigraphic images showing increased uptake in the knees and hands (which on physical exam were shown to be painful and have edema), indicative of RA. Upon further clinical examination, this patient was later re-diagnosed with RA. This case serves to demonstrate the clinical rele-

vance of this imaging technique. GA patients, in comparison, were noted to have an initial increase in articular radioactivity, but this greatly declined as observed on the delayed scan. The authors suggested that the early accumulation of [^{99m}Tc]OKT3 in the joints of GA patients is likely the result of increased vascularity and cell infiltration in patients whose main complaint was edema or edema and pain. And thus, the eventual decrease in articular radioactivity levels reflects the absence of TCR/CD3-mediated T lymphocyte activation in GA pathophysiology.

While promising results, a major drawback to this imaging technique is the safety profile of OKT3 mAbs. Although no adverse events were noted in the Martins *et al.* and Lopes *et al.* studies, a whole host of side effects, particularly cytokine release syndrome (CRS), are associated with OKT3 use, even at microgram doses [203, 205]. CRS appears to be the result of the binding of antibody Fc regions to Fc-γ-receptors on immune effector cells and subsequent activation of these cell populations [209]. In this process, T lymphocytes are activated as well, which ultimately leads to the release of cytokines, mitogenicity, and antibody- and complement-dependent cytotoxicity [209]. Furthermore, as a murine mAb, OKT3 has the potential to elicit a human anti-mouse antibody (HAMA) response. This not only limits follow-up imaging, but also long-term therapeutic use. In an effort to limit these clinical complications, a number of humanized and chimeric OKT3 Fc variants have been developed [210-214].

Malviya *et al.* recently radiolabeled visilizumab (Nuvion®), a non-Fc-γ-receptor binding humanized IgG_2 mAb that binds with the CD3-ε chain with high specificity and high avidity (K_a= 0.5x10^9) [215, 216]. Favorably, this mAb does not activate T lymphocytes and thus has limited potential to induce cytokine release or acute cytotoxicity [216]. This imaging strategy was evaluated in Balb/c and SCID irradiated mice reconstituted with human lymphocytes and shown to be able to accurately map $CD3^+$ cell distribution *in vivo* [215-217]. From these findings, the authors suggested that in addition to offering information about disease localization, [^{99m}Tc]visilizumab could provide a rationale for therapy with unlabeled visilizumab in select candidates. Unfortunately, visilizumab has been withdrawn from production as a therapeutic agent after phase III trials [217]. Insufficient efficacy and, surprisingly, inferior safety profile were cited as the reasons for the withdrawal. While visilizumab could be manufactured solely for imaging purposes, it may be clinically useful to instead radiolabel anti-CD3 mAbs that offer therapeutic benefits and thus allow for the coupling of imaging and treatment.

[^{99m}Tc]anti-CD4 mAb

Anti-CD4 imaging is yet another strategy to visualize the highly relevant molecular process of T lymphocyte infiltration. In contrast to the previous technique, however, CD4 radioimmunodetection does not target a pan-T cell antigen, but instead, a molecule only present in a subset of T lymphocytes. CD4 is a 55 kDa monomeric glycoprotein expressed on the cell surface of all mature T helper cells (T_H, $CD4^+$ T lymphocytes), a majority of thymocytes, and to a lesser extent, monocytes-macrophages and dendritic cells [218]. Its extracellular domains bind to non-polymorphic regions of major histocompatibility complex class II (MHC-II) molecules, stabilizing the interaction between T_H cells and MHC-II-positive antigen-presenting cells (APCs) during T cell activation [219, 220]. In addition to functioning as a co-receptor for the TCR on T_H cells, CD4 plays a role in signal transduction due to the physical association of its short cytoplasmic tail with tyrosine kinase $p56^{lck}$, an important protein integral for the intracellular signaling cascade following T cell activation [221].

CD4 antigen represents a potentially important target in the study of RA, as $CD4^+$ T_H cell clones with abnormal phenotypes are abundant among cell infiltrates in arthritic synovial tissue and fluid [222, 223]. Synovial tissue and fluid also contain monocytes-macrophages, which express, in lower density, the CD4 molecule. Increased numbers of $CD4^+$ T_H cells in the peripheral blood have been noted as well during active disease [224]. Furthermore, a higher frequency of certain MHC-II alleles has been described in RA, suggesting that antigen-specific responses of autoreactive $CD4^+$ T_H cells are critical to the development and possible maintenance of this disease [15, 225, 226].

Based on these considerations, Becker and colleagues evaluated anti-CD4 radioimmunoscintigraphy in 6 patients with severe, clinically active RA [227]. Whole body and joint-specific

planar images were obtained for all patients at 1.5, 4, and 24 hours following intravenous injection of [^{99m}Tc]MAX.16H5, a ^{99m}Tc-labeled murine IgG_1 mAb that binds with high affinity to the human CD4 molecule in 5 patients, and *in vitro* labeled [^{99m}Tc]MAX.16H5 lymphocytes (≥10 MBq) in 1 patient. Scintigraphic findings were compared to those of clinical examination (Ritchie index, joint swelling) of 44 joints and early (5 minutes) and late (2 hours) [^{99m}Tc]HDP bone scans that each patient received within 7 days prior to immunoscintigraphy. [^{99m}Tc]MAX.16H5 imaging allowed clear visualization of diseased joints at 4-6 hours after radiotracer administration in all patients. These results correlated well with those of the early bone scan ($P<0.01$) and clinical scoring of joint swelling ($P<0.01$), but not with the late bone scan ($P>0.05$) or Ritchie index scoring of painful joints. A number of mismatches between joint uptake patterns in late bone scans and [^{99m}Tc]MAX.16H5 scintigrams were noted, suggesting that the latter imaging technique has higher sensitivity in detecting early, active disease, comparable to that of clinical diagnosis. Although not substantiated in this study, CD4 radiolocalization may be able to differentiate between RA and other forms of arthritis, such as septic arthritis, as it binds to infiltrating mononuclear cells, not granulocytes characteristic of acute inflammation. This property would be valuable and an advantage over both bone scanning and radiolabeled leukocyte scintigraphy.

While the Becker *et al.* study demonstrated increased uptake of [^{99m}Tc]MAX.16H5 in arthritic joints, it is unclear from their work as to whether accumulation of radiolabeled anti-CD4 mAbs in inflamed synovium is a consequence of specific target recognition or non-specific mechanisms [227]. To validate the specificity of this technique, Kinne and co-workers compared [^{99m}Tc]MAX.16H5 uptake with that of non-specific polyclonal [^{99m}Tc]HIG in 8 patients with severe, clinically active RA and 2 healthy volunteers [228]. In all examined arthritic joints, accumulation of [^{99m}Tc]MAX.16H5, expressed as percentage of total body radioactivity, did not significantly differ from that of non-specific [^{99m}Tc]HIG. Despite similar total uptake values, [^{99m}Tc]MAX.16H5 had lower background activity and thus significantly higher target-to-background (T/B) ratios as compared to [^{99m}Tc]HIG as early as 4 hours following radiotracer administration. Semi-quantitative visual scoring of scans confirmed higher average counts in the synovial membrane over those in either blood vessels or muscle for radiolabeled anti-CD4 mAbs in arthritic knee and elbow joints as compared to control Ig. ROI analysis of knee joint scans allowed quantification of T/B ratios, corroborating the results from the visual assessment. Kinne *et al.* argued that the improved T/B ratios were solely the result of [^{99m}Tc]MAX.16H5 specificity for $CD4^+$ inflammatory cell infiltrate, and, consequently, radiolabeled anti-CD4 mAbs allow for superior detection of inflammatory foci in RA than [^{99m}Tc]HIG scintigraphy. In support of this claim, another study by the same authors reported that [^{99m}Tc]MAX.16H5 exhibited higher total radioactivity levels and T/B ratios in arthritic joints of a single patient with longstanding, severe RA in comparison to [^{99m}Tc]anti-carcinoembryonic antigen mAb, an isotype-matched non-specific control mAb [229].

Conflicting reports exist, however, as a study utilizing a rat-adjuvant arthritis model has revealed similar levels of uptake and T/B ratios in inflamed synovium for both radiolabeled anti-CD4 mAbs and isotype-matched Ig controls [230]. The authors posited that the low T/B ratios may be the result of non-specific trapping of the anti-CD4 mAb due to its large size and/or binding to Fc receptors in arthritic joints rather than true non-specificity of the molecule [230, 231]. To test this hypothesis, Kinne and co-workers compared the joint uptake and body distribution of [^{99m}Tc]anti-CD4 (W3/25; IgG_1) Fab' fragments, which are smaller in size and devoid of Fc receptor-binding regions, to those of non-specific Fab' fragments ([^{99m}Tc]NCA-90) in a rat-adjuvant arthritis model [231]. Although both Fab' fragments showed increased uptake in arthritic compared to non-arthritic joints, accumulation of anti-CD4 Fab' fragments was significantly higher (approximately 1.6-fold) than that of control Fab' at all time points. Quantification of T/B ratios by ROI analysis confirmed superiority of anti-CD4 Fab' fragments over control Fab' fragments as well as whole anti-CD4 mAbs in delineating inflammatory foci. In addition to having higher specific accumulation in inflamed synovium compared to entire anti-CD4 mAbs, anti-CD4 Fab' fragments favorably had faster blood clearance and renal excretion and lower levels of background plasma radioactivity [232]. It was noted, however, that the Fab' fragments exhibited greater *in vivo* instability than the

whole anti-CD4 molecule [232].

From these studies, it is clear that [^{99m}Tc]anti-CD4 imaging can detect inflammatory foci with high sensitivity; as to whether this imaging technique will play a large role in the routine clinical evaluation of RA patients in the future is unknown. As has been previously discussed, a critical advantage for utilizing radioimmunoscintigraphy over other conventional methods is the ability to localize molecules that can serve as potential targets of therapeutic intervention. Currently, a controversy in the literature exists concerning the therapeutic benefit of anti-CD4 mAbs for RA patients [233-239]. Further evaluation of the efficacy of scintigraphic and therapeutic use of anti-CD4 mAbs and Fab' fragments in RA is needed.

[^{99m}Tc]Anti-CD20 mAb

While T lymphocytes have long been favored as the principal agents in RA pathogenesis, there is increasing evidence that B cell-mediated processes are critical for the development of autoimmunity, warranting the targeting of this cell population for radioimmunoscintigraphy and therapeutic interventions. B cell functions that may contribute to the propagation of chronic inflammation include T cell activation through expression of co-stimulatory molecules (CD80/86 and CD40), antigen presentation to T lymphocytes, secretion of pro-inflammatory cytokines, production of autoantibodies such as Rheumatoid Factor (RF), and their subsequent formation of immune complexes that activate the complement system and bind to Fcγ-receptor-bearing effector cells [240-244]. Additionally, B cell infiltrates have been noted in inflamed synovial tissues, providing the rationale for the use of B cell-targeted imaging in the *in vivo* study of RA patients. Instead of directly tagging B lymphocytes, researchers have developed radiolabeled mAbs that target CD20, a pan-B cell surface antigen that is important for calcium homeostasis and the development and activation of this cell population [245]. CD20 represents a potentially useful target because 95% of circulating normal and malignant B lymphocytes expresses this transmembrane phosphoprotein [246]. Furthermore, it is exclusive to B lymphocytes, specifically in their late pro-B phase to maturity [241, 246, 247]; CD20, however, is not expressed in hematopoietic stem cells and is shed upon differentiation into plasma cells [241, 247, 248].

In a pilot study, Malviya and co-workers radiolabeled Rituximab (Rituxan, MabThera®), a chimeric mouse/human $IgG_1\kappa$ mAb that recognizes epitopes on human CD20 antigen, with ^{99m}Tc to image B cell infiltration in the affected tissues of 10 patients with chronic inflammatory diseases, including RA [249]. Planar images obtained at 6 hours post-injection displayed increased [^{99m}Tc] Rituximab uptake in a majority, but not all, clinically inflamed joints. In one RA patient, [^{99m}Tc] Rituximab scintigraphic results were compared to those of [^{99m}Tc]anti-TNF-α imaging. Interestingly, the authors found a mismatch between the degree of uptake of [^{99m}Tc]Rituximab and radiolabeled anti-TNF-α in various synovial joints. While low radiotracer sensitivity is a possible explanation for this finding, it is more likely an indication that selective inflammatory pathways are in effect in different synovial joints, causing divergent articular phenotypes. Consequently, [^{99m}Tc]Rituximab scintigraphy may allow for the visualization of the degree of local and systemic involvement of B lymphocytes in disease propagation.

Moving forward, this method of mapping B cell infiltration has the potential to establish personalized therapy, select candidates for treatment with unlabeled anti-CD20 mAbs, and monitor the efficacy of these therapies [206, 217]. A later study by the same group of authors supported this approach by citing a high intra-articular and inter-individual variability of [^{99m}Tc] Rituximab uptake and thus B lymphocyte infiltration in RA patients [250]. More studies, however, are needed to test the clinical efficacy and relevance of this imaging technique. As RA patients have been shown to benefit from unlabeled Rituximab and other B cell-depleting therapies, the role of [^{99m}Tc]Rituximab scintigraphy may expand in the near future [251-255].

[^{99m}Tc]Anti-TNF-α

Numerous pro-inflammatory cytokines play a role in the development and maintenance of chronic inflammation. Interleukin-1 (IL-1), interleukin-6 (IL-6), interleukin-2 (IL-2) and tumor necrosis factor-α (TNF-α), in particular, have been identified as important inflammatory mediators in RA [256-258]. Directly and indirectly targeting cytokines and their receptors for imaging purposes is a novel strategy that has only

recently been explored in the context of RA. One study investigated the utility of [^{123}I]IL-1 receptor antagonist ([^{123}I]anakinra), which has a similar binding affinity to IL-1, but no biological activity, in imaging RA patients [259]. Nevertheless, the authors concluded that this probe was not useful for the scintigraphic assessment of RA patients because it did not show higher uptake levels than non-specific radiolabeled albumin, and thus, no follow-up studies were performed. Accordingly, attention has turned toward targeting TNF-α for radioimmunoscintigraphic evaluation of RA patients and unlike [^{123}I]anakinra, this imaging technique has shown promising results.

TNF-α is a pleiotropic pro-inflammatory cytokine that has been implicated as a mediator of key pathophysiological processes in a number of neoplastic and chronic inflammatory autoimmune diseases. It is synthesized, primarily by activated monocytes-macrophages and lymphocytes, as a 27 kDa prohormone that, upon aggregation into a homotrimer, serves as a transmembrane protein [260]. Through proteolytic cleavage by metalloproteinase TNF-α converting enzyme (TACE), soluble trimeric TNF-α (sTNF-α) is produced and secreted extracellularly [261, 262]. In either form, TNF-α carries out its numerous immunoregulatory and inflammatory functions by binding to its cognate cell-surface receptors, type 1 TNF-α receptor (TNFRI, p55) and type 2 TNF-α receptor (TNFRII, p75) [263-265]. These are found on neutrophils, endothelial cells, fibroblasts, and other cell types. The pro-inflammatory functions of TNF-α include the ability to upregulate adhesion molecules on the surface of vascular endothelium, and thus, promote recruitment of granulocytes and mononuclear cells, stimulate fibroblast growth, mediate bone resorption, and induce synthesis of other pro-inflammatory mediators such as IL-1, IL-6, prostaglandin E_2, and IFNγ [266-274].

Based upon these considerations and the fact that elevated levels of membrane-bound and soluble TNF-α and its receptors are found in the sera and inflamed synovial tissue and fluid of patients with active RA, this potent inflammatory cytokine represents a critical target for immunotherapy in these patients [256, 275, 276]. Numerous clinical studies have supported the sustained efficacy of TNF-α antagonists by demonstrating significant reduction of symptoms and disease severity and slowing or arresting of joint erosive progression in RA patients when used in combination with conventional DMARDs [277-280]. Consequently, TNF-α blockade has become an established therapeutic approach, particularly in cases of refractory RA. Current FDA-approved TNF-α inhibitors for the treatment of RA include infliximab (Remicade®), adalimumab (Humira®), golimumab (Simponi®), certolizumab pegol (Cimzia®), and etanercept (Enbrel®). While TNF-α antagonists have revolutionized rheumatologic intervention, it is important to note that some RA patients do not respond to these agents [281]. This is likely the result of high inter-individual and intra-articular variation in the concentrations of TNF-α and other inflammatory cytokines [258]. Determining the quantity and distribution of TNF-α *in vivo* in all inflamed joints prior to initiating therapy may therefore prove to be useful in selecting candidates likely to respond to TNF-α inhibition. This technique moreover has the potential to provide an objective measure of disease activity and treatment efficacy. To date, 2 TNF-α antagonists have been radiolabeled and utilized in the study of RA- infliximab and adalimumab.

Infliximab is a bivalent, chimeric (murine-human) IgG_1 monoclonal antibody that binds to both membrane-bound and soluble TNF-α with high specificity and affinity (K_D= 1x10^{-10} M) [282]. It has a biological half-life of 9.5 days and functions as a TNF-α inhibitor by blocking the interaction between TNF-α and its receptors (p55 and p75) [283]. In addition, infliximab can induce antibody-dependent cellular cytotoxicity (ADCC) or complement-mediated cytotoxicity (CDC) of membrane-bound TNF-α expressing cells [283-286]. Recently, infliximab was radiolabeled with ^{99m}Tc and shown to have the same affinity for TNF-α as its unradiolabeled counterpart [287]. It has since been tested in patients with various infectious and chronic immune-mediated inflammatory diseases. In a preliminary study, Conti and co-workers scintigraphically assessed the *in vivo* levels of TNF-α in the inflamed knee of a patient with undifferentiated spondylarthropathy [288]. Following administration of [^{99m}Tc]infliximab (15 mCi), planar images of the knee joints were acquired at 6 and 24 hours post-injection. Significant uptake of [^{99m}Tc]infliximab was observed for the inflamed knee as compared to the clinically uninvolved knee, indicating high intra-lesional levels of TNF-α. These scintigraphic findings served as the rationale for the patient receiving an intra-

articular injection of unradiolabeled infliximab. Clinical follow-up for a period of 4 months showed no signs of active disease (VAS score for pain= 0; no swelling or tenderness) in the injected knee, which was confirmed by negative scintigraphic findings, suggesting a role for [^{99m}Tc]infliximab imaging in localizing disease activity and monitoring therapeutic response in RA patients.

The utility of [^{99m}Tc]infliximab scintigraphy for the detection of TNF-α-mediated inflammation in the joints of RA patients was assessed in another pilot study [289], evaluating patients pre- and post-therapy. Planar images of the inflamed joints were obtained for all patients at 3, 6, and 24 hours following intravenous administration of [^{99m}Tc]infliximab. Pre-treatment scans demonstrated increased regional radiotracer accumulation in inflamed joints with high target-to-background (T/B) ratios; no uptake was observed for clinically uninvolved joints. [^{99m}Tc] infliximab uptake in joints, however, showed more variability in scans performed 3 months after therapy. In comparison to the previous scan, 4 joints exhibited significantly reduced or no radiotracer uptake while 6 joints showed little to no change in [^{99m}Tc]infliximab accumulation. Patients with higher pre-therapy levels of TNF-α, as determined by scintigraphy, and significantly decreased [^{99m}Tc]infliximab uptake post-treatment were shown to have a better clinical response (improved swelling and pain) to infliximab treatment. These findings, in addition to those from the Conti *et al.* study, support the use of [^{99m}Tc]infliximab scintigraphy in the objective selection of potential candidates that are likely to benefit from local or systemic infliximab treatment [288]. Although promising, a proof-of-mechanism study has yet to be performed with a larger patient cohort. Furthermore, as a chimeric mAb, infliximab use can trigger a human anti-mouse antibody (HAMA) response, which not only can hamper follow-up imaging studies, but also markedly decrease the efficacy of repeated therapeutic doses of infliximab.

In an effort to reduce immunogenicity, adalimumab, a recombinant humanized anti-TNF-α IgG_1 mAb, was engineered and has been approved for use in RA patients [290]. Adalimumab binds to membrane-bound and soluble TNF-α with high specificity and affinity (K_D= $6x10^{-10}$ M) [291]. Similar to infliximab, adalimumab neutralizes TNF-α by blocking its interaction with p55 and p75 and inducing ADCC and CDC of TNF-α-expressing cells [292]. Adalimumab has been radiolabeled with ^{99m}Tc as well and employed in clinical trials. In a two-part study, Barrera and co-workers investigated the feasibility and validity of using [^{99m}Tc]adalimumab scintigraphy in the study of 10 RA patients [293]. In the first scintigraphic session, whole-body and joint-specific planar images were acquired for each patient 5 minutes, 4 and 24 hours following intravenous injection of [^{99m}Tc] adalimumab to assess tissue biodistribution and imaging properties. The same imaging procedure was utilized in the second scintigraphic assessment that took place 2 weeks later, but an excess of unlabeled adalimumab (10 mg/kg) was co-administered in a subset of 5 patients to evaluate the degree of specific binding. The remaining 5 patients received a single intramuscular dose of methylprednisolone (120 mg) 2 days before scintigraphic evaluation to study the ability of [^{99m}Tc]adalimumab imaging to detect clinically significant changes in intra-articular disease activity in response to systemic corticosteroid therapy.

In all patients studied by Barrera *et al*., significant physiologic uptake of [^{99m}Tc]adalimumab was seen in the liver and spleen [293]. Joints were clearly delineated at 4 and 24 hours following radiotracer injection, with inflamed joints demonstrating a 2- to 4-fold increase in radiotracer uptake over normal tissues. Not all clinically active joints, however, showed accumulation of radiolabeled anti-TNF-α mAbs; this was particularly true for the small joints of the hands and feet. Although no explanation was offered, this finding likely reflects the high intra- and inter-individual variability of TNF-α expression in inflammatory foci. Conversely, no uptake was observed in clinically uninvolved joints. Scintigraphic results from the second imaging session showed that the uptake of radiolabeled adalimumab is partly the result of specific binding to TNF-α; co-administered excess unlabeled adalimumab abrogated the signal of radiolabeled anti-TNF-α mAbs by a median of 16% and 25% at 4 and 24 hours, respectively. These results were reproduced in later studies [294, 295]. Anti-TNF-α radioimmunoscintigraphy was also able to detect clinically relevant changes in synovitis following systemic corticosteroid treatment. The 5 patients who received treatment exhibited a decrease in clinical disease activity,

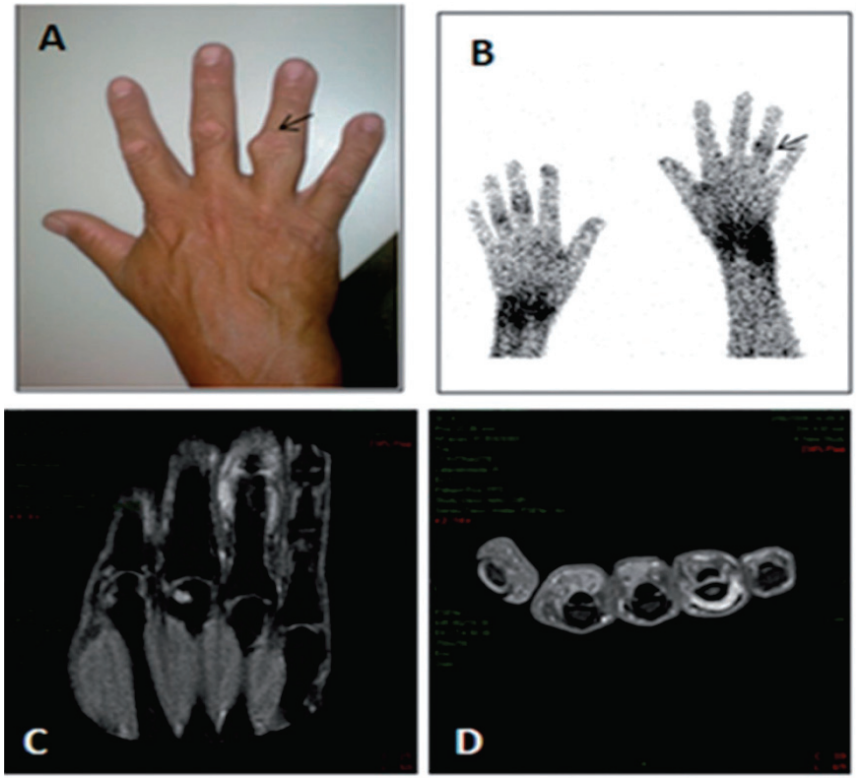

Figure 6. (A) Right hand with fourth PIP joint swelling and capsular bulging. (B) Hand scintigraphy scan, showing increase in uptake of ^{99m}Tc-anti-TNF-a in the fourth right (PIP) (arrow), third and fourth left PIP and wrists. (C and D) Right-hand MRI coronal (C) and axial (D) slices showing fourth PIP synovitis. (Reprinted from Roimicher L, Lopes FP, de Souza SA, Mendes LF, Domingues RC, da Fonseca LM and Gutfilen B. ^{99m}Tc-anti-TNF-α scintigraphy in RA: a comparison pilot study with MRI and clinical examination. Rheumatology (Oxford) 2011; 50: 2044-2050; by permission of Oxford University Press).

as expected, and a concomitant decline in [^{99m}Tc]adalimumab uptake in inflamed joints. No adverse events were reported.

Further validating this imaging technique, Roimicher and co-workers compared the results of [^{99m}Tc]adalimumab scintigraphy to those of MRI and clinical evaluation in 8 patients with active RA and 1 healthy volunteer [295]. Whole-body and anterior planar images of hands and wrists were acquired for each patient at 30 minutes and 3 hours following injection of a subtherapeutic dose (15% of treatment dose) of [^{99m}Tc] adalimumab. Two nuclear medicine specialists visually evaluated the scintigraphic scans for intensity and pattern of [^{99m}Tc]adalimumab uptake. All patients underwent clinical examination and MR imaging of hands and wrists. Axial and coronal pre- and post-Gadolinium contrast T1-weighted spin echo MR images were obtained for each patient, as were axial and coronal short tau inversion recovery (STIR) images. Two radiologists evaluated the scans for synovitis, according to the definition put forth by the OMERACT MRI collaborative subgroup (see below). Representative MR and scintigraphic images can be seen in **Figure 6**.

Of 198 examined joints in the study by Roimicher *et al*., 49 joints were determined to be positive for synovitis on MRI and 48 joints on scintigraphy [295]; agreement between the methods was found for 44 joints (sensitivity of 89.8%). One hundred and forty-five joints were found to be negative on both MRI and scintigraphy, resulting in a specificity of 97.3%. Five false-negatives and 4 false-positives were reported. The authors suggested that these false-negative scintigraphs were likely the result of the absence of detectable TNF-α levels in those inflamed joints. It has previously been shown that other cytokines besides TNF-α can act as the primary mediator of inflammation in some clinically active joints [258]. The ability to indirectly measure intra-lesional levels of TNF-α expression is a major advantage of this imaging technique, as it allows for evidence-based biologic therapy and patient selection. A number of studies have indicated that patients with higher pre-therapy uptake of [^{99m}Tc]adalimumab were more likely to respond to treatment with unlabeled anti-TNF-α mAbs than patients with lower or no radiotracer accumulation [294, 296]. Consequently, both positive and negative scintigraphic findings appear to offer clinically rele-

vant data. In addition to finding comparable results between MRI and [^{99m}Tc]adalimumab scintigraphy, the authors found that the latter technique was more sensitive and specific than clinical examination in detecting synovitis, suggesting a possible diagnostic role for [^{99m}Tc] adalimumab scintigraphy.

Overall, anti-TNF-α scintigraphy represents a promising tool in the study of RA. High quality whole-body scans with relatively low doses can be rapidly acquired for RA patients. Scintigraphic findings give clinically relevant data that may assist in accurate diagnosis, evidence-based biologic therapy, and localization and measuring of disease activity. Moving forward, it may be of interest to radiolabel anti-TNF-α Fab' or F(ab')$_2$ fragments for scintigraphic use to reduce non-specific uptake and immunogenicity associated with Fcγ-receptor binding as well as to improve imaging properties such as plasma clearance and excretion time. Larger studies that determine the prognostic value of anti-TNF-α scintigraphy are needed as well.

[^{99m}Tc]Annexin V

Radioimmunodetection of apoptosis is another novel imaging strategy being employed in the study of RA. As apoptosis is a highly regulated, complex cascade of enzymatic activity, there are numerous and diverse potential targets for molecular imaging. Among these targets, phosphatidylserine (PS), an anionic aminophospholipid that constitutes 10-15% of plasma membrane content, has garnered the most interest, as its location within the lipid bilayer not only reflects but also has a direct bearing on the apoptotic status of a cell [297, 298]. In normal, healthy tissue, PS expression is actively restricted to the inner (cytoplasmic) leaflet of the plasma membrane through the enzymatic activity of an ATP-dependent aminophospholipid translocase (APLT) [297, 299]. In comparison, other phospholipids are largely constrained to the outer (exoplasmic) leaflet, resulting in the deliberate establishment of an asymmetrical phospholipid distribution [297, 299].

With the onset of apoptosis, however, this asymmetry collapses as PS residues are rapidly externalized through the simultaneous inhibition of APLT and activation of scramblase, a non-selective enzyme that bi-directionally transports phospholipids between leaflets [300, 301]. Cell-surface exposure of PS occurs early in the apoptotic cascade and only later serves as a signal for macrophages to phagocytize the PS-expressing cell [302-305]. Under normal circumstances, macrophages and neighboring cells can efficiently remove and thus minimize the presence of apoptotic cells and cell remnants. On the other hand, in diseased states, there is a sustained presence of PS-expressing cells due to the increased activation of apoptotic cellular pathways and the inability of phagocytes to efficiently clear dying cells in pathological tissue [306-308]. Radiotracers that specifically target and bind to cell-surface exposed PS, therefore, have the potential to non-invasively assess the presence, extent, and, with long-term follow-up, rate of apoptosis in its early to intermediate phase.

Although various PS-targeting compounds have been reported in the literature, radiolabeled annexin V is the only radioligand that has been validated as a reliable *in vivo* cell marker of apoptosis and has been utilized in both preclinical and clinical imaging studies. Annexin V is an endogenous human protein (molecular weight, 35.8 kDa) that is widely expressed intracellularly and has been supposed to play a role in anti-coagulation and inhibition of protein kinase C and phospolipase A_2 [309-311]. While the exact physiologic function of annexin V is unknown, its biological activity is thought to stem from its ability to bind to anionic phospholipids in the presence of calcium [312]. In particular, annexin V selectively binds to the phosphoserine head of cell-surface exposed PS residues in all cell lines with high affinity (k_D= 0.1-2 nM) [313]. Consequently, upon initiation of apoptosis and subsequent PS externalization, there is a concurrent increase in the concentration of annexin V and the number of annexin V binding sites per cell [314-316]. Binding to PS, annexin V is internalized by the PS-expressing cell through a modified form of pinocytosis [317]. To date, several radiolabeled recombinant human annexin V derivatives with various chelators and co-ligands have been developed for use in apoptotic imaging.

Apoptosis imaging as it relates to the study of RA has only recently been explored. To investigate this potential application, Post and co-workers performed autoradiographic imaging studies with [^{99m}Tc]annexin V in a murine collagen-induced arthritis model [318]. The front and

hind paws of collagen-inoculated DBA/1 mice showed increased multifocal uptake of [^{99m}Tc] annexin V in peri-articular and ligamentous structures. Localization of [^{99m}Tc]annexin V to these sites of scattered mononuclear infiltration, confirmed histologically, was evidenced to be specific when compared to that of [^{125}I] bovine serum albumin, a non-specific radiotracer. At maximum effect size, [^{99m}Tc]annexin V uptake values in the digits and pads of front and rear paws and Achilles tendon sheaths of collagen-inoculated mice were 2- to 6 times higher than those for age-matched controls. Advantageously, this difference was discernible early in the disease course when there was no evidence of bone or joint erosions. Minimal focal radiotracer accumulation, however, was noted for control mice in the physeal growth plates of the digits and the Achilles tendon sheaths; uptake in these regions is most likely physiologic in nature, as previous studies have reported that normal apoptosis occurs at these sites [319]. Post and co-workers did not specifically identify the apoptotic cells that served as the radiotracer's target(s). Clarifying the exact mechanism of [^{99m}Tc]annexin V localization in arthritic joints will prove to be crucial moving forward. Additionally, this study opened the door to the possibility of using [^{99m}Tc]annexin V imaging to monitor treatment response in RA patients by showing that collagen-inoculated mice exhibited reduced radiotracer uptake in their extremities following 5 days of treatment with methylprednisolone.

While only the Post *et al.* [318] study specifically explored apoptosis imaging in RA, there are several pre-clinical and clinical studies that have validated the use of this technique in the study of cardiac ischemic-reperfusion injury, heart failure, acute allograft rejection, active myocarditis, malignant intracardiac tumors, Alzheimer's disease, neonatal and adult cerebral hypoxic-ischemic injury, and atherosclerotic plaques vulnerable to thrombosis [320-327]. This imaging strategy also has been shown to accurately monitor and predict response to chemotherapy in oncology patients [328]. These studies lend themselves to the validation of apoptosis imaging in RA since they demonstrate that [^{99m}Tc] annexin V has a high sensitivity and specificity for detecting apoptosis, rapid blood clearance ($t_{1/2}$ =24 minutes) and renal excretion devoid of bowel activity (23% at 24 hours), favorable human biodistribution (although high radioactivity concentration in renal cortex), and a high signal-to-background ratio that is achieved relatively quickly, allowing for shorter imaging times [329, 330]. Moreover, this radiotracer has an acceptable effective dose comparable to that of other ^{99m}Tc-labeled radiopharmaceuticals and a low immunogenicity due to its human origin [331, 332]. Possible disadvantages are that it cannot accurately differentiate between apoptosis and necrosis, as the latter process results in increased PS availability as well, and the biologic half-life of the radiopharmaceutical ($t_{1/2}$= 70 hours) is long in comparison to its physical half-life [333, 334].

Overall, apoptosis imaging is in its infancy. Although [^{99m}Tc]annexin V is the most prevalent probe for apoptosis scintigraphy and SPECT, various other agents have been or are being developed. Moving forward, it is likely that these other apoptosis-seeking radiotracers will be tested so as to maximize the sensitivity and specificity of this technique. Future options include [^{99m}Tc]annexin V derivatives with different chelators and co-ligands, radiolabeled anti-annexin V mAbs, and non-annexin V PS-binding radiotracers [325, 336, 335]. As PET has better spatial resolution than SPECT and allows for quantitative analysis, efforts to develop and test annexin V derivatives labeled with positron-emitting radionuclides are underway [337, 338]. Annexin V derivates conjugated to superparamagnetic iron oxide nanoparticles for MRI have been introduced, as this imaging modality offers high tissue contrast without patient radiation [339]. It is unclear at this time as to the direction apoptosis imaging will take.

Other molecular imaging strategies for RA

Magnetic resonance imaging (MRI)

The goals for MRI imaging of RA are similar to those for nuclear and molecular imaging: namely, to detect the manifestations of RA at an earlier stage, identify patients at risk for progressive disease, and monitor progression that may prompt the need for altering therapy. Early and aggressive treatment may prevent subsequent development of irreversible joint damage, which underscores the need for accurate early diagnoses. While MRI is fundamentally an anatomic technique, it bridges the gap between anatomy and physiology. T1-weighted images, for example, clearly show peri-articular erosions

and synovial thickening, but it is the contrast enhancement pattern following Gadolinium administration that identifies the hyperemia suggestive of active inflammation from synovitis. There continues to be progressive advancement and better understanding of the significance of MRI findings in RA [340-342].

MRI versus radiography

Radiography has long been the standard for detection of joint damage in established RA. It is readily available, low-cost, and reliably demonstrates many of the more advanced changes, such as erosions, joint space narrowing, and juxta-articular bone loss. Radiographically-based scoring systems such as the Larsen and Sharp scoring methods are extremely reproducible [343, 344]. It is over 20 years, however, since the initial report of the utility of MRI over radiographs in early RA [345]. Since then, numerous authors have concluded that MRI is superior to plain radiographs in detecting erosions in early active disease. In one study of RA patients evaluated in their first year after presentation by McQueen *et al*., MRI revealed erosions in 45% of patients versus only 15% of patients on radiography at 4 months. This increased to 75% on MRI and 29% on radiographs at 1-year follow-up [346, 347]. This not only shows the superior sensitivity of MRI, but also that the development of erosions is a very dynamic process. Less than 20% of patients with RA of less than 6 months duration will have erosions on radiographs [347].

There are 3 reasons why it is logical that MRI is more sensitive than radiography in early RA. MRI is a 2D/3D technique and does not attempt to project the findings onto a single planar image (i.e., a film). The superimposition that occurs on a "flat", single dimensional image can hide significant pathology. Second, since plain radiographs lack the contrast resolution of MRI, they do not discretely visualize and discriminate the various soft tissue structures from one another; in particular, they do not differentiate the synovium from other overlying soft-tissues. Third, for erosions to be visible on radiographs, significant loss of bony mineral must have occurred. This is most pronounced in established RA.

MRI technical issues

While there has been some variability in the MRI imaging techniques used in the literature, most exams are conducted consistent with the OMERACT working group recommendations [348]. These include imaging in at least 2 planes, with T1-weighted images before and after Gadolinium-based contrast administration, plus a T2-weighted fat-saturated image (or STIR sequence if fat-saturation is not available). Most contemporary systems do allow fat-saturation, and this also is commonly used on post-contrast T1-weighted images. If available, many sites perform gradient echo 3D acquisitions pre- and post-contrast, and reconstruct the images in 2 dimensions to reduce exam time and improve spatial resolution; a minority prefer or are limited to direct axial and coronal acquisition of 2D images using spin-echo sequences for pre- and post-contrast imaging.

Most clinical practices focus on imaging the dominant symptomatic wrist and metacarpal-phalangeal (MCP) joints [349]. This has proven equivalent for follow-up and detection of progression as compared to serial radiographs of the hands and feet [242, 350]. Recently, it has been shown that creative combinations of surface coils can produce whole body assessment of the major joints (13 per patient including the hands and wrists) in examination times comparable to single joint assessments [351]. This technique, while close to true MR screening, suffers from reduced spatial resolution compared to the traditional approach. Furthermore, the overall synovitis burden correlated quite closely with semi-quantitative hand/MCP synovitis scores and therefore yielded little additional information.

There is extensive experience now with both low-field (.2-.6 Tesla (T)) and high-field (1.0-1.5 Tesla) MRI. The low-field machines have lower spatial resolution and somewhat longer exam times, and earlier studies suggested that this adversely affected the detection of bone marrow edema (osteitis) [352]. More recent experience [353] has shown no such difference. In addition, erosions and synovitis appear equally well seen with both field strengths [354] with good intra- and inter-reader reproducibility [355].

MRI findings and their significance in RA

MRI is capable of demonstrating the broad spectrum of findings seen in rheumatoid arthritis [349].

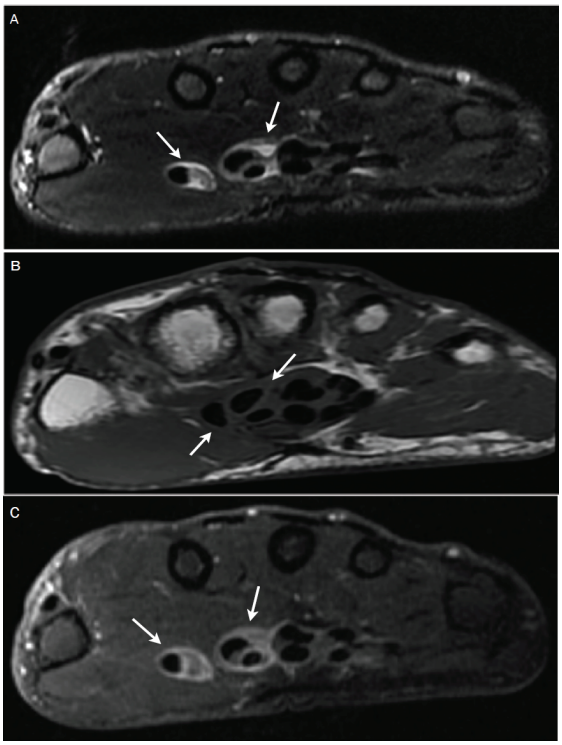

Figure 7. Tenosynovitis. (A) T2-weighted fat-suppressed axial image shows high signal surrounding the flexor tendons (arrows), which represents fluid or edema. (B) T1-weighted axial image shows intermediate signal surrounding the flexor tendons (arrows). (C) T1-weighted fat-suppressed axial image after Gadolinium contrast administration shows high signal enhancement (arrows), representing tenosynovitis surrounding the flexor tendons (Image courtesy of Dr. Kathleen Brindle, the George Washington University, Washington D.C.).

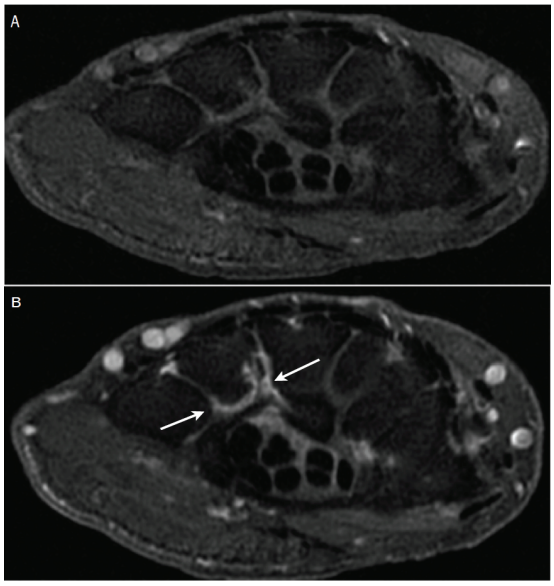

Figure 8. Synovitis/synovial hypertrophy. (A) T1-weighted fat-suppressed axial image shows intermediate signal of the synovium surrounding the metacarpal bases. (B) T1-weighted fat-suppressed axial image after Gadolinium contrast administration shows high signal enhancing synovium (arrows) around the base of the fourth metacarpal. The findings suggest synovitis or synovial hypertrophy (Image courtesy of Dr. Kathleen Brindle, the George Washington University, Washington D.C.).

Synovitis: Synovitis is one of the earliest abnormalities detected in RA. The synovial lining should be barely perceptible in normal patients with minimal or no contrast enhancement with Gadolinium administration. Thickening, increased water content producing high signal on T2-weighted images, or more than minimal contrast enhancement suggests synovitis (**Figures 7** and **8**). MRI appears to be more sensitive than clinical exam in detecting synovitis [356], and synovitis correlates well with development of subsequent erosive disease [357, 358]. The degree of enhancement can be used as a surrogate marker for hyperemia, and can help distinguish active from inactive disease [359].

Bone Marrow Edema: Bone marrow edema or osteitis, albeit non-specific, also occurs in early RA. On fat-suppressed T2-weighted images, it appears as high signal in the subchondral bone (**Figure 9**). At times osteitis is seen surrounding an erosion or clusters of erosions. Since marrow edema is a marker for generalized early inflammation, it is not surprising that it often correlates with an elevation of C-reactive protein and erythrocyte sedimentation rate serum levels; all 3 (along with synovitis) are early predictors of subsequent erosive change [353, 358].

Erosions: Erosions, when they develop in early RA, strongly imply that irreversible joint damage has developed (**Figure 10**). It is controversial as to whether erosions may "heal" but this appears to be a rare event. In a detailed analysis of specific erosions, McQueen and colleagues found that virtually all erosions seen on baseline MRI studies were also visualized one year later by 2 radiologists [360]. In that same study, erosion scores on baseline MRI were predictive of the radiographic erosion score at 2 years. Bony erosions in early RA predict a more aggressive dis-

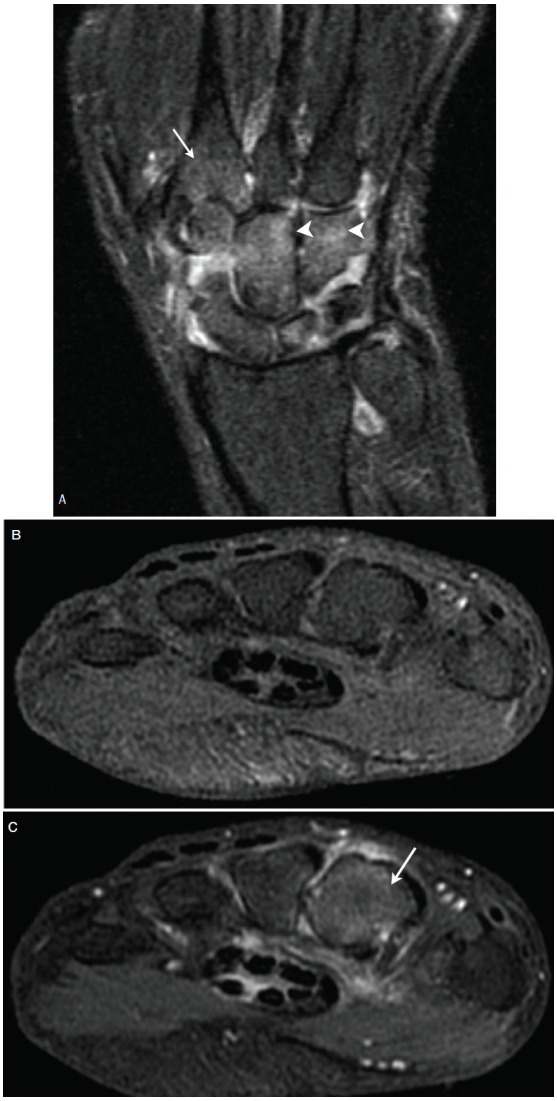

Figure 9. (A) Bone edema. T2-weighted fat-suppressed coronal image shows intermediate signal in the bone of the second metacarpal (arrow) and in the carpal bones (arrowheads). In the setting of RA this can represent edema. (B) T1-weighted fat-suppressed axial image shows uniform intermediate signal through the metacarpal bases. T1-weighted images without contrast are not sensitive for detection of bone edema. (C) T1-weighted fat-suppressed axial image after Gadolinium contrast enhancement shows diffusely increased bone signal at the base of the second metacarpal (arrow), consistent with enhancing edema (Image courtesy of Dr. Kathleen Brindle, the George Washington University, Washington D.C.).

ease with radiographic progression and reduced functional outcomes. In one such study, hand and wrist tendon function were strongly predicted by the presence of erosions (and even more strongly predicted by bone edema) [361].

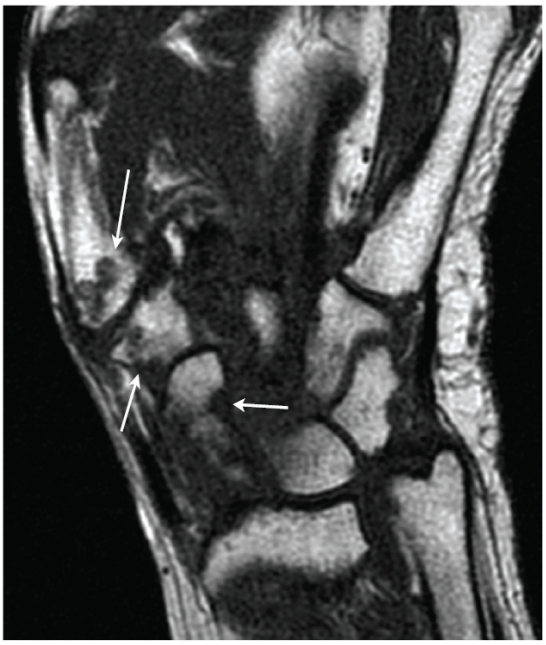

Figure 10. Erosions. T1-weighted coronal image shows erosive changes of the navicular, multangular, and first metacarpal (arrows) (Image courtesy of Dr. Kathleen Brindle, the George Washington University, Washington D.C.).

Other Findings: Tendinopathy is a common finding in RA. Most commonly this takes the form of tenosynovitis, which exhibits MR evidence of fluid in the tendon sheath or increased thickness or enhancement of the tendon sheath synovium. Tendonitis may also occur. Tenosynovitis is not included in the RAMRIS scoring system (see below), but is important since early evidence of tendinopathy has been reported to predict tendon rupture at 6 years [362]. Joint effusions occur in RA often in association with synovitis. Fibrotic pannus may also be present in RA, but is more common in long-standing disease. Loss of cartilage and joint space narrowing occur late in long-standing disease.

While not an imaging finding, it is worth mentioning anticyclic citrullinated peptide (anti-CCP) antibodies. This autoantibody has similar sensitivity to rheumatoid factor, but with greater specificity and greater likelihood of being positive in early disease [363]. If positive it represents a risk factor for development of erosive disease.

Three of the above major imaging findings have been the focus of the OMERACT Rheumatoid Arthritis Magnetic Resonance Imaging Scoring (RAMRIS) system [348]. These are synovitis, bone erosions, and bone edema. Synovitis is scored in 3 regions of the wrist from 0 to 3 with 3 representing severe synovitis (thickening and enhancement). Bone erosions are scored from 0 to 10 based on 10% volume intervals of bone eroded within any given area of assessed bone volume. Bone edema or osteitis is scored on a scale of 0 to 3, each representing intervals of 33% volume involvement. Edema may be the most difficult to assess of the RAMRIS categories, as it is often feathery and indistinct in nature.

While it requires training and experience to recognize the varied manifestations of RA, there is generally good agreement among readers. Prior to the development of the RAMRIS scoring system, Østergaard and colleagues, using a similar scoring system, showed good agreement between readers for synovitis (86%) and erosions/bone lesions (97%) [364]. Using the RAMRIS system, similar results were obtained with strong agreement for MCP erosions, wrist erosions, and wrist synovitis [365]. Slightly less agreement was seen for MCP synovitis, MCP bone edema, and wrist bone edema.

Progression of disease

The advent of biologic therapies such as the anti-TNF-α class of drugs and continued use of immunosuppressive agents such as methotrexate have created a growing emphasis on treating early disease before the development of structural joint damage. As mentioned above, MR excels at identifying erosions, and does so far earlier than radiographs. If erosions are present, there is ample evidence supporting early treatment [366, 367]. If no erosions are present on initial MRI, however, McQueen *et al.* found that 82% of his RA cohort at 2 years did not develop erosions on radiograph [347]. Conservative management to avoid the toxicity, immunosuppressive effects, and cost of the biologic agents may better serve patients without early erosions. This issue, however, remains controversial, as the presence of bone marrow edema, positive anti-CCP antibodies, and synovitis may pose sufficient risk of developing erosions, that treatment is warranted even in the absence of early erosions.

For patients undergoing treatment, the promise of MRI is its great potential for monitoring response to therapy and disease arrest or progression. There have been numerous reports using parameters such as the RAMRIS score, the number of erosions, the volume of erosions, the volume or thickness of synovitis, and the peak synovial enhancement to track response to treatment. An earlier version of the synovial component of the RAMRIS score showed good correlation to the volume of enhancing synovium [368]. Similarly, Dohn *et al.* showed good correlation between RAMRIS score, MR erosion volume, and CT erosion volume [369]. Until more automated techniques are developed to monitor disease activity and progression, one can expect to see variation in the parameters followed by individual investigators.

Examples of the successful use of these MRI parameters to track response to treatment included reduction in synovial and effusion volumes in response to intra-articular steroid injection [370], reduction in thickness of synovial enhancement in response to intra-articular steroids and methotrexate [371], reduced degree of enhancement of the synovium in response to infliximab [372], reduction in tenosynovitis in response to etanercept [373], reduced synovitis and arrested erosion development in response to adalimumab [374], and reduction in MRI findings of synovitis and bone edema in response to golimumab and methotrexate [375]. While all of these studies exhibited success in using MR to monitor response, low-grade synovitis may persist without erosion progression [376] or clinical progression [374]. Bone marrow edema may persist in patients in clinical remission as well [377]. The latter may explain why patients continue to develop erosions, despite clinically doing well and appearing to be in remission.

New MRI techniques

MRI scanning techniques have continued to be refined and are being actively investigated. There has been a gradual migration to using 3T systems for imaging because of their enhanced signal-to-noise ratios, and better spatial resolution as compared to 1.5T. Some of the resultant gain in signal may also be used to shorten exam times. 3T magnets are not as universally available as 1.5T, and equipment costs are considerably greater. Nevertheless, it can be expected

to see more studies done at 3T. Future studies of cartilage and cartilage loss in small joints may really benefit from use of the higher field 3T systems [378].

Diffusion-weighted imaging is a relatively new technique that is currently being used on 1.5T scanners for a wide variety of neuroradiologic and body imaging applications. By applying additional RF pulses and assessing the relative dephasing of spins of mobile versus less mobile protons, MRI can assess the relative diffusion protons in structures and abnormalities. In the context of cerebral infarcts, edema appears high signal on diffusion-weighted images but low signal on apparent diffusion coefficient (ADC) maps due to restricted diffusion of edema fluid. There are many MRI-related physical factors, which affect diffusion, not just the biologic properties of the tissue or fluid being imaged, but it may be possible to apply some of the quantitative measures such as ADC maps to bone marrow edema assessment. Clinical trials studying this are underway.

Synovitis is an important predictor of future erosion development. The degree of contrast enhancement has been used as a marker for the degree of synovitis [359]. Increasingly sophisticated pharmacokinetic modeling is also being applied [379]. The relative early enhancement and "shape" of the enhancement curve may have prognostic implications that can be quantitated in a more precise way than visual analysis of the enhancement of the synovium on the images. Accurate placement of representative region-of-interest curves to generate this data is a potential pitfall, but more rapid automated methods are now available that allow multiple enhancement data sets to be quickly reviewed and optimized.

Non-contrast techniques for assessing perfusion, such as arterial spin labeling, are becoming established techniques as well, and show good correlation with disease activity and traditional Gadolinium-based enhancement [380]. In patients who may need multiple MRI exams throughout their clinical care, non-contrast techniques may be beneficial in reducing cost and risk, especially if the patient has significant renal dysfunction that would preclude the use of Gadolinium.

Progress continues to be made on MRI quantification of rheumatoid arthritis in the hopes that less subjective and less time consuming automated methods may replace manual scoring. Scoring, however, still remains the standard against which other techniques are compared [381]. While subjective, manual scoring does, in general, result in good inter-reader reliability. There are 2 excellent reviews of quantification techniques, that the reader is referred to, which describe scoring methods, manual, and automated segmentation methods that are being developed [341, 382].

Conclusion

The clinical role of imaging in RA is greatly expanding. As this field rapidly progresses, imaging strategies are becoming increasingly integrated into the multi-disciplinary approach to RA patient management. Spearheading this change are the advances in imaging technologies and a further understanding of the molecular basis of RA. In particular, the current trend we are seeing is a shift toward more functional imaging. This not only means a more inclusive role for functional imaging modalities, such as SPECT and PET, but also a push for newer imaging sequences and strategies that allow MRI to move beyond anatomic imaging. Gadolinium-enhanced MRI and diffusion-weighted MRI are just two examples of how this imaging modality can provide more 'physiological' data. Furthermore, it is becoming more commonplace to use multi-modal imaging. PET/CT, SPECT/CT, and PET/MRI allow the fusion of complementary anatomic and functional data and thus offer high sensitivity, excellent tissue contrast, and improved spatial resolution. These hybrid imaging modalities are likely to be a future mainstay of the rapidly developing field of molecular imaging.

As we learn more about the active inflammatory processes specific to RA, we are gradually moving toward a molecular basis for imaging this disease. Imaging reporter agents have been and are being constructed that relay information about leukocyte trafficking, endothelial activation, cytokine-mediated inflammatory pathways, and apoptosis. When used in conjunction with the appropriate imaging modality, these probes have the potential to provide an earlier and more reliable assessment of clinical outcome, disease activity, severity, and location, and treatment response. Molecular imaging

may also allow for diagnoses early in the disease course prior to irreversible changes in joint anatomy, as evidence suggests there is a subclinical phase of RA, in which cellular and molecular changes precede any anatomic, physiological, or metabolic alterations. The future holds great promise for this field.

Acknowledgements

A special thanks is given to Dr. Kathleen Brindle, MD for her assistance in gathering the included imaging studies and Dr. Esma Akin, MD for her guidance on the covered content. We also thank the University of Michigan Undergraduate Research Opportunity Program (UROP) for financial support of MNZ.

Address correspondence to: Dr. Peter J. H. Scott, Department of Radiology, University of Michigan Medical School, 2276 Medical Science Building I / SPC 5610, Ann Arbor, MI, USA E-mail: pjhscott@umich.edu

References

[1] Gabriel SE. The epidemiology of rheumatoid arthritis. Rheum Dis Clin North Am 2001; 27: 269-281.

[2] Pincus T, Callahan LF, Sale WG, Brooks AL, Payne LE and Vaughn WK. Severe functional declines, work disability, and increased mortality in seventy-five rheumatoid arthritis patients studied over nine years. Arthritis Rheum 1984; 27: 864-872.

[3] Wolfe F, Mitchell DM, Sibley JT, Fries JF, Bloch DA, Williams CA, Spitz PW, Haga M, Kleinheksel SM and Cathey MA. The mortality of rheumatoid arthritis. Arthritis Rheum 1994; 37: 481-494.

[4] Choy EH, Kingsley GH, Panayi GS. Monoclonal antibody therapy in rheumatoid arthritis. Br J Rheumatol 1998; 37: 484-490.

[5] Fan PT and Leong KH. The use of biological agents in the treatment of rheumatoid arthritis. Ann Acad Med Singapore 2007; 36: 128-134.

[6] Smolen JS, Aletaha D, Koeller M, Weisman MH and Emery P. New therapies for treatment of rheumatoid arthritis. Lancet 2007; 370: 1861-1874.

[7] O'Dell JR, Haire CE, Erikson N, Drymalski W, Palmer W, Eckhoff PJ, Garwood V, Maloley P, Klassen LW, Wees S, Klein H and Moore GF. Treatment of rheumatoid arthritis with methotrexate alone, sulfasalazine and hydroxychloroquine, or a combination of all three medications. N Engl J Med 1996; 334: 1287-1291.

[8] Landewè RB, Boers M, Verhoeven AC, Westhovens R, van de Laar MA, Markusse HM, van Denderen JC, Westedt ML, Peeters AJ, Dijkmans BA, Jacobs P, Boonen A, van der Heijde DM and van der Linden S. COBRA combination therapy in patients with early rheumatoid arthritis: long-term structural benefits of a brief intervention. Arthritis Rheum 2002; 46: 347-356.

[9] Scott DL, Kingsley GH. Tumor necrosis factor inhibitors for rheumatoid arthritis. N Engl J Med 2006; 355: 704-712.

[10] Emery P. The Roche Rheumatology Prize Lecture. The optimal management of early rheumatoid disease: the key to preventing disability. Br J Rheumatol 1994; 33: 765-768.

[11] Pichler BJ, Wehrl HF and Judenhofer MS. Latest advances in molecular imaging instrumentation. J Nucl Med 2008; 49 (Suppl 2): 5S-23S.

[12] Wunder A, Straub RH, Gay S, Funk J and Müller-Ladner U. Molecular imaging: novel tools in visualizing rheumatoid arthritis. Rheumatology (Oxford) 2005; 44: 1341-1349.

[13] Tak PP, Smeets TJ, Daha MR, Kluin PM, Meijers KA, Brand R, Meinders AE and Breedveld FC. Analysis of the synovial cell infiltrate in early rheumatoid synovial tissue in relation to local disease activity. Arthritis Rheum 1997; 40: 217-225.

[14] Kraan MC, Versendaal H, Jonker M, Bresnihan B, Post WJ, t Hart BA, Breedveld FC and Tak PP. Asymptomatic synovitis precedes clinically manifest arthritis. Arthritis Rheum 1998; 41: 1481-1488.

[15] Gregersen PK, Silver J and Winchester RJ. The shared epitope hypothesis. An approach to understanding the molecular genetics of susceptibility to rheumatoid arthritis. Arthritis Rheum 1987; 30: 1205-1213.

[16] Mueller DL, Jenkins MK and Schwartz RH. Clonal expansion versus functional clonal inactivation: a costimulatory signalling pathway determines the outcome of T cell antigen receptor occupancy. Annu Rev Immunol 1989; 7: 445-480.

[17] Frauwirth KA, Thompson CB. Activation and inhibition of lymphocytes by costimulation. J Clin Invest 2002; 109: 295-299.

[18] Steiner G, Tohidast-Akrad M, Witzmann G, Vesely M, Studnicka-Benke A, Gal A, Kunaver M, Zenz P and Smolen JS. Cytokine production by synovial T cells in rheumatoid arthritis. Rheumatology (Oxford) 1999; 38: 202-213.

[19] Bombara MP, Webb DL, Conrad P, Marlor CW, Sarr T, Ranges GE, Aune TM, Greve JM, and Blue ML. Cell contact between T cells and synovial fibroblasts causes induction of adhesion molecules and cytokines. J Leukoc Biol 1993; 54: 399-406.

[20] Kong YY, Feige U, Sarosi I, Bolon B, Tafuri A, Morony S, Capparelli C, Li J, Elliott R, McCabe S, Wong T, Campagnuolo G, Moran E, Bogoch ER, Van G, Nguyen LT, Ohashi PS, Lacey DL, Fish E,

Boyle WJ and Penninger JM. Activated T cells regulate bone loss and joint destruction in adjuvant arthritis through osteoprotegerin ligand. Nature 1999; 402: 304-309.
[21] Firestein GS, Alvaro-Gracia JM and Maki R. Quantitative analysis of cytokine gene expression in rheumatoid arthritis. J Immunol 1990; 144: 3347-3353.
[22] Feldmann M, Brennan FM, Foxwell BM and Maini RN. The role of TNF α and IL-1 in rheumatoid arthritis. Curr Dir Autoimmun 2001; 3: 188 -199.
[23] Zwerina J, Redlich K, Schett G and Smolen JS. Pathogenesis of rheumatoid arthritis: targeting cytokines. Ann N Y Acad Sci 2005; 1051: 716-729.
[24] Springer TA. Adhesion receptors of the immune system. Nature 1990; 346: 425-434.
[25] Levick JR. Permeability of rheumatoid and normal human synovium to specific plasma proteins. Arthritis Rheum 1981; 24: 1550-1560.
[26] Firestein GS. Invasive fibroblast-like synoviocytes in rheumatoid arthritis. Passive responders or transformed aggressors? Arthritis Rheum 1996; 39: 1781-1790.
[27] Gravallese EM, Harada Y, Wang JT, Gorn AH, Thornhill TS and Goldring SR. Identification of cell types responsible for bone resorption in rheumatoid arthritis and juvenile rheumatoid arthritis. Am J Pathol 1998; 152: 943-951.
[28] Pap T, Claus A, Ohtsu S, Hummel KM, Schwartz P, Drynda S, Pap G, Machner A, Stein B, George M, Gay RE, Neumann W, Gay S and Aicher WK. Osteoclast-independent bone resorption by fibroblast-like cells. Arthritis Res Ther 2003; 5: R163-173.
[29] Mettler FA Jr, Guiberteau MJ. Positron Emission Tomography (PET) Imaging. Essentials of Nuclear Medicine Imaging. 5th edition. Philadelphia: Saunders; 2006; p. 359-423.
[30] Kubota R, Yamada S, Kubota K, Ishiwata K, Tamahashi N and Ido T. Intratumoral distribution of fluorine-18-fluorodeoxyglucose *in vivo*: high accumulation in macrophages and granulation tissues studied by microautoradiography. J Nucl Med 1992; 33: 1972-1980.
[31] Kubota K, Kubota R and Yamada S. FDG accumulation in tumor tissue. J Nucl Med 1993; 34: 419-421.
[32] Yamada S, Kubota K, Kubota R, Ido T and Tamahashi N. High accumulation of fluorine-18 -fluorodeoxyglucose in turpentine-induced inflammatory tissue. J Nucl Med 1995; 36: 1301-1306.
[33] Carey K, Saboury B, Basu S, Brothers A, Ogdie A, Werner T, Torigian DA and Alavi A. Evolving role of FDG PET imaging in assessing joint disorders: a systematic review. Eur J Nucl Med Mol Imaging 2011; 38: 1939-1955.
[34] Matsui T, Nakata N, Nagai S, Nakatani A, Takahashi M, Momose T, Ohtomo K and Koyasu S. Inflammatory cytokines and hypoxia contribute to ^{18}F-FDG uptake by cells involved in pannus formation in rheumatoid arthritis. J Nucl Med 2009; 50: 920-926.
[35] Palmer WE, Rosenthal DI, Schoenberg OI, Fischman AJ, Simon LS, Rubin R and Polisson RP. Quantification of inflammation in the wrist with gadolinium-enhanced MR imaging and PET with 2-[F-18]-fluoro-2-deoxy-D-glucose. Radiology 1995; 196: 647-655.
[36] Polisson RP, Schoenberg OI, Fischman A, Rubin R, Simon LS, Rosenthal D and Palmer WE. Use of magnetic resonance imaging and positron emission tomography in the assessment of synovial volume and glucose metabolism in patients with rheumatoid arthritis. Arthritis Rheum 1995; 38: 819-825.
[37] Beckers C, Ribbens C, Andre B, Marcelis S, Kaye O, Mathy L, Kaiser MJ, Hustinx R, Foidart J and Malaise MG. Assessment of disease activity in rheumatoid arthritis with ^{18}F-FDG PET. J Nucl Med 2004; 45: 956-964.
[38] Brenner W. ^{18}F-FDG PET in rheumatoid arthritis: there still is a long way to go. J Nucl Med 2004; 45: 927-929.
[39] Beckers C, Jeukens X, Ribbens C, Andre B, Marcelis S, Leclercq P, Kaiser MJ, Foidart J, Hustinx R and Malaise MG. ^{18}F-FDG PET imaging of rheumatoid knee synovitis correlates with dynamic magnetic resonance and sonographic assessments as well as with the serum level of metalloproteinase-3. Eur J Nucl Med Mol Imaging 2006; 33: 275-280.
[40] Goerres GW, Forster A, Uebelhart D, Seifert B, Treyer V, Michel B, von Schulthess GK and Kaim AH. F-18 FDG whole-body PET for the assessment of disease activity in patients with rheumatoid arthritis. Clin Nucl Med 2006; 31: 386-390.
[41] Elzinga EH, van der Laken CJ, Comans EF, Boellaard R, Hoekstra OS, Dijkmans BA, Lammertsma AA and Voskuyl AE. ^{18}F-FDG PET as a tool to predict the clinical outcome of infliximab treatment of rheumatoid arthritis: an explorative study. J Nucl Med 2011; 52: 77-80.
[42] Vogel WV, van Riel PL and Oyen WJ. FDG-PET/CT can visualise the extent of inflammation in rheumatoid arthritis of the tarsus. Eur J Nucl Med Mol Imaging 2007; 34: 439.
[43] dos Anjos DA, do Vale GF, Campos Cde M, do Prado LF, Sobrinho AB, da Cunha AL and Santos AC. Extra-articular inflammatory sites detected by F-18 FDG PET/CT in a patient with rheumatoid arthritis. Clin Nucl Med 2010; 35: 540-541.
[44] Kaneta T, Hakamatsuka T, Yamada T, Takase K, Sato A, Higano S, Ito H, Fukuda H, Takahashi S and Yamada S. Atlantoaxial osteoarthritis in rheumatoid arthritis: FDG PET/CT findings. Clin Nucl Med 2006; 31: 209.
[45] Ju JH, Kang KY, Kim IJ, Yoon JU, Kim HS, Park SH and Kim HY. Visualization and localization of rheumatoid knee synovitis with FDG-PET/CT

images. Clin Rheumatol 2008; 27(Suppl 2): S39-41.
[46] Kubota K, Ito K, Morooka M, Mitsumoto T, Kurihara K, Yamashita H, Takahashi Y and Mimori A. Whole-body FDG-PET/CT on rheumatoid arthritis of large joints. Ann Nucl Med 2009; 23: 783-791.
[47] Kubota K, Ito K, Morooka M, Minamimoto R, Miyata Y, Yamashita H, Takahashi Y and Mimori A. FDG PET for rheumatoid arthritis: basic considerations and whole-body PET/CT. Ann N Y Acad Sci 2011; 1228: 29-38.
[48] Neva MH, Hakkinen A, Makinen H, Hannonen P, Kauppi M and Sokka T. High prevalence of asymptomatic cervical spine subluxation in patients with rheumatoid arthritis waiting for orthopaedic surgery. Ann Rheum Dis 2006; 65: 884-888.
[49] Linn-Rasker SP, van der Helm-van Mil AH, Breedveld FC and Huizinga TW. Arthritis of the large joints - in particular, the knee - at first presentation is predictive for a high level of radiological destruction of the small joints in rheumatoid arthritis. Ann Rheum Dis 2007; 66: 646-650.
[50] Chaudhari AJ, Bowen SL, Burkett GW, Packard NJ, Godinez F, Joshi AA, Naguwa SM, Shelton DK, Hunter JC, Boone JM, Buonocore MH and Badawi RD. High-resolution ^{18}F-FDG PET with MRI for monitoring response to treatment in rheumatoid arthritis. Eur J Nucl Med Mol Imaging 2010; 37: 1047.
[51] El-Haddad G, Kumar R, Pamplona R and Alavi A. PET/MRI depicts the exact location of meniscal tear associated with synovitis. Eur J Nucl Med Mol Imaging 2006; 33: 507-508.
[52] Miese F, Scherer A, Ostendorf B, Heinzel A, Lanzman RS, Kropil P, Blondin D, Hautzel H, Wittsack HJ, Schneider M, Antoch G, Herzog H and Shah NJ. Hybrid ^{18}F-FDG PET-MRI of the hand in rheumatoid arthritis: initial results. Clin Rheumatol 2011; 30: 1247-1250.
[53] Zeisel SH. Dietary choline: biochemistry, physiology, and pharmacology. Annu Rev Nutr 1981; 1: 95-121.
[54] Ishidate K. Choline transport and choline kinase. Phoshatidylcholine metabolism. Edited by Vance DE. Boca Raton: CRC Press; 1989; p. 9-32.
[55] Zeisel SH. Choline phospholipids: signal transduction and carcinogenesis. FASEB J 1993; 7: 551-557.
[56] Katz-Brull R, Degani H. Kinetics of choline transport and phosphorylation in human breast cancer cells; NMR application of the zero trans method. Anticancer Res 1996; 16: 1375-1380.
[57] Shinoura N, Nishijima M, Hara T, Haisa T, Yamamoto H, Fujii K, Mitsui I, Kosaka N and Kondo T. Brain tumors: detection with C-11 choline PET. Radiology 1997; 202: 497-503.
[58] Ohtani T, Kurihara H, Ishiuchi S, Saito N, Oriuchi N, Inoue T and Sasaki T. Brain tumour imaging with carbon-11 choline: comparison with FDG PET and gadolinium enhanced MR imaging. Eur J Nucl Med 2001; 28: 1664-1670.
[59] Utriainen M, Komu M, Vuorinen V, Lehikoinen P, Sonninen P, Kurki T, Utriainen T, Roivainen A, Kalimo H and Minn H. Evaluation of brain tumor metabolism with [^{11}C]choline PET and ^{1}H-MRS. J Neurooncol 2003; 62: 329-338.
[60] Kobori O, Kirihara Y, Kosaka N and Hara T. Positron emission tomography of esophageal carcinoma using ^{11}C-choline and ^{18}F-fluorodeoxyglucose: a novel method of preoperative lymph node staging. Cancer 1999; 86: 1638-1648.
[61] Jager PL, Que TH, Vaalburg W, Pruim J, Elsinga P and Plukker JT. Carbon-11 choline or FDG-PET for staging of oesophageal cancer? Eur J Nucl Med 2001; 28: 1845-1849.
[62] Hara T, Inagaki K, Kosaka N and Morita T. Sensitive detection of mediastinal lymph node metastasis of lung cancer with ^{11}C-choline PET. J Nucl Med 2000; 41: 1507-1513.
[63] Kotzerke J, Prang J, Neumaier B, Volkmer B, Guhlmann A, Kleinschmidt K, Hautmann R and Reske SN. Experience with carbon-11 choline positron emission tomography in prostate carcinoma. Eur J Nucl Med 2000; 27: 1415-1419.
[64] de Jong IJ, Pruim J, Elsinga PH, Jongen MM, Mensink HJ and Vaalburg W. Visualisation of bladder cancer using ^{11}C-choline PET: first clinical experience. Eur J Nucl Med Mol Imaging 2002; 29: 1283-1288.
[65] Roivainen A, Parkkola R, Yli-Kerttula T, Lehikoinen P, Viljanen T, Möttönen T, Nuutila P and Minn H. Use of positron emission tomography with methyl-^{11}C-choline and 2-^{18}F-fluoro-2-deoxy-D-glucose in comparison with magnetic resonance imaging for the assessment of inflammatory proliferation of synovium. Arthritis Rheum 2003; 48: 3077-3084.
[66] Patlak CS, Blasberg RG and Fenstermacher JD. Graphical evaluation of blood-to-brain transfer constants from multiple-time uptake data. J Cereb Blood Flow Metab 1983; 3: 1-7.
[67] Roivainen A and Yli-Kerttula T. Whole-body distribution of ^{11}C-choline and uptake in knee synovitis. Eur J Nucl Med Mol Imaging 2006; 33: 1372-1373.
[68] Tolvanen T, Yli-Kerttula T, Ujula T, Autio A, Lehikoinen P, Minn H and Roivainen A. Biodistribution and radiation dosimetry of [^{11}C]choline: a comparison between rat and human data. Eur J Nucl Med Mol Imaging 2010; 37: 874-883.
[69] DeGrado TR, Reiman RE, Price DT, Wang S and Coleman RE. Pharmacokinetics and radiation dosimetry of ^{18}F-fluorocholine. J Nucl Med 2002; 43: 92-96.
[70] Zavala F, Lenfant M. Benzodiazepines and PK 11195 exert immunomodulating activities by binding on a specific receptor on macrophages. Ann N Y Acad Sci 1987; 496: 240-249.

[71] Canat X, Carayon P, Bouaboula M, Cahard D, Shire D, Roque C, Le Fur G and Casellas P. Distribution profile and properties of peripheral-type benzodiazepine receptors on human hemopoietic cells. Life Sci 1993; 52: 107-118.
[72] Bazzichi L, Betti L, Giannaccini G, Rossi A and Lucacchini A. Peripheral-type benzodiazepine receptors in human mononuclear cells of patients affected by osteoarthritis, rheumatoid arthritis or psoriasic arthritis. Clin Biochem 2003; 36: 57-60.
[73] Papadopoulos V, Baraldi M, Guilarte TR, Knudsen TB, Lacapere JJ, Lindemann P, Norenberg MD, Nutt D, Weizman A, Zhang MR and Gavish M. Translocator protein (18kDa): new nomenclature for the peripheral-type benzodiazepine receptor based on its structure and molecular function. Trends Pharmacol Sci 2006; 27: 402-409.
[74] Giusti L, Betti L, Giannaccini G, Mascia G, Bazzichi L and Lucacchini A. [^{3}H]PK11195 binding sites in human neutrophils: effect of fMLP stimulation and modulation in rheumatic diseases. Clin Biochem 2004; 37: 61-66.
[75] Veenman L, Papadopoulos V and Gavish M. Channel-like functions of the 18-kDa translocator protein (TSPO): regulation of apoptosis and steroidogenesis as part of the host-defense response. Curr Pharm Des 2007; 13: 2385-2405.
[76] Scarf AM, Kassiou M. The translocator protein. J Nucl Med 2011; 52: 677-680.
[77] Krueger KE. Molecular and functional properties of mitochondrial benzodiazepine receptors. Biochim Biophys Acta 1995; 1241: 453-470.
[78] Casellas P, Galiegue S and Basile AS. Peripheral benzodiazepine receptors and mitochondrial function. Neurochem Int 2002; 40: 475-486.
[79] Rosenberg N, Rosenberg O, Weizman A, Leschiner S, Sakoury Y, Fares F, Soudry M, Weisinger G, Veenman L and Gavish M. In vitro mitochondrial effects of PK 11195, a synthetic translocator protein 18 kDa (TSPO) ligand, in human osteoblast-like cells. J Bioenerg Biomembr 2011; 43: 739-746.
[80] Banati RB, Newcombe J, Gunn RN, Cagnin A, Turkheimer F, Heppner F, Price G, Wegner F, Giovannoni G, Miller DH, Perkin GD, Smith T, Hewson AK, Bydder G, Kreutzberg GW, Jones T, Cuzner ML and Myers R. The peripheral benzodiazepine binding site in the brain in multiple sclerosis: quantitative *in vivo* imaging of microglia as a measure of disease activity. Brain 2000; 123: 2321-2337.
[81] Hammoud DA, Endres CJ, Chander AR, Guilarte TR, Wong DF, Sacktor NC, McArthur JC and Pomper MG. Imaging glial cell activation with [^{11}C]-R-PK11195 in patients with AIDS. J Neurovirol 2005; 11: 346-355.
[82] Rojas S, Martín A, Arranz MJ, Pareto D, Purroy J, Verdaguer E, Llop J, Gómez V, Gispert JD, Millán O, Chamorro A and Planas AM. Imaging brain inflammation with [^{11}C]PK11195 by PET and induction of the peripheral-type benzodiazepine receptor after transient focal ischemia in rats. J Cereb Blood Flow Metab 2007; 27: 1975-1986.
[83] van der Laken CJ, Elzinga EH, Kropholler MA, Molthoff CF, van der Heijden JW, Maruyama K, Boellaard R, Dijkmans BA, Lammertsma AA and Voskuyl AE. Noninvasive imaging of macrophages in rheumatoid synovitis using ^{11}C-*(R)*-PK11195 and positron emission tomography. Arthritis Rheum 2008; 58: 3350-3355.
[84] Gent YY, Voskuyl AE, Kloet RW, van Schaardenburg D, Hoekstra OS, Dijkmans BA, Lammertsma AA and van der Laken CJ. Macrophage positron emission tomography imaging as a biomarker for preclinical rheumatoid arthritis: Findings of a prospective pilot study. Arthritis Rheum 2012; 64: 62-66.
[85] Luoto P, Laitinen I, Suilamo S, Nagren K and Roivainen A. Human dosimetry of carbon-11 labeled *N*-butan-2-yl-1-(2-chlorophenyl)-*N*-methylisoquinoline-3 carboxamide extrapolated from whole-body distribution kinetics and radiometabolism in rats. Mol Imaging Biol 2010; 12: 435-442.
[86] Roivainen A, Någren K, Hirvonen J, Oikonen V, Virsu P, Tolvanen T and Rinne JO. Whole body distribution and metabolism of [N-methyl-^{11}C] *(R)*-1-(2-chlorophenyl)-*N*-(1 methylpropyl)-3-isoquinolinecarb oxamide in humans; an imaging agent for in vivo assessment of peripheral benzodiazepine receptor activity with positron emission tomography. Eur J Nucl Med Mol Imaging 2009; 36: 671-682.
[87] Hirvonen J, Roivainen A, Virta J, Helin S, Någren K and Rinne JO. Human biodistribution and radiation dosimetry of ^{11}C-*(R)*-PK11195, the prototypic PET ligand to image inflammation. Eur J Nucl Med Mol Imaging 2010; 37: 606-612.
[88] Venneti S, Lopresti BJ and Wiley CA. The peripheral benzodiazepine receptor (Translocator protein 18kDa) in microglia: from pathology to imaging. Prog Neurobiol 2006; 80: 308-322.
[89] Arlicot N, Vercouillie J, Ribeiro MJ, Tauber C, Venel Y, Baulieu JL, Maia S, Corcia P, Stabin MG, Reynolds A, Kassiou M, Guilloteau D. Initial evaluation in healthy humans of [^{18}F]DPA-714, a potential PET biomarker for neuroinflammation. Nucl Med Biol 2011.
[90] Chauveau F, Boutin H, Van Camp N, Dollé F and Tavitian B. Nuclear imaging of neuroinflammation: a comprehensive review of [^{11}C]PK11195 challengers. Eur J Nucl Med Mol Imaging 2008; 35: 2304-2319.
[91] Boutin H, Chauveau F, Thominiaux C, Grégoire MC, James ML, Trebossen R, Hantraye P, Dollé F, Tavitian B and Kassiou M. ^{11}C-DPA-713: a novel peripheral benzodiazepine receptor PET ligand for in vivo imaging of neuroinflammation.

J Nucl Med 2007; 48: 573-581.
[92] Endres CJ, Pomper MG, James M, Uzuner O, Hammoud DA, Watkins CC, Reynolds A, Hilton J, Dannals RF and Kassiou M. Initial evaluation of ^{11}C-DPA-713, a novel TSPO PET ligand, in humans. J Nucl Med 2009; 50: 1276-1282.
[93] Chauveau F, Van Camp N, Dollé F, Kuhnast B, Hinnen F, Damont A, Boutin H, James M, Kassiou M and Tavitian B. Comparative evaluation of the translocator protein radioligands ^{11}C-DPA-713, ^{18}F-DPA-714, and ^{11}C-PK11195 in a rat model of acute neuroinflammation. J Nucl Med 2009; 50: 468-476.
[94] Doorduin J, Klein HC, Dierckx RA, James M, Kassiou M and de Vries EF. [^{11}C]-DPA-713 and [^{18}F]-DPA-714 as new PET tracers for TSPO: a comparison with [^{11}C]-*(R)*-PK11195 in a rat model of herpes encephalitis. Mol Imaging Biol 2009; 11: 386-398.
[95] Ikoma Y, Yasuno F, Ito H, Suhara T, Ota M, Toyama H, Fujimura Y, Takano A, Maeda J, Zhang MR, Nakao R and Suzuki K. Quantitative analysis for estimating binding potential of the peripheral benzodiazepine receptor with [^{11}C] DAA1106. J Cereb Blood Flow Metab 2007; 27: 173-184.
[96] Venneti S, Wang G and Wiley CA. The high affinity peripheral benzodiazepine receptor ligand DAA1106 binds to activated and infected brain macrophages in areas of synaptic degeneration: implications for PET imaging of neuroinflammation in lentiviral encephalitis. Neurobiol Dis 2008; 29: 232-241.
[97] Miyoshi M, Ito H, Arakawa R, Takahashi H, Takano H, Higuchi M, Okumura M, Otsuka T, Kodaka F, Sekine M, Sasaki T, Fujie S, Seki C, Maeda J, Nakao R, Zhang MR, Fukumura T, Matsumoto M and Suhara T. Quantitative analysis of peripheral benzodiazepine receptor in the human brain using PET with ^{11}C-AC-5216. J Nucl Med 2009; 50: 1095-1101.
[98] Dickstein LP, Zoghbi SS, Fujimura Y, Imaizumi M, Zhang Y, Pike VW, Innis RB and Fujita M. Comparison of ^{18}F- and ^{11}C-labeled aryloxyanilide analogs to measure translocator protein in human brain using positron emission tomography. Eur J Nucl Med Mol Imaging 2011; 38: 352-357.
[99] Fujimura Y, Ikoma Y, Yasuno F, Suhara T, Ota M, Matsumoto R, Nozaki S, Takano A, Kosaka J, Zhang MR, Nakao R, Suzuki K, Kato N and Ito H. Quantitative analyses of ^{18}F-FEDAA1106 binding to peripheral benzodiazepine receptors in living human brain. J Nucl Med 2006; 47: 43-50.
[100] Takano A, Gulyas B, Varrone A, Karlsson P, Sjoholm N, Larsson S, Jonsson C, Odh R, Sparks R, Al Tawil N, Hoffmann A, Zimmermann T, Thiele A and Halldin C. Biodistribution and radiation dosimetry of the 18 kDa translocator protein (TSPO) radioligand [^{18}F]FEDAA1106: a human whole-body PET study. Eur J Nucl Med Mol Imaging 2011; 38: 2058-2065.
[101] Hoffer P. Gallium: mechanisms. J Nucl Med 1980; 21: 282-285.
[102] Tzen KY, Oster ZH, Wagner HN Jr and Tsan MF. Role of iron-binding proteins and enhanced capillary permeability on the accumulation of gallium-67. J Nucl Med 1980; 21: 31-35.
[103] Weiner R. The role of transferrin and other receptors in the mechanism of ^{67}Ga localization. Int J Rad Appl Instrum B 1990; 17: 141-149.
[104] Gelrud LG, Arseneau JC, Milder MS, Kramer RJ, Swann SJ, Canellos GP and Johnston GS. The kinetics of ^{67}gallium incorporation into inflammatory lesions: experimental and clinical studies. J Lab Clin Med 1974; 83: 489-495.
[105] Handmaker H and O'Mara RE. Gallium imaging in pediatrics. J Nucl Med 1977; 18: 1057-1063.
[106] Tsan MF, Chen WY, Scheffel U and Wagner HN Jr. Studies on gallium accumulation in inflammatory lesions: I. Gallium uptake by human polymorphonuclear leukocytes. J Nucl Med 1978; 19: 36-43.
[107] Otsuki H, Brunetti A, Owens ES, Finn RD and Blasberg RG. Comparison of iron-59, indium-111, and gallium-69 transferrin as a macromolecular tracer of vascular permeability and the transferrin receptor. J Nucl Med 1989; 30: 1676-1685.
[108] Menon S, Wagner HN Jr and Tsan MF. Studies on gallium accumulation in inflammatory lesions: II. Uptake by Staphylococcus aureus: concise communication. J Nucl Med 1978; 19: 44-47.
[109] Brunetti A, Blasberg RG, Finn RD and Larson SM. Gallium-transferrin as a macromolecular tracer of vascular permeability. Int J Rad Appl Instrum B 1988; 15: 665-672.
[110] Wilkins M, Williams P and Cavill I. Transferrin iron uptake by human synovium. Ann Rheum Dis 1977; 36: 474-475.
[111] Lee SI, Kim EM, Kim SL, Lee CM, Jang KY, Yun HJ, Yoo WH, Sohn MH and Jeong HJ. Molecular scintigraphic imaging using ^{99m}Tc-transferrin is useful for early detection of synovial inflammation of collagen-induced arthritis mouse. Rheumatol Int 2008; 29: 153-157.
[112] Seabold JE, Palestro CJ, Brown ML, Datz FL, Forstrom LA, Greenspan BS, McAfee JG, Schauwecker DS and Royal HD. Procedure guideline for gallium scintigraphy in inflammation. Society of Nuclear Medicine. J Nucl Med 1997; 38: 994-997.
[113] Ercan MT, Aras T, Ünlenen E, Ünlü M, Ünsal IS and Hasçelik Z. ^{99m}Tc-citrate versus ^{67}Ga-citrate for the scintigraphic visualization of inflammatory lesions. Nucl Med Biol 1993; 20: 881-887.
[114] Coleman RE, Samuelson CO Jr, Baim S, Christian PE and Ward JR. Imaging with Tc-99m MDP and Ga-67 citrate in patients with rheumatoid arthritis and suspected septic arthritis: concise communication. J Nucl Med 1982; 23: 479-

482.
[115] McCall IW, Sheppard H, Haddaway M, Park WM and Ward DJ. Gallium 67 scanning in rheumatoid arthritis. Br J Radiol 1983; 56: 241-243.
[116] Palestro CJ. The current role of gallium imaging in infection. Semin Nucl Med 1994; 24: 128-141.
[117] Liberatore M, Clemente M, Iurilli AP, Zorzin L, Marini M, Di Rocco E, Colella AC. Scintigraphic evaluation of disease activity in rheumatoid arthritis: a comparison of technetium-99m human non-specific immunoglobulins, leucocytes and albumin nanocolloids. Eur J Nucl Med 1992; 19: 853-857.
[118] Vesterskiöld L, Schnell PO and Jacobsson H. Comparison between scintigraphy with polyclonal immunoglobulin ($^{99}Tc^{m}$-HIG) and physical examination in polyarthritic disease. Scand J Rheumatol 1996; 25: 159-163.
[119] Sahin M, Bernay I, Basoglu T and Canturk F. Comparison of Tc-99m MDP, Tc-99m HAS and Tc-99m HIG uptake in rheumatoid arthritis and its variants. Ann Nucl Med 1999; 13: 389-395.
[120] Pons F, Sanmarti R, Herranz R, Collado A, Piera C, Vidal-Sicart S, Muñoz-Gomez J and Setoain J. Scintigraphic evaluation of the severity of inflammation of the joints with $^{99}Tc^{m}$-HIG in rheumatoid arthritis. Nucl Med Commun 1996; 17: 523-528.
[121] de Bois MH, Arndt JW, Speyer I, Pauwels EK and Breedveld FC. Technetium-99m labelled human immunoglobulin scintigraphy predicts rheumatoid arthritis in patients with arthralgia. Scand J Rheumatol 1996; 25: 155-158.
[122] de Bois MH, Tak PP, Arndt JW, Kluin PM, Pauwels EK and Breedveld FC. Joint scintigraphy for quantification of synovitis with ^{99m}Tc-labelled human immunoglobulin G compared to histological examination. Clin Exp Rheumatol 1995; 13: 155-159.
[123] Desaulniers M, Fuks A, Hawkins D, Lacourciere Y and Rosenthall L. Radiotechnetium polyphosphate joint imaging. J Nucl Med 1974; 15: 417-423.
[124] Möttönen TT, Hannonen P, Toivanen J, Rekonen A and Oka M. Value of joint scintigraphy in the prediction of erosiveness in early rheumatoid arthritis. Ann Rheum Dis 1988; 47: 183-189.
[125] Peepre K, Shah D, Solanki S, Tiwari AN and Pisal R. Clinical utility of nuclear medicine 99mTc-MDP bone scan in the early diagnosis of rheumatoid arthritis. Turk J Pediatr 2008; 50: 194-195.
[126] Rosenthall L. Nuclear medicine techniques in arthritis. Rheum Dis Clin North Am 1991; 17: 585-597.
[127] Sandrock D, Backhaus M, Burmester G and Munz DL. Imaging techniques in rheumatology: scintigraphy in rheumatoid arthritis. Z Rheumatol 2003; 62: 476-480.
[128] Jamar F, Houssiau FA, Devogelaer JP, Chapman PT, Haskard DO, Beaujean V, Beckers C, Manicourt DH and Peters AM. Scintigraphy using a technetium 99m labelled anti-E-selectin Fab fragment in rheumatoid arthritis. Rheumatology (Oxford) 2002; 41: 53-61.
[129] Helfgott S, Rosenthall L, Esdaile J and Tannenbaum H. Generalized skeletal response to ^{99m}technetium methylene diphosphonate in rheumatoid arthritis. J Rheumatol 1982; 9: 939-941.
[130] Ostendorf B, Mattes-Gyorgy K, Reichelt DC, Blondin D, Wirrwar A, Lanzman R, Muller HW, Schneider M, Modder U and Scherer A. Early detection of bony alterations in rheumatoid and erosive arthritis of finger joints with high-resolution single photon emission computed tomography, and differentiation between them. Skeletal Radiol 2010; 39: 55-61.
[131] Schramm NU, Ebel G, Engeland U, Schurrat T, Behe M and Behr TM. High-resolution SPECT using multipinhole collimation. IEEE Trans Nucl Sci 2003; 50: 315-320.
[132] Ostendorf B, Scherer A, Wirrwar A, Hoppin JW, Lackas C, Schramm NU, Cohnen M, Modder U, van den Berg WB, Muller HW, Schneider M and Joosten LA. High-resolution multipinhole single-photon-emission computed tomography in experimental and human arthritis. Arthritis Rheum 2006; 54: 1096-1104.
[133] Ercan MT, Kostakoğlu L. Radiopharmaceuticals for the visualization of infectious and inflammatory lesions. Curr Pharm Des 2000; 6: 1159-1177.
[134] Van Hemert FJ, Voermans C, Van Eck-Smit BL and Bennink RJ. Labeling monocytes for imaging chronic inflammation. Q J Nucl Med Mol Imaging 2009; 53: 78-88.
[135] Gaál J, Mezes A, Siro B, Varga J, Galuska L, Janoky G, Garai I, Bajnok L and Suranyi P. ^{99m}Tc-HMPAO labelled leukocyte scintigraphy in patients with rheumatoid arthritis: a comparison with disease activity. Nucl Med Commun 2002; 23: 39-46.
[136] Al-Janabi MA, Jones AK, Solanki K, Sobnack R, Bomanji J, Al-Nahhas AA, Doyle DV, Britton KE and Huskisson EC. $^{99}Tc^{m}$-labelled leucocyte imaging in active rheumatoid arthritis. Nucl Med Commun 1988; 9: 987-991.
[137] Bennink RJ, Thurlings RM, van Hemert FJ, Voermans C, Dohmen SE, van Eck-Smit BL, Tak PP and Busemann-Sokole E. Biodistribution and radiation dosimetry of ^{99m}Tc HMPAO-labeled monocytes in patients with rheumatoid arthritis. J Nucl Med 2008; 49: 1380-1385.
[138] Thurlings RM, Wijbrandts CA, Bennink RJ, Dohmen SE, Voermans C, Wouters D, Izmailova ES, Gerlag DM, van Eck-Smit BL and Tak PP. Monocyte scintigraphy in rheumatoid arthritis: the dynamics of monocyte migration in immune-mediated inflammatory disease. PLoS One 2009; 4: e7865.
[139] Hmama Z, Kouassi E, Panaye G, Delassan S,

Normier G, Binz H and Revillard JP. Binding of a bacterial acylpoly(1,3)galactoside to human blood leucocytes. Scand J Immunol 1992; 36: 11-20.
[140] Hmama Z, Normier G, Kouassi E, Flacher M, Binz H and Revillard JP. Binding of a membrane proteoglycan from *Klebsiella pneumoniae* and its derivatives to human leukocytes. Immunobiology 1992; 186: 183-198.
[141] Kouassi E, Hmama Z, Lina G, Vial J, Faure-Barba F, Normier G, Binz H and Revillard JP. Activation of human monocyte chemiluminescence response by acylpoly(1,3)galactosides derived from *Klebsiella pneumoniae*. J Leukoc Biol 1992; 52: 529-536.
[142] Le Pape A. The targeting of macrophages with bacterial proteoglycans: a new strategy for the scintigraphic imaging of tumors and inflammatory lesions. Eur J Nucl Med 1989; 15: 424.
[143] Hmama Z, Mey A, Normier G, Binz H and Revillard JP. CD14 and CD11b mediate serum-independent binding to human monocytes of an acylpolygalactoside isolated from *Klebsiella pneumoniae*. Infect Immun 1994; 62: 1520-1527.
[144] Hmama Z, Lina G, Normier G, Binz H and Revillard JP. Role of acyl residues in polyclonal murine B cell activation by acylpoly(1,3) galactosides from *Klebsiella pneumoniae*. J Immunol 1993; 151: 5440-5449.
[145] Fenton MJ, Golenbock DT. LPS-binding proteins and receptors. J Leukoc Biol 1998; 64: 25-32.
[146] Diot P, Le Pape A, Nolibe D, Normier G, Binz H, Revillard JP, Lasfargues G, Lavandier M and Lemarié E. Scintigraphy with J001X, a Klebsiella membrane glycolipid, for the early diagnosis of chronic berylliosis: results from an experimental model. Br J Ind Med 1992; 49: 359-364.
[147] Perin F, Pittet JC, Hoffschir D, Normier G, Binz H and Le Pape A. Scintigraphic potentials of J001X acylated poly-galactoside for imaging inflammatory lesions in pigs. Nucl Med Biol 1993; 20: 963-971.
[148] Perin F, Pittet JC, Hoffschir D, Daburon F, Normier G and Le Pape A. ^{201}T1 and ^{99}Tc^{m} J001X macrophage scintigraphy: two radionuclide imaging techniques for the surveillance of acute localized radiation over-exposures. Nucl Med Commun 1995; 16: 608-614.
[149] Pittet JC, Pepin M, Normier G, Binz H and Le Pape A. Lymphoscintigraphy via the targeting of macrophages with ^{99m}Tc-J001X poly-galactoside in a model of pyogranulomas developed in sheep lymph nodes. Nucl Med Biol 1995; 22: 355-365.
[150] Goupille P, Chevalier X, Valat JP, Garaud P, Perin F and Le Pape A. Macrophage targeting with ^{99m}Tc-labelled J001 for scintigraphic assessment of experimental osteoarthritis in the rabbit. Br J Rheumatol 1997; 36: 758-762.
[151] Diot P, Diot E, Lemarie E, Guilmot JL, Baulieu JL, Asquier E, Valat C, Delarue A and Le Pape A. Imaging of pulmonary disease in scleroderma with J001X scintigraphy. Thorax 1994; 49: 504-508.
[152] Goupille P, Diot P, Valat JP, Lemarie E, Valat C, Asquier E, Delarue A and Le Pape A. Imaging of pulmonary disease in rheumatoid arthritis using J001X scintigraphy: preliminary results. Eur J Nucl Med 1995; 22: 1411-1415.
[153] Miot-Noirault E, Perin F, Routledge L, Normier G and Le Pape A. Macrophage targeting with technetium-99m labelled J001 acylated poly-galactoside for scintigraphy of inflammation: optimization and assessment of imaging specificity in experimental arthritis. Eur J Nucl Med 1996; 23: 61-68.
[154] Perin F, Routledge L, N'Doye O, M'Bodj M, Normier G and Le Pape A. Influence of technetium-99m-labeling conditions on physicochemical and related biological properties of an acylated poly-galactosidic macrophage targeting agent for inflammation imaging. Nucl Med Biol 1996; 23: 947-955.
[155] Caveliers V, Goodbody AE, Tran LL, Peers SH, Thornback JR and Bossuyt A. Evaluation of ^{99m}Tc-RP128 as a potential inflammation imaging agent: human dosimetry and first clinical results. J Nucl Med 2001; 42: 154-161.
[156] Chaudhuri MK, Konopinska D, Bump NJ and Najjar VA. The similarity between tuftsin (Thr-Lys-Pro-Arg) receptors and tuftsin antibody: a case of induced molecular mimicry. Ann N Y Acad Sci 1983; 419: 135-142.
[157] Fridkin M, Najjar VA. Tuftsin: its chemistry, biology, and clinical potential. Crit Rev Biochem Mol Biol 1989; 24: 1-40.
[158] Albelda SM, Smith CW and Ward PA. Adhesion molecules and inflammatory injury. FASEB J 1994; 8: 504-512.
[159] Tarrant TK, Patel DD. Chemokines and leukocyte trafficking in rheumatoid arthritis. Pathophysiology 2006; 13: 1-14.
[160] Austrup F, Vestweber D, Borges E, Löhning M, Bräuer R, Herz U, Renz H, Hallmann R, Scheffold A, Radbruch A and Hamann A. P- and E-selectin mediate recruitment of T helper-1 but not T-helper-2 cells into inflamed tissues. Nature 1997; 385: 81-83.
[161] Garrood T, Lee L and Pitzalis C. Molecular mechanisms of cell recruitment to inflammatory sites: general and tissue-specific pathways. Rheumatology (Oxford) 2006; 45: 250-260.
[162] Koch AE, Burrows JC, Haines GK, Carlos TM, Harlan JM and Leibovich SJ. Immunolocalization of endothelial and leukocyte adhesion molecules in human rheumatoid and osteoarthritic synovial tissues. Lab Invest 1991; 64: 313-320.
[163] Johnson BA, Haines GK, Harlow LA and Koch AE. Adhesion molecule expression in human synovial tissue. Arthritis Rheum 1993; 36: 137-146.

[164] Kriegsmann J, Keyszer GM, Geiler T, Lagoo AS, Lagoo-Deenadayalan S, Gay RE and Gay S. Expression of E-selectin messenger RNA and protein in rheumatoid arthritis. Arthritis Rheum 1995; 38: 750-754.
[165] Tak PP, Thurkow EW, Daha MR, Kluin PM, Smeets TJ, Meinders AE and Breedveld FC. Expression of adhesion molecules in early rheumatoid synovial tissue. Clin Immunol Immunopathol 1995; 77: 236-242.
[166] Elewaut D, De Keyser F, De Wever N, Baeten D, Van Damme N, Verbruggen G, Cuvelier C and Veys EM. A comparative phenotypical analysis of rheumatoid nodules and rheumatoid synovium with special reference to adhesion molecules and activation markers. Ann Rheum Dis 1998; 57: 480-486.
[167] Kuuliala A, Eberhardt K, Takala A, Kautiainen H, Repo H and Leirisalo-Repo M. Circulating soluble E-selectin in early rheumatoid arthritis: a prospective five year study. Ann Rheum Dis 2002; 61: 242-246.
[168] Keelan ET, Harrison AA, Chapman PT, Binns RM, Peters AM and Haskard DO. Imaging vascular endothelial activation: an approach using radiolabeled monoclonal antibodies against the endothelial cell adhesion molecule E-selectin. J Nucl Med 1994; 35: 276-281.
[169] Keelan ET, Licence ST, Peters AM, Binns RM and Haskard DO. Characterization of E selectin expression *in vivo* with use of a radiolabeled monoclonal antibody. Am J Physiol 1994; 266: H278-290.
[170] Chapman PT, Jamar F, Harrison AA, Binns RM, Peters AM and Haskard DO. Noninvasive imaging of E-selectin expression by activated endothelium in urate crystal-induced arthritis. Arthritis Rheum 1994; 37: 1752-1756.
[171] Jamar F, Chapman PT, Harrison AA, Binns RM, Haskard DO and Peters AM. Inflammatory arthritis: imaging of endothelial cell activation with an indium-111 labeled F(ab')$_2$ fragment of anti-E-selectin monoclonal antibody. Radiology 1995; 194: 843-850.
[172] Chapman PT, Jamar F, Keelan ET, Peters AM and Haskard DO. Use of a radiolabeled monoclonal antibody against E-selectin for imaging of endothelial activation in rheumatoid arthritis. Arthritis Rheum 1996; 39: 1371-1375.
[173] Jamar F, Chapman PT, Manicourt DH, Glass DM, Haskard DO and Peters AM. A comparison between ^{111}In-anti-E-selectin mAb and ^{99}Tc^{m}-labelled human non-specific immunoglobulin in radionuclide imaging of rheumatoid arthritis. Br J Radiol 1997; 70: 473-481.
[174] Martens CL, Cwirla SE, Lee RY, Whitehorn E, Chen EY, Bakker A, Martin EL, Wagstrom C, Gopalan P, Smith CW, Tate E, Koller KJ, Schatz PJ, Dower WJ and Barrett RW. Peptides which bind to E-selectin and block neutrophil adhesion. J Biol Chem 1995; 270: 21129-21136.
[175] Zinn KR, Chaudhuri TR, Smyth CA, Wu Q, Liu HG, Fleck M, Mountz JD and Mountz JM. Specific targeting of activated endothelium in rat adjuvant arthritis with a ^{99m}Tc radiolabeled E-selectin-binding peptide. Arthritis Rheum 1999; 42: 641-649.
[176] Funovics M, Montet X, Reynolds F, Weissleder R and Josephson L. Nanoparticles for the optical imaging of tumor E-selectin. Neoplasia 2005; 7: 904-911.
[177] Reynolds PR, Larkman DJ, Haskard DO, Hajnal JV, Kennea NL, George AJ and Edwards AD. Detection of vascular expression of E-selectin in vivo with MR imaging. Radiology 2006; 241: 469-476.
[178] Gompels LL, Madden L, Lim NH, Inglis JJ, McConnell E, Vincent TL, Haskard DO and Paleolog EM. *In vivo* fluorescence imaging of E-selectin: quantitative detection of endothelial activation in a mouse model of arthritis. Arthritis Rheum 2010; 63: 107-117.
[179] Brazeau P. Somatostatin: a peptide with unexpected physiologic activities. Am J Med 1986; 81: 8-13.
[180] Pearse AG, Polak JM and Bloom SR. The newer gut hormones. Cellular sources, physiology, pathology, and clinical aspects. Gastroenterology 1977; 72: 746-761.
[181] Reichlin S. Somatostatin. N Engl J Med 1983; 309: 1495-1501.
[182] Patel YC. Somatostatin and its receptor family. Front Neuroendocrinol 1999; 20: 157-198.
[183] Dalm VA, van Hagen PM and Krenning EP. The role of octreotide scintigraphy in rheumatoid arthritis and sarcoidosis. Q J Nucl Med 2003; 47: 270-278.
[184] Duet M and Lioté F. Somatostatin and somatostatin analog scintigraphy: any benefits for rheumatology patients? Joint Bone Spine 2004; 71: 530-535.
[185] Cascini GL, Cuccurullo V and Mansi L. The non tumour uptake of ^{111}In-octreotide creates new clinical indications in benign diseases, but also in oncology. Q J Nucl Med Mol Imaging 2010; 54: 24-36.
[186] Bakker WH, Krenning EP, Reubi JC, Breeman WA, Setyono-Han B, de Jong M, Kooij PP, Bruns C, van Hagen PM, Marbach P, Visser TJ, Pless J and Lamberts SWJ. *In vivo* application of [^{111}In-DTPA-D-Phe1]-octreotide for detection of somatostatin receptor positive tumors in rats. Life Sci 1991; 49: 1593-1601.
[187] Kwekkeboom DJ, Krenning EP, Bakker WH, Oei HY, Kooij PP and Lamberts SW. Somatostatin analogue scintigraphy in carcinoid tumours. Eur J Nucl Med 1993; 20: 283-292.
[188] van Eijck CH, Krenning EP, Bootsma A, Oei HY, van Pel R, Lindemans J, Jeekel J, Reubi JC and Lamberts SW. Somatostatin-receptor scintigraphy in primary breast cancer. Lancet 1994; 343: 640-643.
[189] Postema PT, De Herder WW, Reubi JC, Oei HY, Kwekkeboom DJ, Bruining HJ, Bonjer J, van

Toor H, Hennemann G and Krenning EP. Somatostatin receptor scintigraphy in non-medullary thyroid cancer. Digestion 1996; 57 (Suppl 1): 36-37.
[190] Lebtahi R, Cadiot G, Mignon M and Le Guludec D. Somatostatin receptor scintigraphy: a first-line imaging modality for gastroenteropancreatic neuroendocrine tumors. Gastroenterology 1998; 115: 1025-1027.
[191] Reisinger I, Bohuslavitzki KH, Brenner W, Braune S, Dittrich I, Geide A, Kettner B, Otto HJ, Schmidt S and Munz DL. Somatostatin receptor scintigraphy in small-cell lung cancer: results of a multicenter study. J Nucl Med 1998; 39: 224-227.
[192] van Hagen PM, Krenning EP, Kwekkeboom DJ, Reubi JC, Anker-Lugtenburg PJ, Lowenberg B and Lamberts SW. Somatostatin and the immune and haematopoetic system; a review. Eur J Clin Invest 1994; 24: 91-99.
[193] Vanhagen PM, Markusse HM, Lamberts SW, Kwekkeboom DJ, Reubi JC and Krenning EP. Somatostatin receptor imaging. The presence of somatostatin receptors in rheumatoid arthritis. Arthritis Rheum 1994; 37: 1521-1527.
[194] Reubi JC, Waser B, Markusse HM, Krenning EP, VanHagen M and Laissue JA. Vascular somatostatin receptors in synovium from patients with rheumatoid arthritis. Eur J Pharmacol 1994; 271: 371-378.
[195] ten Bokum AM, Melief MJ, Schonbrunn A, van der Ham F, Lindeman J, Hofland LJ, Lamberts SW and van Hagen PM. Immunohistochemical localization of somatostatin receptor sst_{2A} in human rheumatoid synovium. J Rheumatol 1999; 26: 532-535.
[196] Takeba Y, Suzuki N, Takeno M, Asai T, Tsuboi S, Hoshino T and Sakane T. Modulation of synovial cell function by somatostatin in patients with rheumatoid arthritis. Arthritis Rheum 1997; 40: 2128-2138.
[197] Paran D, Elkayam O, Mayo A, Paran H, Amit M, Yaron M and Caspi D. A pilot study of a long acting somatostatin analogue for the treatment of refractory rheumatoid arthritis. Ann Rheum Dis 2001; 60: 888-891.
[198] Paran D, Kidron D, Mayo A, Ziv O, Chowers Y, Caspi D, Yaron M and Paran H. Somatostatin analogue treatment attenuates histological findings of inflammation and increases mRNA expression of interleukin-1 beta in the articular tissues of rats with ongoing adjuvant-induced arthritis. Rheumatol Int 2005; 25: 350-356.
[199] Imhof AK, Gluck L, Gajda M, Lupp A, Brauer R, Schaible HG and Schulz S. Differential antiinflammatory and antinociceptive effects of the somatostatin analogs octreotide and pasireotide in a mouse model of immune-mediated arthritis. Arthritis Rheum 2011; 63: 2352-2362.
[200] Geisler C. The T cell receptor: structural and functional studies. Dan Med Bull 1995; 42: 342-357.
[201] Cantrell DA. T cell antigen receptor signal transduction pathways. Cancer Surv 1996; 27: 165-175.
[202] Kane LP, Lin J and Weiss A. Signal transduction by the TCR for antigen. Curr Opin Immunol 2000; 12: 242-249.
[203] Ferran C, Sheehan K, Dy M, Schreiber R, Merite S, Landais P, Noel LH, Grau G, Bluestone J, Bach JF and Chatenoud L. Cytokine-related syndrome following injection of anti-CD3 monoclonal antibody: further evidence for transient *in vivo* T cell activation. Eur J Immunol 1990; 20: 509-515.
[204] Hooks MA, Wade CS and Millikan WJ. Muromonab CD-3: a review of its pharmacology, pharmacokinetics, and clinical use in transplantation. Pharmacotherapy 1991; 11: 26-37.
[205] Marcus C, Thakur ML, Huynh TV, Louie JS, Leibling M, Minami C and Diggles L. Imaging rheumatic joint diseases with anti-T lymphocyte antibody OKT-3. Nucl Med Commun 1994; 15: 824-830.
[206] Malviya G, Conti F, Chianelli M, Scopinaro F, Dierckx RA and Signore A. Molecular imaging of rheumatoid arthritis by radiolabelled monoclonal antibodies: new imaging strategies to guide molecular therapies. Eur J Nucl Med Mol Imaging 2010; 37: 386-398.
[207] Martins FP, Gutfilen B, de Souza SA, de Azevedo MN, Cardoso LR, Fraga R, and da Fonseca LM. Monitoring rheumatoid arthritis synovitis with ^{99m}Tc-anti-CD3. Br J Radiol 2008; 81: 25-29.
[208] Lopes FP, de Azevedo MN, Marchiori E, da Fonseca LM, de Souza SA and Gutfilen B. Use of ^{99m}Tc-anti-CD3 scintigraphy in the differential diagnosis of rheumatic diseases. Rheumatology (Oxford) 2010; 49: 933-939.
[209] Bugelski PJ, Achuthanandam R, Capocasale RJ, Treacy G and Bouman-Thio E. Monoclonal antibody-induced cytokine-release syndrome. Expert Rev Clin Immunol 2009; 5: 499-521.
[210] Alegre ML, Peterson LJ, Xu D, Sattar HA, Jeyarajah DR, Kowalkowski K, Thistlethwaite JR, Zivin RA, Jolliffe L and Bluestone JA. A non-activating "humanized" anti-CD3 monoclonal antibody retains immunosuppressive properties *in vivo*. Transplantation 1994; 57: 1537-1543.
[211] Routledge EG, Falconer ME, Pope H, Lloyd IS and Waldmann H. The effect of aglycosylation on the immunogenicity of a humanized therapeutic CD3 monoclonal antibody. Transplantation 1995; 60: 847-853.
[212] Cole MS, Anasetti C and Tso JY. Human IgG_2 variants of chimeric anti-CD3 are nonmitogenic to T cells. J Immunol 1997; 159: 3613-3621.
[213] Cole MS, Stellrecht KE, Shi JD, Homola M, Hsu DH, Anasetti C, Vasquez M and Tso JY. HuM291, a humanized anti-CD3 antibody, is immunosuppressive to T cells while exhibiting reduced mitogenicity *in vitro*. Transplantation

1999; 68: 563-571.
[214] Woodle ES, Xu D, Zivin RA, Auger J, Charette J, O'Laughlin R, Peace D, Jollife LK, Haverty T, Bluestone JA and Thistlethwaite JR Jr. Phase I trial of a humanized, Fc receptor nonbinding OKT3 antibody, huOKT3γ1(Ala-Ala) in the treatment of acute renal allograft rejection. Transplantation 1999; 68: 608-616.
[215] Malviya G, de Vries EFJ, Dierckx RA and Signore A. Radiopharmaceuticals for imaging chronic lymphocytic inflammation. Brazilian Archives of Biology and Technology 2007; 50: 1-13.
[216] Malviya G, D'Alessandria C, Bonanno E, Vexler V, Massari R, Trotta C, Scopinaro F, Dierckx R and Signore A. Radiolabeled humanized anti-CD3 monoclonal antibody visilizumab for imaging human T-lymphocytes. J Nucl Med 2009; 50: 1683-1691.
[217] Malviya G, Signore A, Lagana B and Dierckx RA. Radiolabelled peptides and monoclonal antibodies for therapy decision making in inflammatory diseases. Curr Pharm Des 2008; 14: 2401-2414.
[218] Scoazec JY, Feldmann G. Both macrophages and endothelial cells of the human hepatic sinusoid express the CD4 molecule, a receptor for the human immunodeficiency virus. Hepatology 1990; 12: 505-510.
[219] Doyle C, Strominger JL. Interaction between CD4 and class II MHC molecules mediates cell adhesion. Nature 1987; 330: 256-259.
[220] Janeway CA Jr. The role of CD4 in T-cell activation: accessory molecule or co receptor? Immunol Today 1989; 10: 234-238.
[221] Barber EK, Dasgupta JD, Schlossman SF, Trevillyan JM and Rudd CE. The CD4 and CD8 antigens are coupled to a protein-tyrosine kinase ($p56^{lck}$) that phosphorylates the CD3 complex. Proc Natl Acad Sci USA 1989; 86: 3277-3281.
[222] Namekawa T, Wagner UG, Goronzy JJ and Weyand CM. Functional subsets of CD4 T cells in rheumatoid synovitis. Arthritis Rheum 1998; 41: 2108-2116.
[223] Dejaco C, Duftner C, Klauser A and Schirmer M. Altered T-cell subtypes in spondyloarthritis, rheumatoid arthritis and polymyalgia rheumatica. Rheumatol Int 2010; 30: 297-303.
[224] Veys EM, Hermanns P, Verbruggen G, Schindler G and Goldstein G. T lymphocytes in blood and synovial fluid in rheumatoid arthritis. Lancet 1982; 1: 225-226.
[225] Schiff B, Mizrachi Y, Orgad S, Yaron M and Gazit E. Association of HLA-Aw31 and HLA DR1 with adult rheumatoid arthritis. Ann Rheum Dis 1982; 41: 403-404.
[226] Fox DA. The role of T cells in the immunopathogenesis of rheumatoid arthritis: new perspectives. Arthritis Rheum 1997; 40: 598-609.
[227] Becker W, Emmrich F, Horneff G, Burmester G, Seiler F, Schwarz A, Kalden J and Wolf F. Imaging rheumatoid arthritis specifically with technetium 99m CD4-specific (T helper lymphocytes) antibodies. Eur J Nucl Med 1990; 17: 156-159.
[228] Kinne RW, Becker W, Schwab J, Horneff G, Schwarz A, Kalden JR, Emmrich F, Burmester GR and Wolf F. Comparison of $^{99}Tc^{m}$-labelled specific murine anti-CD4 monoclonal antibodies and nonspecific human immunoglobulin for imaging inflamed joints in rheumatoid arthritis. Nucl Med Commun 1993; 14: 667-675.
[229] Kinne RW, Becker W, Schwab J, Schwarz A, Kalden JR, Emmrich F, Burmester GR and Wolf F. Imaging rheumatoid arthritis joints with technetium-99m labelled specific anti-CD4- and non-specific monoclonal antibodies. Eur J Nucl Med 1994; 21: 176-180.
[230] Kinne RW, Becker W, Simon G, Paganelli G, Palombo-Kinne E, Wolski A, Bloch S, Schwarz A, Wolf F and Emmrich F. Joint uptake and body distribution of a technetium 99m-labeled anti-rat-CD4 monoclonal antibody in rat adjuvant arthritis. J Nucl Med 1993; 34: 92-98.
[231] Kinne RW, Becker W, Koscheck T, Kuhlmann J, Sharkey RM, Behr T, Palombo-Kinne E, Goldenberg DM, Wolf F and Emmrich F. Rat adjuvant arthritis: imaging with technetium-99m-anti-CD4 Fab' fragments. J Nucl Med 1995; 36: 2268-2275.
[232] Kinne RW, Schemer K, Behr T, Sharkey RM, Palombokinne E, Emmrich F, Goldenberg D M , Wolf F and Becker W. *In vivo* stability and metabolism of $^{99}Tc^{m}$-labelled anti-CD4 monoclonal antibodies and Fab' fragments. Nucl Med Commun 1999; 20: 67-75.
[233] Walker C, Herzog C, Rieber P, Riethmuller G, Muller W and Pichler WJ. Anti-CD4 antibody treatment of patients with rheumatoid arthritis: II. Effect of in vivo treatment on *in vitro* proliferative response of CD4 cells. J Autoimmun 1989; 2: 643-649.
[234] Fox DA. Biological therapies: a novel approach to the treatment of autoimmune disease. AM J Med 1995; 99: 82-88.
[235] Moreland LW, Pratt PW, Mayes MD, Postlethwaite A, Weisman MH, Schnitzer T, Lightfoot R, Calabrese L, Zelinger DJ, Woody JN and Koopman WJ. Double-blind, placebo controlled multicenter trial using chimeric monoclonal anti-CD4 antibody, cM-T412, in rheumatoid arthritis patients receiving concomitant methotrexate. Arthritis Rheum 1995; 38: 1581-1588.
[236] Tak PP, van der Lubbe PA, Cauli A, Daha MR, Smeets TJ, Kluin PM, Meinders AE, Yanni G, Panayi GS and Breedveld FC. Reduction of synovial inflammation after anti CD4 monoclonal antibody treatment in early rheumatoid arthritis. Arthritis Rheum 1995; 38: 1457-1465.
[237] van der Lubbe PA, Dijkmans BA, Markusse HM, Nassander U and Breedveld FC. A randomized, double-blind, placebo-controlled study of CD4 monoclonal antibody therapy in early rheuma-

toid arthritis. Arthritis Rheum 1995; 38: 1097-1106.
[238] Choy EH, Pitzalis C, Cauli A, Bijl JA, Schantz A, Woody J, Kingsley GH and Panayi GS. Percentage of anti-CD4 monoclonal antibody-coated lymphocytes in the rheumatoid joint is associated with clinical improvement. Implications for the development of immunotherapeutic dosing regimens. Arthritis Rheum 1996; 39: 52-56.
[239] Choy EH, Kingsley GH and Panayi GS. Anti-CD4 monoclonal antibodies in rheumatoid arthritis. Springer Semin Immunopathol 1998; 20: 261-273.
[240] Kim HJ, Berek C. B cells in rheumatoid arthritis. Arthritis Res 2000; 2: 126-131.
[241] Shaw T, Quan J and Totoritis MC. B cell therapy for rheumatoid arthritis: the rituximab (anti-CD20) experience. Ann Rheum Dis 2003; 62 (Suppl 2): ii55-59.
[242] Kotzin BL. The role of B cells in the pathogenesis of rheumatoid arthritis. J Rheumatol Suppl 2005; 73: 14-18; discussion 29-30.
[243] Waubant E. Spotlight on anti-CD20. Int MS J 2008; 15: 19-25.
[244] Taylor PC. Rituximab in the treatment of rheumatoid arthritis. Expert Rev Clin Immunol 2007; 3: 17-26.
[245] Riley JK, Sliwkowski MX. CD20: a gene in search of a function. Semin Oncol 2000; 27: 17-24.
[246] Stashenko P, Nadler LM, Hardy R and Schlossman SF. Characterization of a human B lymphocyte-specific antigen. J Immunol 1980; 125: 1678-1685.
[247] Stopar TG, Mlinaric-Rascan I, Fettich J, Hojker S and Mather SJ. ^{99m}Tc-rituximab radiolabelled by photo-activation: a new non-Hodgkin's lymphoma imaging agent. Eur J Nucl Med Mol Imaging 2006; 33: 53-59.
[248] Tedder TF, Boyd AW, Freedman AS, Nadler LM and Schlossman SF. The B cell surface molecule B1 is functionally linked with B cell activation and differentiation. J Immunol 1985; 135: 973-979.
[249] Malviya G, Laganà B, Milanetti F, Del Mastro C, Familiari D, Dierckx RA, Scopinaro F, D'Amelio R and Signore A. Use of 99m-technetium labelled Rituximab for imaging of patients with chronic inflammatory diseases. Eur J Nucl Med Mol Imaging 2008; 35 (Suppl 2): S142-S143.
[250] Malviya G, Anzola KL, Podesta E, Lagana B, Del Mastro C, Dierckx RA, Scopinaro F and Signore A. ^{99m}Tc-labeled Rituximab for Imaging B Lymphocyte Infiltration in Inflammatory Autoimmune Disease Patients. Mol Imaging Biol 2011.
[251] Kneitz C, Wilhelm M and Tony HP. Improvement of refractory rheumatoid arthritis after depletion of B cells. Scand J Rheumatol 2004; 33: 82-86.
[252] Roll P, Palanichamy A, Kneitz C, Dorner T and Tony HP. Regeneration of B cell subsets after transient B cell depletion using anti-CD20 antibodies in rheumatoid arthritis. Arthritis Rheum 2006; 54: 2377-2386.
[253] Smolen JS, Aletaha D, Koeller M, Weisman MH and Emery P. New therapies for treatment of rheumatoid arthritis. Lancet 2007; 370: 1861-1874.
[254] Kormelink TG, Tekstra J, Thurlings RM, Boumans MH, Vos K, Tak PP, Bijlsma JW, Lafeber FP, Redegeld FA and van Roon JA. Decrease in immunoglobulin free light chains in patients with rheumatoid arthritis upon rituximab (anti-CD20) treatment correlates with decrease in disease activity. Ann Rheum Dis 2010; 69: 2137-2144.
[255] Taylor PC, Quattrocchi E, Mallett S, Kurrasch R, Petersen J and Chang DJ. Ofatumumab, a fully human anti-CD20 monoclonal antibody, in biological-naive, rheumatoid arthritis patients with an inadequate response to methotrexate: a randomised, double-blind, placebo-controlled clinical trial. Ann Rheum Dis 2011; 70: 2119-2125.
[256] Tetta C, Camussi G, Modena V, Di Vittorio C and Baglioni C. Tumour necrosis factor in serum and synovial fluid of patients with active and severe rheumatoid arthritis. Ann Rheum Dis 1990; 49: 665-667.
[257] McNiff PA, Stewart C, Sullivan J, Showell HJ and Gabel CA. Synovial fluid from rheumatoid arthritis patients contains sufficient levels of IL-1 beta and IL-6 to promote production of serum amyloid A by Hep3B cells. Cytokine 1995; 7: 209-219.
[258] Ulfgren AK, Grondal L, Lindblad S, Khademi M, Johnell O, Klareskog L and Andersson U. Interindividual and intra-articular variation of proinflammatory cytokines in patients with rheumatoid arthritis: potential implications for treatment. Ann Rheum Dis 2000; 59: 439-447.
[259] Barrera P, van der Laken CJ, Boerman OC, Oyen WJ, van de Ven MT, van Lent PL, van de Putte LB and Corstens FH. Radiolabelled interleukin-1 receptor antagonist for detection of synovitis in patients with rheumatoid arthritis. Rheumatology (Oxford) 2000; 39: 870-874.
[260] Kriegler M, Perez C, DeFay K, Albert I and Lu SD. A novel form of TNF/cachectin is a cell surface cytotoxic transmembrane protein: ramifications for the complex physiology of TNF. Cell 1988; 53: 45-53.
[261] Black RA, Rauch CT, Kozlosky CJ, Peschon JJ, Slack JL, Wolfson MF, Castner BJ, Stocking KL, Reddy P, Srinivasan S, Nelson N, Boiani N, Schooley KA, Gerhart M, Davis R, Fitzner JN, Johnson RS, Paxton RJ, March CJ and Cerretti DP. A metalloproteinase disintegrin that releases tumour-necrosis factor-α from cells. Nature 1997; 385: 729-733.
[262] Moss ML, Jin SL, Becherer JD, Bickett DM, Burkhart W, Chen WJ, Hassler D, Leesnitzer MT, McGeehan G, Milla M, Moyer M, Rocque W, Seaton T, Schoenen F, Warner J and Willard D.

Structural features and biochemical properties of TNF-α converting enzyme (TACE). J Neuroimmunol 1997; 72: 127-129.
[263] Brockhaus M, Schoefeld H-J. Schlaeger EJ, Hunziker W, Lesslauer W and Loetscher H. Identification of two types of tumor necrosis factor receptors on human cell lines by monoclonal antibodies. Proc Natl Acad Sci USA 1990; 87: 3127-3131.
[264] Erikstein BK, Smeland EB, Blomhoff HK, Funderud S, Prydz K, Lesslauer W and Espevik T. Independent regulation of 55-kDa and 75-kDa tumor necrosis factor receptors during activation of human peripheral blood B lymphocytes. Eur J Immunol 1991; 21: 1033-1037.
[265] Naume B, Shalaby R, Leslauer W and Espevik T. Involvement of the 55- and 75-kDa tumor necrosis factor receptors in the generation of lymphokine-activated killer cell activity and proliferation of natural killer cells. J Immunol 1991; 146: 3045-3048.
[266] Dayer JM, Beutler B and Cerami A. Cachectin/tumor necrosis factor stimulates collagenase and prostaglandin E2 production by human synovial cells and dermal fibroblasts. J Exp Med 1985; 162: 2163-2168.
[267] Bertolini DR, Nedwin GE, Bringman TS, Smith DD and Mundy GR. Stimulation of bone resorption and inhibition of bone formation in vitro by human tumour necrosis factors. Nature 1986; 319: 516-518.
[268] Bevilacqua MP, Pober JS, Majeau GR, Fiers W, Cotran RS and Gimbrone MA Jr. Recombinant tumor necrosis factor induces procoagulant activity in cultured human vascular endothelium: characterization and comparison with the actions of interleukin 1. Proc Natl Acad Sci USA 1986; 83: 4533-4537.
[269] Nawroth PP, Bank I, Handley D, Cassimeris J, Chess L and Stern D. Tumor necrosis factor/cachectin interacts with endothelial cell receptors to induce release of interleukin 1. J Exp Med 1986; 163: 1363-1375.
[270] Saklatvala J. Tumour necrosis factor alpha stimulates resorption and inhibits synthesis of proteoglycan in cartilage. Nature 1986; 322: 547-549.
[271] Vilçek J, Palombella VJ, Henriksen-DeStefano D, Swenson C, Feinman R, Hirai M and Tsujimoto M. Fibroblast growth enhancing activity of tumor necrosis factor and its relationship to other polypeptide growth factors. J Exp Med 1986; 163: 632-643.
[272] Cavender D, Saegusa Y and Ziff M. Stimulation of endothelial cell binding of lymphocytes by tumor necrosis factor. J Immunol 1987; 139: 1855-1860.
[273] Le J and Vilçek J. Tumor necrosis factor and interleukin 1: cytokines with multiple overlapping biological activities. Lab Invest 1987; 56: 234-248.
[274] Brennan FM, Chantry D, Jackson A, Maini R and Feldmann M. Inhibitory effect of TNF-α antibodies on synovial cell interleukin-1 production in rheumatoid arthritis. Lancet 1989; 2: 244-247.
[275] Chu CQ, Field M, Feldmann M and Maini RN. Localization of tumor necrosis factor α in synovial tissues and at the cartilage-pannus junction in patients with rheumatoid arthritis. Arthritis Rheum 1991; 34: 1125-1132.
[276] Deleuran BW, Chu CQ, Field M, Brennan FM, Mitchell T, Feldmann M and Maini RN. Localization of tumor necrosis factor receptors in the synovial tissue and cartilage pannus junction in patients with rheumatoid arthritis. Implications for local actions of tumor necrosis factor α. Arthritis Rheum 1992; 35: 1170-1178.
[277] den Broeder AA, Joosten LA, Saxne T, Heinegard D, Fenner H, Miltenburg AM, Frasa WL, van Tits LJ, Buurman WA, van Riel PL, van de Putte LB and Barrera P. Long term anti tumour necrosis factor α monotherapy in rheumatoid arthritis: effect on radiological course and prognostic value of markers of cartilage turnover and endothelial activation. Ann Rheum Dis 2002; 61: 311-318.
[278] Keystone EC, Kavanaugh AF, Sharp JT, Tannenbaum H, Hua Y, Teoh LS, Fischkoff SA and Chartash EK. Radiographic, clinical, and functional outcomes of treatment with adalimumab (a human anti-tumor necrosis factor monoclonal antibody) in patients with active rheumatoid arthritis receiving concomitant methotrexate therapy: a randomized, placebo-controlled, 52-week trial. Arthritis Rheum 2004; 50: 1400-1411.
[279] Breedveld FC, Weisman MH, Kavanaugh AF, Cohen SB, Pavelka K, van Vollenhoven R, Sharp J, Perez JL and Spencer-Green GT. The PREMIER study: A multicenter, randomized, double-blind clinical trial of combination therapy with adalimumab plus methotrexate versus methotrexate alone or adalimumab alone in patients with early, aggressive rheumatoid arthritis who had not had previous methotrexate treatment. Arthritis Rheum 2006; 54: 26-37.
[280] Smolen JS, Van Der Heijde DM, St Clair EW, Emery P, Bathon JM, Keystone E, Maini RN, Kalden JR, Schiff M, Baker D, Han C, Han J and Bala M. Predictors of joint damage in patients with early rheumatoid arthritis treated with high -dose methotrexate with or without concomitant infliximab: results from the ASPIRE trial. Arthritis Rheum 2006; 54: 702-710.
[281] Hochberg MC, Lebwohl MG, Plevy SE, Hobbs KF and Yocum DE. The benefit/risk profile of TNF-blocking agents: findings of a consensus panel. Semin Arthritis Rheum 2005; 34: 819-836.
[282] Knight DM, Trinh H, Le J, Siegel S, Shealy D, McDonough M, Scallon B, Moore MA, Vilcek J, Daddona P and Ghrayeb J. Construction and initial characterization of a mouse-human chimeric anti-TNF antibody. Mol Immunol 1993; 30: 1443-1453.

[283] Scallon BJ, Moore MA, Trinh H, Knight DM and Ghrayeb J. Chimeric anti-TNF-alpha monoclonal antibody cA2 binds recombinant transmembrane TNF-α and activates immune effector functions. Cytokine 1995; 7: 251-259.
[284] Siegel SA, Shealy DJ, Nakada MT, Le J, Woulfe DS, Probert L, Kollias G, Ghrayeb J, Vilcek J and Daddona PE. The mouse/human chimeric monoclonal antibody cA2 neutralizes TNF in vitro and protects transgenic mice from cachexia and TNF lethality *in vivo*. Cytokine 1995; 7: 15-25.
[285] Barone D, Krantz C, Lambert D, Maggiora K and Mohler K. Comparative analysis of the ability of Etanercept and infliximab to lyse TNF-expressing cells in a complement dependent fashion. Arthritis Rheum 1999; 42 (Suppl): S90.
[286] ten Hove T, van Montfrans C, Peppelenbosch MP and van Deventer SJ. Infliximab treatment induces apoptosis of lamina propria T lymphocytes in Crohn's disease. Gut 2002; 50: 206-211.
[287] Annovazzi A, D'Alessandria C, Caprilli R, Viscido A, Corsetti F and Parisella MG. Radiolabelling of a monoclonal anti-TNF-α antibody with ^{99m}Tc: *in vitro* studies. Q J Nucl Med 2002; 46 (Suppl 1): 27.
[288] Conti F, Priori R, Chimenti MS, Coari G, Annovazzi A, Valesini G and Signore A. Successful treatment with intraarticular infliximab for resistant knee monarthritis in a patient with spondylarthropathy: a role for scintigraphy with ^{99m}Tc-infliximab. Arthritis Rheum 2005; 52: 1224-1226.
[289] Chianelli M, D'Alessandria C, Conti F, Priori R, Valesini G, Annovazzi A and Signore A. New radiopharmaceuticals for imaging rheumatoid arthritis. Q J Nucl Med Mol Imaging 2006; 50: 217-225.
[290] Anderson PJ. Tumor necrosis factor inhibitors: clinical implications of their different immunogenicity profiles. Semin Arthritis Rheum 2005; 34: 19-22.
[291] Salfeld J, Kaymakçalan Z, Tracey D, Roberts A and Kamen R. Generation of fully human anti-TNF antibody D2E7. Ann Rheum Dis 1999; 58 (Suppl): 170-172.
[292] Rau R. Adalimumab (a fully human anti-tumour necrosis factor alpha monoclonal antibody) in the treatment of active rheumatoid arthritis: the initial results of five trials. Ann Rheum Dis 2002; 61 (Suppl 2): ii70-73.
[293] Barrera P, Oyen WJ, Boerman OC and van Riel PL. Scintigraphic detection of tumour necrosis factor in patients with rheumatoid arthritis. Ann Rheum Dis 2003; 62: 825-828.
[294] Malviya G, D'Alessandria C, Lanzolla T, Lenza A, Conti F and Valesini G. ^{99m}Technetium labelled anti-TNF-α antibodies for the therapy-decision making and follow-up of patients with rheumatoid arthritis. Q J Nucl Med 2008; 52: 13-14.
[295] Roimicher L, Lopes FP, de Souza SA, Mendes LF, Domingues RC, da Fonseca LM and Gutfilen B. ^{99m}Tc-anti-TNF-α scintigraphy in RA: a comparison pilot study with MRI and clinical examination. Rheumatology (Oxford) 2011; 50: 2044-2050.
[296] Annovazzi A, D'Alessandria C, Lenza A, Lanzolla T, Conti F, Priori R, Valesini G, Scopinaro F and Signore A. Radiolabelled anti-TNF-α antibodies for therapy decision making and follow-up in rheumatoid arthritis. Eur J Nucl Med 2006; 33 (Suppl 2): S146.
[297] Williamson P, Schlegel RA. Back and forth: the regulation and function of transbilayer phospholipid movement in eukaryotic cells. Mol Membr Biol 1994; 11: 199-216.
[298] Zwaal RF, Schroit AJ. Pathophysiologic implications of membrane phospholipid asymmetry in blood cells. Blood 1997; 89: 1121-1132.
[299] Reutelingsperger CP, van Heerde WL. Annexin V, the regulator of phosphatidylserine catalyzed inflammation and coagulation during apoptosis. Cell Mol Life Sci 1997; 53: 527-532.
[300] Schroit AJ, Zwaal RF. Transbilayer movement of phospholipids in red cell and platelet membranes. Biochim Biophys Acta 1991; 1071: 313-329.
[301] Bevers EM, Comfurius P, Dekkers DW and Zwaal RF. Lipid translocation across the plasma membrane of mammalian cells. Biochim Biophys Acta 1999; 1439: 317-330.
[302] Martin SJ, Reutelingsperger CP, McGahon AJ, Rader JA, van Schie RC, LaFace DM and Green DR. Early redistribution of plasma membrane phosphatidylserine is a general feature of apoptosis regardless of the initiating stimulus: inhibition by overexpression of Bcl-2 and Abl. J Exp Med 1995; 182: 1545-1556.
[303] Vermes I, Haanen C, Steffens-Nakken H and Reutelingsperger C. A novel assay for apoptosis. Flow cytometric detection of phosphatidylserine expression on early apoptotic cells using fluorescein labelled Annexin V. J Immunol Methods 1995; 184: 39-51.
[304] Denecker G, Dooms H, Van Loo G, Vercammen D, Grooten J, Fiers W, Declercq W and Vandenabeele P. Phosphatidyl serine exposure during apoptosis precedes release of cytochrome c and decrease in mitochondrial transmembrane potential. FEBS Lett 2000; 465: 47-52.
[305] Li MO, Sarkisian MR, Mehal WZ, Rakic P and Flavell RA. Phosphatidylserine receptor is required for clearance of apoptotic cells. Science 2003; 302: 1560-1563.
[306] Tait JF, Gibson D. Measurement of membrane phospholipid asymmetry in normal and sickle-cell erythrocytes by means of annexin V binding. J Lab Clin Med 1994 123: 741-748.
[307] Wood BL, Gibson DF and Tait JF. Increased erythrocyte phosphatidylserine exposure in sickle cell disease: flow-cytometric measurement and clinical associations. Blood 1996;

88: 1873-1880.
[308] Schutters K, Reutelingsperger C. Phosphatidylserine targeting for diagnosis and treatment of human diseases. Apoptosis 2010; 15: 1072-1082.
[309] Reutelingsperger CP, Hornstra G and Hemker HC. Isolation and partial purification of a novel anticoagulant from arteries of human umbilical cord. Eur J Biochem 1985; 151: 625-629.
[310] Huber R, Romisch J and Paques EP. The crystal and molecular structure of human annexin V, an anticoagulant protein that binds to calcium and membranes. EMBO J 1990; 9: 3867-3874.
[311] Blankenberg FG, Strauss HW. Nuclear medicine applications in molecular imaging: 2007 update. Q J Nucl Med Mol Imaging 2007; 51: 99-110.
[312] Walker JH, Boustead CM, Koster JJ, Bewley M and Waller DA. Annexin V, a calcium dependent phospholipid-binding protein. Biochem Soc Trans 1992; 20: 828-833.
[313] van Heerde WL, de Groot PG and Reutelingsperger CP. The complexity of the phospholipid binding protein Annexin V. Thromb Haemost 1995; 73: 172-179.
[314] Sugimura M, Donato R, Kakkar VV and Scully MF. Annexin V as a probe of the contribution of anionic phospholipids to the procoagulant activity of tumour cell surfaces. Blood Coagul Fibrinolysis 1994; 5: 365-373.
[315] Meers P, Mealy T. Calcium-dependent annexin V binding to phospholipids: stoichiometry, specificity, and the role of negative charge. Biochemistry 1993; 32: 11711-11721.
[316] Bennett MR, Gibson DF, Schwartz SM and Tait JF. Binding and phagocytosis of apoptotic vascular smooth muscle cells is mediated in part by exposure of phosphatidylserine. Circ Res 1995; 77: 1136-1142.
[317] Kenis H, van Genderen H, Bennaghmouch A, Rinia HA, Frederik P, Narula J, Hofstra L and Reutelingsperger CP. Cell surface-expressed phosphatidylserine and annexin A5 open a novel portal of cell entry. J Biol Chem 2004; 279: 52623-52629.
[318] Post AM, Katsikis PD, Tait JF, Geaghan SM, Strauss HW and Blankenberg FG. Imaging cell death with radiolabeled annexin V in an experimental model of rheumatoid arthritis. J Nucl Med 2002; 43: 1359-1365.
[319] Bronckers AL, Goei W, van Heerde WL, Dumont EA, Reutelingsperger CP and van den Eijnde SM. Phagocytosis of dying chondrocytes by osteoclasts in the mouse growth plate as demonstrated by annexin-V labelling. Cell Tissue Res 2000; 301: 267-272.
[320] Blankenberg FG, Katsikis PD, Tait JF, Davis RE, Naumovski L, Ohtsuki K, Kopiwoda S, Abrams MJ, Darkes M, Robbins RC, Maecker HT and Strauss HW. *In vivo* detection and imaging of phosphatidylserine expression during programmed cell death. Proc Natl Acad Sci USA 1998; 95: 6349-6354.
[321] Hofstra L, Liem IH, Dumont EA, Boersma HH, van Heerde WL, Doevendans PA, De Muinck E, Wellens HJ, Kemerink GJ, Reutelingsperger CP and Heidendal GA. Visualisation of cell death *in vivo* in patients with acute myocardial infarction. Lancet 2000; 356: 209-212.
[322] Narula J, Acio ER, Narula N, Samuels LE, Fyfe B, Wood D, Fitzpatrick JM, Raghunath PN, Tomaszewski JE, Kelly C, Steinmetz N, Green A, Tait JF, Leppo J, Blankenberg FG, Jain D and Strauss HW. Annexin-V imaging for noninvasive detection of cardiac allograft rejection. Nat Med 2001; 7: 1347-1352.
[323] Thimister PW, Hofstra L, Liem IH, Boersma HH, Kemerink G, Reutelingsperger CP and Heidendal GA. *In vivo* detection of cell death in the area at risk in acute myocardial infarction. J Nucl Med 2003; 44: 391-396.
[324] Tokita N, Hasegawa S, Maruyama K, Izumi T, Blankenberg FG, Tait JF, Strauss HW and Nishimura T. ^{99m}Tc-Hynic-annexin V imaging to evaluate inflammation and apoptosis in rats with autoimmune myocarditis. Eur J Nucl Med Mol Imaging 2003; 30: 232-238.
[325] Blankenberg FG. Recent advances in the imaging of programmed cell death. Curr Pharm Des 2004; 10: 1457-1467.
[326] Kietselaer BL, Reutelingsperger CP, Heidendal GA, Daemen MJ, Mess WH, Hofstra L and Narula J. Noninvasive detection of plaque instability with use of radiolabeled annexin A5 in patients with carotid-artery atherosclerosis. N Engl J Med 2004; 350: 1472-1473.
[327] Lampl Y, Lorberboym M, Blankenberg FG, Sadeh M and Gilad R. Annexin V SPECT imaging of phosphatidylserine expression in patients with dementia. Neurology 2006; 66: 1253-1254.
[328] Belhocine T, Steinmetz N, Hustinx R, Bartsch P, Jerusalem G, Seidel L, Rigo P and Green A. Increased uptake of the apoptosis-imaging agent ^{99m}Tc recombinant human Annexin V in human tumors after one course of chemotherapy as a predictor of tumor response and patient prognosis. Clin Cancer Res 2002; 8: 2766-2774.
[329] Boersma HH, Liem IH, Kemerink GJ, Thimister PW, Hofstra L, Stolk LM, van Heerde W L , Pakbiers MT, Janssen D, Beysens AJ, Reutelingsperger CP and Heidendal GA. Comparison between human pharmacokinetics and imaging properties of two conjugation methods for ^{99m}Tc-annexin A5. Br J Radiol 2003; 76: 553-560.
[330] Kemerink GJ, Liu X, Kieffer D, Ceyssens S, Mortelmans L, Verbruggen AM, Steinmetz ND, Vanderheyden JL, Green AM and Verbeke K. Safety, biodistribution, and dosimetry of ^{99m}Tc-HYNIC-annexin V, a novel human recombinant annexin V for human application. J Nucl Med 2003; 44: 947-952.
[331] Kemerink GJ, Boersma HH, Thimister PW, Hof-

stra L, Liem IH, Pakbiers MT, Janssen D, Reutelingsperger CP and Heidendal GA. Biodistribution and dosimetry of ^{99m}Tc BTAP annexin-V in humans. Eur J Nucl Med 2001; 28: 1373-1378.

[332] Kemerink GJ, Liem IH, Hofstra L, Boersma HH, Buijs WC, Reutelingsperger CP and Heidendal GA. Patient dosimetry of intravenously administered ^{99m}Tc-annexin V. J Nucl Med 2001; 42: 382-387.

[333] Ohtsuki K, Akashi K, Aoka Y, Blankenberg FG, Kopiwoda S, Tait JF and Strauss HW. Technetium-99m HYNIC-annexin V: a potential radiopharmaceutical for the in-vivo detection of apoptosis. Eur J Nucl Med 1999; 26: 1251-1258.

[334] Vannier MW. Imaging apoptosis in rheumatoid arthritis. J Nucl Med 2002; 43: 1366-1367.

[335] Kietselaer BL, Hofstra L, Dumont EA, Reutelingsperger CP and Heidendal GA. The role of labeled Annexin A5 in imaging of programmed cell death. From animal to clinical imaging. Q J Nucl Med 2003; 47: 349-361.

[336] Lahorte CM, Vanderheyden JL, Steinmetz N, Van de Wiele C, Dierckx RA and Slegers G. Apoptosis-detecting radioligands: current state of the art and future perspectives. Eur J Nucl Med Mol Imaging 2004; 31: 887-919.

[337] Grierson JR, Yagle KJ, Eary JF, Tait JF, Gibson DF, Lewellen B, Link JM and Krohn KA. Production of [F-18]fluoroannexin for imaging apoptosis with PET. Bioconjug Chem 2004; 15: 373-379.

[338] Murakami Y, Takamatsu H, Taki J, Tatsumi M, Noda A, Ichise R, Tait JF and Nishimura S. ^{18}F-labelled annexin V: a PET tracer for apoptosis imaging. Eur J Nucl Med Mol Imaging 2004; 31: 469-474.

[339] Zhao M, Beauregard DA, Loizou L, Davletov B and Brindle KM. Non-invasive detection of apoptosis using magnetic resonance imaging and a targeted contrast agent. Nat Med 2001; 7: 1241-1244.

[340] McQueen FM, Østergaard M. Established rheumatoid arthritis-new imaging modalities. Best Practices and Research Clinical Rheumatology 2007; 21: 841-856.

[341] Boesen M, Østergaard M, Cimmino MA, Kubassova O, Jensen KE and Bliddal H. MRI quantification of rheumatoid arthritis: Current knowledge and future perspectives. Eur J Radiol 2009; 71: 189-196.

[342] Bird P, Joshua F. New applications of imaging techniques for monitoring progression of rheumatoid arthritis and predicting outcome. Imaging Med 2011; 3: 107-122.

[343] Larsen A, Dale K and Eck M. Radiographic evaluation of rheumatoid arthritis and related conditions by standard reference films. Acta Radiolo Diag 1977; 18: 481-491.

[344] Sharp JT, Young DY, Bluhm GB, Brook A, Brower AC, Corbett M, Decker JL, Genant HK, Gofton JP, Goodman N, Larsen A, Lidsky MD, Pussila P, Weinstein AS and Weissman BN. How many joints in the hands and wrists should be included in a score of radiologic abnormalities used to assess rheumatoid arthritis? Arthritis Rheum 1985; 28: 1326-1335.

[345] Gilkeson G, Polisson R, Sinclair H, Vogler J, Rice J, Caldwell D, Spritzer C and Martinez S. Early detection of carpal erosions in patients with rheumatoid arthritis; a pilot study of magnetic resonance imaging. J Rheumatol 1988; 15: 1361-1366.

[346] McQueen FM, Stewart N, Crabbe J, Robinson E, Yeoman S, Tan PL and McLean L. Magnetic resonance imaging of the wrist in early rheumatoid arthritis reveals a high prevalence of erosions at four months after symptom onset. Ann Rheum Dis 1998; 57: 350-356.

[347] McQueen FM, Stewart N, Crabbe J, Robinson E, Yeoman S, Tan PL and McLean L. Magnetic resonance imaging of the wrist in early rheumatoid arthritis reveals progression of erosions despite clinical improvements. Ann Rheum Dis 1999; 58: 156-163.

[348] Østergaard M, Peterfy C, Conaghan P, McQueen F, Bird P, Ejbjerg B, Shnier R, O'Connor P, Klarlund M, Emery P, Genant H, Lassere M and Edmonds J. OMERACT rheumatoid arthritis magnetic resonance imaging studies. Core set of MRI acquisitions, joint pathology definitions, and the OMERACT RA-MRI scoring system. J Rheumatol 2003; 30: 1385-1386.

[349] Narvaez JA, Narvaez J, De Lama E and De Albert M. MR imaging of early rheumatoid arthritis. Radiographics 2010; 30: 143-165.

[350] Ejbjerg BJ, Vestergaard A, Jacobsen S, Thomsen HS and Østergaard M. The smallest detectable difference and sensitivity to change of magnetic resonance imaging and radiographic scoring of structural joint damage in rheumatoid arthritis finger, wrist, and toe joints: a comparison of the OMERACT rheumatoid arthritis magnetic esonance imaging score applied to different joint combinations and the Sharp/van der Heijde radiographic score. Arthritis Rheum 2005; 52: 2300-2306.

[351] Kamishima T, Fujieda Y, Atsumi T, Mimura R, Koike T, Terae S and Shirato H. Contrast-enhanced whole-body joint MRI in patients with unclassified arthritis who develop early rheumatoid arthritis within 2 years: feasibility study and correlation with MRI findings of the hands. AJR Am J Roentgenol 2010; 195: W287-W292.

[352] Ejbjerg B, Narvestad E, Jacobsen S, Thomsen HS and Østergaard M. Optimised low cost, low field dedicated extremity MRI is highly specific and sensitive for synovitis and bone erosions in rheumatoid arthritis wrist and finger joints: a comparison with conventional high-field MRI and radiography. Ann Rheum Dis 2004; 50: 1097-1106.

[353] Hetland ML, Ejbjerg BJ Horslev-Petersen K,

Jacobsen S, Vestergaard A, Jurik AG, Stengaard -Pedersen K, Junker P, Lottenburger T, Hansen I, Andersen LS, Tarp U, Skjodt H, Pedersen JK, Majgaard O, Svendsen AJ, Ellingsen T, Lindegaard H, Christensen AF, Vallo J, Torfing T, Narvestad E, Thomsen HS and Østergaard M. MRI bone oedema is the strongest predictor of subsequent radiographic progression in early rheumatoid arthritis. Results from a 2 year randomized controlled trial (CIMESTRA). Ann Rheum Dis 2009; 68: 384-390.

[354] Taouli B, Zaim S, Peterfy CG, Lynch JA, Stork A, Guermazi A, Fan B, Fye KH and Genant HK. Rheumatoid arthritis of the hand and wrist: comparison of three imaging techniques. AJR Am J Roentgenol 2004; 182: 937-943.

[355] Haavardsholm EA, Østergaard M, Ejbjerg BJ, Kvan NP, Uhlig TA, Lilleas FG and Kvien TK. Reliability and sensitivity to change of the OMERACT rheumatoid arthritis magnetic resonance imaging score in a multi-reader, longitudinal setting. Arthritis Rheum 2005; 52: 3860-3867.

[356] Goupille P, Roulot B, Akoka S, Avimadje AM, Garaud P, Naccache L, Le Pape A and Valat JP. Magnetic resonance imaging: a valuable method for the detection of synovial inflammation in rheumatoid arthritis. J Rheumatol 2001; 28: 35-40.

[357] Conaghan P, O'Connor P, McGonacle D, Astin P, Wakefield RJ, Gibbon WW, Quinn M, Karim Z, Green MJ, Proudman S, Isaacs J and Emery P. Elucidation of the relationship between synovitis and bone damage: a randomized magnetic resonance imaging study of individual joints in patients with early rheumatoid arthritis. Arthritis Rheum 2003; 48: 64-71.

[358] Boyesen P, Haavardsholm EA, Østergaard M, van der Heijde D, Sesseng S and Kvien TK. MRI in early rheumatoid arthritis: synovitis and bone marrow oedema are independent predictors of subsequent radiographic progression. Ann Rheum 2011; 70: 428-433.

[359] Cimmino MA, Innocenti S, Livrone F, Magnaguagno F, Silvestri E and Garlaschi G. Dynamic gadolinium-enhanced magnetic resonance imaging of the wrist in patients with rheumatoid arthritis can discriminate active from inactive disease. Arthritis Rheum 2003; 48: 120-1213.

[360] McQueen FM, Benton N, Crabbe J, Robinson E, Yeoman S, McLean L and Stewart N. What is the fate of erosions in early rheumatoid arthritis? Tracking individual lesions using x-rays and magnetic resonance imaging over the first two years of disease. Ann Rheum Dis 2001; 60: 859-868.

[361] Zheng S, Robinson E, Yeoman S, Stewart N, Crabbe J, Rouse J and McQueen FM. MRI bone oedema predicts eight year tendon function of the wrist but not requirements for orthopedic surgery in rheumatoid arthritis. Ann Rheum Dis 2006; 65: 607-611.

[362] McQueen FM, Beckley V, Crabbe J, Robinson E, Yeoman S and Stewart N. Magnetic resonance imaging of tendinopathy in early RA predicts tendon rupture at six years. Arthritis Rheum 2005; 52: 744-751.

[363] Bell DA. Can we rely on anti-citrulline antibody determination for the diagnosis of early rheumatoid arthritis? J Rheumatol 2006; 33: 2369-2371.

[364] Østergaard M, Klarlund M, Lassere M, Conaghan P, Peterfy C, McQueen F, O'Connor P, Shnier R, Stewart N, McGonagle D, Emery P, Genant H and Edmonds J. Interreader agreement in the assessment of magnetic resonance images of rheumatoid arthritis wrist and finger joints-an international multicenter study. J Rheumatol 2001; 28: 1143-1150.

[365] Lassere M, McQueen F, Østergaard M, Conaghan P, Shnier R, Peterfy C, Klarlund M, Bird P, O'Connor P, Stewart N, Emery P, Genant H and Edmonds J. OMERACT rheumatoid arthritis magnetic resonance imaging studies. exercise 3: an international multicenter reliability study using the RA-MRI score. J Rheumatol 2003; 30: 1366-1375.

[366] Irvine S, Munro R and Porter D. Early referral, diagnosis, and treatment of rheumatoid arthritis: evidence for changing medical practice. Ann Rheum Dis 1999; 58: 510-513.

[367] Emery P. Evidence supporting the benefit of early intervention in rheumatoid arthritis. J Rheumatol 2002; 29 (suppl 66): 3-6.

[368] Østergaard M, Hansen M, Stoltenberg M and Lorenzen I. Quantitative assessment of the synovial membrane in the rheumatoid wrist: an early obtained MRI score reflects the synovial volume. Br J Rheumatol 1996; 35: 965-971.

[369] Dohn UM, Ejbjerg BJ, Hasselquist M, Narvestad E, Court-Payen M, Szkudlarek M, Moller J, Thomsen HS and Østergaard M. Rheumatoid arthritis bone erosion volumes on CT and MRI: reliability and correlation with erosion scores on CT, MRI, and radiography. Ann Rheum Dis 2007; 66: 1388-1392.

[370] Østergaard M, Stoltenberg M, Gideon P, Sorensen K, Henriksen O and Lorenzen I. Changes in synovial membrane and joint effusion volumes after intraarticular methylprednisolone. Quantitative assessment of inflammatory and destructive changes in arthritis by MRI. J Rheumatol 1996; 23: 1151-1161.

[371] Conaghan PG, O' Connor P, McGonacle D, Astin P, Wakefield RJ, Gibbon WW, Quinn M, Karim Z, Green MJ, Proudman S, Isaacs J and Emery P. Elucidation of the relationship between synovitis and bone damage: a randomized magnetic resonance imaging study of individual joints in patients with early rheumatoid arthrits. Arthritis Rheum 2003; 48: 64-71.

[372] Kalden-Nemeth D, Grebmeier J, Antoni C, Manger B, Wolf F and Kalden JR. NMR monitoring of rheumatoid arthritis patients receiving anti-TNF-

α monoclonal antibody therapy. Rheumatol Int 1997; 16: 249-255.
[373] Lisbona MP, Maymo J, Perich J, Almirall M and Carbonell J. Rapid reduction in tenosynovitis of the wrist and fingers evaluated by MRI in patients with rheumatoid arthritis after treatment with etanercept. Ann Rheum Dis 2010; 69: 1117-1122.
[374] Dohn UM, Ejbjerg B, Boonen A, Hetland ML, Hansen MS, Knudsen LS, Hansen A, Madsen OR, Hasselquist M, Moller JM and Østergaard M. No overall progression and occassional repair of erosions despite persistent inflammation in adalimumab treated rheumatoid arthritis patients: results from a longitudinal comparative MRI, ultrasonography, CT, and radiography study. Ann Rheum Dis 2011; 70: 252-258.
[375] Conaghan PG, Emery P, Østergaard M, Keystone EC, Genovese MC, Hsia EC, Xu W and Rahman MU. Assessment by MRI of inflammation and damage in rheumatoid arthritis patients with methotrexate inadequate response receiving golimumab: results of the GO-FORWARD trial. Ann Rheum Dis 2011; 70: 1968-1974.
[376] Fonseca JE, Canhao H, Tavares NJ, Cruz M, Branco J and Queiroz MV. Persistent low grade synovitis without erosive progression in magnetic resonance imaging of rheumatoid arthritis patients treated with infliximab over 1 year. Clin Rheumatol 2009; 28: 1213-1216.
[377] Gandjbakhch F, Conaghan PG, Ejbjerg B, Haavardsholm EA, Foltz V, Brown AK, Moller Dohn U, Lassere M, Freeston J, Boyesen P, Bird P, Fautrel B, Hetland ML, Emery P, Bourgeois P, Horslev-Petersen K, Kvien TK, McQueen F and Østergaard M. Synovitis and osteitis are very frequent in rheumatoid arthritis clinical remission: results from an MRI study of 294 patients in clinical remission or low disease activity state. J Rheumatol 2011; 38: 2039-2044.
[378] McQueen F, Clarke A, McHaffie A, Reeves Q, Williams M, Robinson E, Dong J, Chand A, Mulders D and Dalbeth N. Assessment of cartilage loss at the wrist in rheumatoid arthritis using a new MRI scoring system. Ann Rheum Dis 2010; 11: 1971-1975.
[379] Hodgson RJ, Connolly S, Barnes T, Eyes B, Campbell RS and Moots R. Pharmacokinetic modeling of dynamic contrast enhanced MRI of the hand and wrist in rheumatoid arthritis and the response to anti-tumor necrosis factor-α therapy. Magn Reson Med 2007; 58: 482-489.
[380] Boss A, Martirosian P, Fritz J, Kotter I, Henes JC, Claussen CD, Schick F and Horger M. Magnetic resonance spin-labeling perfusion imaging of synovitis in inflammatory arthritis at 3.0T. MAGMA 2009; 22: 175-180.
[381] Crowley AR, Dong J, McHaffie A, Clarke AW, Reeves Q, Williams M, Robinson E, Dalbeth N and McQueen FM. Measuring bone erosion and edema in rheumatoid arthritis: a comparison of manual segmentation and RAMRIS methods. J Magn Reson Imaging 2011; 33: 364-71.
[382] Hodgson RJ, O'Connor P and Moots R. MRI of rheumatoid arthritis-image application for the assessment of disease activity, progression and response to therapy. Rheumatology (Oxford) 2008; 47: 13-21.